

**Processing and Characterization of Polymer Based  
Composites With Superior Impact Resistance**

**By**

**Abdullah Tuğrul SEYHAN**

**A Dissertation Submitted to the  
Graduate School in Partial Fulfillment of the  
Requirements for the Degree of**

**MASTER OF SCIENCE**

**Department: Materials Science and Engineering Programme  
Major : Materials Science and Engineering Programme**

**İzmir Institute of Technology  
İzmir, Turkey**

**August, 2003**

We approve the thesis of **Abdullah Tuğrul SEYHAN**

**Date of Signature**

-----  
**Asst. Prof. Dr. Metin TANOĞLU**  
Supervisor  
Department of Mechanical Engineering

-----  
**Asst. Prof. Dr. Funda TIHMINLIOĞLU**  
Co-Supervisor  
Department of Chemical Engineering

-----  
**Prof. Dr. Muhsin ÇİFTÇİOĞLU**  
Head of Material Science and Engineering Programme

-----  
**Asst. Prof. Dr. Seçil ARTEM**  
Department of Mechanical Engineering

-----  
**Assc. Prof. Dr. Mustafa GÜDEN**  
Department of Mechanical Engineering

## **ACKNOWLEDGEMENTS**

I am very grateful to Assistant Professor Metin Tanođlu for his supervision, kind guidance and support during my studies. I would like to thank Assistant Professor Funda Tihminliođlu for her valuable comments and recommendations. I would like to thank İYTE - MAM personals for their helps during my material characterization studies. I would like to acknowledge the financial support from İYTE Ar-Fon Projects under the contact of MÜH 21,2001 and MÜH 06,2002. I acknowledge Mr. Can Candan of Turkish Military Service for help on ballistic testing and TAI for ultrasonic inspection. I would like to thank also Mr. Saeed Ziaee for helpful discussions.

## ABSTRACT

Fiber reinforced polymeric composite materials have recently gained widespread use in military, transportation, energy and civil engineering applications. Resin Transfer Molding (RTM) and Vacuum Assisted Resin Transfer Molding (VARTM) process have become important in the manufacture of these types of composites. In those techniques, use of fiber preforms offer some distinct advantages. Using thermoplastic binders that bond the fabrics together allows the plies to be consolidated into near net shape preform.

In the present work, glass preforms were consolidated by application of heat and pressure over plies of the glass fabrics that were coated with various concentration of thermoplastic polyester binder. Composite laminates with and without binder were fabricated by utilizing VARTM technique. The peel strength of the preforms with various binder contents was measured to determine the optimum binder concentration. The highest peel strength was obtained from preforms that were prepared with about 9 wt.% of the binder. Preform compression test was also performed using universal test machine with preforms composed of eight plies of glass fabrics with binder (3,6 and 9 wt.%) and without binder. It was observed that the binder has significant effect on the degree of preform compaction. The highest thickness reduction and therefore fiber volume fraction of the preforms was reached via 3 wt.% of binder. The flexural strength and modulus, compressive strength and modulus through ply-lay up and in-plane loading directions, apparent interlaminar shear strength, mode I interlaminar fracture toughness of the composites with and without binder were measured to evaluate the effects of the binder on the mechanical properties of the composite plates. It was found that the flexural strength, mode I interlaminar fracture toughness of the E-glass/polyester composite system decreases 30 and 40 percentage, respectively due to the presence of 3 wt.% and 6 wt.% of binder. On the other hand, the flexural modulus of the composite increases while the apparent interlaminar shear strength remains almost constant by the introduction of the binder. The ply-lay up compressive strength and modulus were found to increase up to 3 wt.% of binder and decrease upon further addition of binder. The same findings are valid for the compressive strength and modulus through in-plane loading direction. Ballistic test was performed on E-glass/polyester composite panels according to NATO standards 2920 using 1.1-gr. fragment-simulating projectiles (FSPs) to evaluate the effects of the binder on the

ballistic performance of the E-glass/polyester composite laminates. The ultrasonic C-scan test method was used to monitor the extent of the damage on the panels due to ballistic impact. It was seen that the damage on the ballistically impacted composite panels decreases with increasing binder. A model matrix material was prepared adding various concentrations of the binder to the reacting resin system in order to follow the extend of binder dissolution within the matrix resin. It was found that there is no complete dissolution of the binder in the matrix resin.

## ÖZ

Fiberlerle mukavetlendirilmiş kompozit malzemeler, askeri, taşıma, enerji ve inşaat mühendisliği uygulamalarında son zamanlarda artan bir kullanım alanı bulmaktadır. Reçine Transfer Kalıplama (RTK) ve Vakum Destekli Reçine Kalıplama (VDRK) teknikleri, bu tip kompozitlerin üretiminde önemli duruma gelmiştir. Bu proses teknolojilerinde, ön şekillendirilmiş elyafın (fiber preform) kullanımı bir takım avantajlar sunmaktadır. Fabrikleri bir arada bağlayan termoplastik bağlayıcıların kullanımı, katmanların net şekilli preformların konsolidasyonuna izin vermektedir.

Bu çalışmada, cam preformlar değişik termoplastik bağlayıcı konsantrasyonları ile kaplanmış fabrik katmanlarının ısı ve basınç uygulaması ile elde edilmiştir. Bağlayıcı içeren ve içermeyen kompozit laminalar (VDRK) tekniği kullanılarak üretilmiştir. Farklı oranlarda termoplastik bağlayıcı içeren ön şekillendirilmiş cam elyafların ayrılma mukavemeti optimum binder konsantrasyonunu belirlemek için ölçülmüştür. En yüksek ayrılma mukavemeti bağlayıcı oranının ağırlıkça % 9 olduğu preformlarda elde edilmiştir. Ayrıca preform basma testi universal test cihazı kullanarak 8 katmanda oluşan ve bağlayıcı içeren (% 3,6, ve 9 ağırlıkça) ve içermeyen preformlar ile gerçekleştirilmiştir. Bunun sonucunda, bağlayıcının preform kompaktlanma seviyesi üzerinde oldukça önemli etkisinin olduğu gözlenmiştir. En yüksek kalınlık azalması ve böylece fiber hacim oranının % 3 ağırlıkça bağlayıcı ile ulaşılmıştır. Bağlayıcının kompozit plakaların mekanik özelliklerine olan etkilerinin belirlenmesi için, bağlayıcı içeren ve içermeyen kompozitlerin eğme mukavemeti ve modülü, Mode I laminalar arası kırılma tokluğu, laminalar arası akma mukavemeti, ply-lay up ve in-plane yükleme yönünde basma mukavemeti ve modülü ölçülmüştür. Kompozit eğme mukavemeti ve Mode I laminalar arası kırılma tokluğunun % 3 ağırlıkça oranında bağlayıcının bulunması ile sırasıyla % 30 ve 40 oranında azaldığı gözlemlenmiştir. Diğer yandan kompozit eğme modülü plastik bağlayıcı miktarına bağlı olarak artarken akma mukavemeti hemen hemen sabit kalmaktadır. Hem kompozit ply-lay up basma mukavemeti hem de modülü % 3 ağırlıkça bağlayıcıya kadar artmakta ve daha fazla plastik bağlayıcı eklenmesiyle birlikte azalma eğilimi göstermektedir. Aynı sonuçlar, in-plane yönünde basma mukavemeti ve modülü değerleri içinde bulunmuştur. Termoplastik bağlayıcının E-cam/polyester panellerin balistik performansına olan etkilerin değerlendirmek için, NATO 2920 standardına göre 1.1 gr fragment simule eden mermiler kullanılarak balistik test gerçekleştirilmiştir.

Tahribatsız C-scan ultrasonik muayene testi kompozit panellerin üzerinde balistik testten sonra oluşan hasar oranının saptanması için kullanılmıştır. Sonuç olarak plastik bağlayıcının oranının artmasıyla panellerin üzerindeki balistik hasar oranının azaldığı gözlemlenmiştir. Termoplastik bağlayıcının reaktif reçine sisteminde çözünmesini takip edebilmek amacıyla, reaktif reçine sistemine çeşitli oranlarda termoplastik bağlayıcı eklenerek bir model matriks malzeme hazırlanmıştır. Sonuç olarak termoplastik bağlayıcının reçine içerisindeki çözünürlüğünün sınırlı oranda olduğu gözlemlenmiştir.

# TABLE OF CONTENTS

## LIST OF FIGURES

## LIST OF TABLES

Chapter 1. INTRODUCTION.....	1
Chapter 2. FIBER-REINFORCED POLYMER COMPOSITES.....	4
2.1 Matrix Materials.....	5
2.1.1 Polyester Resin.....	7
2.2 Fiber Materials.....	7
2.2.1 Glass Fibers.....	9
2.2.2 Fiber Reinforcement Architecture .....	10
Chapter 3. LIGHT-WEIGHT COMPOSITE ARMOR.....	11
3.1 Ballistic Impact Performance of Fiber Reinforced Polymer Composites.....	13
3.2 Energy Absorption Through Fiber Reinforced Polymer Composites Upon Ballistic Impact.....	16
Chapter 4. FIBER REINFORCED POLYMER COMPOSITE MANUFACTURING METHODS.....	20
4.1 Wet-Lay up/Spray-Lay up.. ..	21
4.2 Prepreg Lay-up.....	22
4.3 Compression Molding .....	23
4.4 Filament Winding.....	25
4.5 Pultrusion.....	27
4.6 Resin Transfer Molding (RTM).....	28
4.7 Vacuum Assisted Resin Transfer Molding (VARTM).....	29
Chapter 5. FIBER PREFORMING .....	31
5.1 Advantages of Fiber Preforming.....	31
5.2 Fiber Preforming Techniques.....	32
5.2.1 Cut and Place Preforming.....	32
5.2.2 Directed Fiber Preforming.....	33
5.2.3 Textile Preforming.....	33
5.2.3.1 Braided Preforms.....	34
5.2.3.2 Knitted Preforms.....	34
5.2.3.3 Stitched Preforms.....	34
5.2.3.4 Woven Preforms.....	34
5.2.4 Use of Preforming Binder .....	35
5.3 Fiber Preform Compressibility.....	36
5.4 Effect of Preforming Binder on The Final Properties of the Composites.....	39
Chapter 6. EXPERIMENTAL.....	43
6.1 Materials.....	43
6.1.1 Binder Characterization.....	44
6.2 Preform Consolidation and Characterization of Peel Strength and Compaction Behaviour.....	45



6.2.1 Preform Consolidation.....	45
6.2.2 Preform T-Peel Test.....	45
6.2.3 Preform Compaction Test.....	46
6.3 Composite Fabrication.....	47
6.4 Matrix Burn-Out Test.....	48
6.5 Ballistic Testing.....	48
6.5.1 Ultrasonic C-scan Test.....	49
6.6 Mechanical Property Characterization.....	49
6.6.1 Flexural Tests.....	49
6.6.2 Short Beam Shear (SBS) Test.....	51
6.6.3 Double Beam Cantilever (DCB) Test.....	51
6.6.4 Compression Tests.....	53
6.7 Microstructure Characterization .....	53
6.8 Determining the Interactions Between Preforming Binder and Matrix Resin.....	53
 Chapter 7.RESULTS AND DISCUSSION .....	 55
7.1 Peel Strength of Glass Preforms.....	55
7.2 Effect of binder on Preform Compaction.....	56
7.3 Effect of the Binder on the Ballistic Performance of the Composites.....	58
7.4 Effect of the Binder on the Mechanical Properties of the Composites.....	63
7.4.1 Flexural Strength and Modulus.....	63
7.4.2 Interlaminar Shear Strength.....	63
7.4.3 Interlaminar Fracture Toughness .....	64
7.4.4 Compression Properties of the Composites.....	67
7.5 Interactions between Preforming Binder and Matrix Resin.....	76
 Chapter 8. CONCLUSIONS AND RECOMMENDATIONS.....	 82
 REFERENCES.....	 84

## LIST OF FIGURES

<b>Figure 3.1</b>	Schematic of Integral Composite Armor .....	12
<b>Figure 4.1</b>	Schematic of RTM process.....	27
<b>Figure 4.2</b>	Schematic of VARTM Process.....	30
<b>Figure 5.1</b>	An example to the preformed structure.....	35
<b>Figure 5.2</b>	Influence of Preform Compressibility on Microstructure.....	36
<b>Figure 6.1</b>	Gelation time as a function of CoNAP and MEKP weight percentage.....	43
<b>Figure 6.2</b>	Chemical Structure of ATLAC-363E binder.....	44
<b>Figure 6.3</b>	DSC profile of the ATLAC 363E polyester preforming binder.....	44
<b>Figure 6.4</b>	Schematic of Preform Consolidation.....	45
<b>Figure 6.5</b>	Photo showing Peel Test Configuration.....	46
<b>Figure 6.6</b>	Schematic of VARTM.....	47
<b>Figure 6.7</b>	Schematic of Ballistic Set up.....	49
<b>Figure 6.8</b>	Photo of Flexural Test Configuration.....	50
<b>Figure 6.9</b>	Photo showing SBS specimen under load.....	51
<b>Figure 6.10</b>	DCB test sample under load and configuration of test set-up.....	52
<b>Figure 7.1</b>	Average peel strength of the specimens as a function of binder weight percentage.....	56
<b>Figure 7.2</b>	Preform thickness per layer as a function of fabric pressure for various binder content (A, B,C,D refer to initial thickness of the preforms with 0,3,6 and 9wt.% of binder, respectively).....	57
<b>Figure 7.3</b>	Photos showing the ballistic impact damage on front and back face of VARTM processed composite panels. (a and b – panels without binder), (c and d – panels with 3 wt. % binder).....	59
<b>Figure 7.4</b>	C-scan imaging of the ballistically impacted panels (a, b refer to 0 and 6 wt.% of the binder, respectively ).....	60
<b>Figure 7.5</b>	Cross sections of the impacted panels with various binder Concentrations.....	61
<b>Figure 7.6</b>	Optical micrographs from the cross-section of E-glass/polyester composite panel (with 3 wt. % of the binder) after ballistic impact showing delamination and intra-bundle cracking.....	62

<b>Figure 7.7</b>	Optical micrographs from the cross-section of E-glass/polyester composite panel (with 3 wt. % of the binder) after ballistic impact showing fiber fracture and buckling around cavity region.....	63
<b>Figure 7.8</b>	Flexural strength and modulus of the E-glass/polyester composites as a function of binder weight percentage.....	63
<b>Figure 7.9</b>	Apparent interlaminar shear strength of the composites as a function of binder weight percentage.....	64
<b>Figure 7.10</b>	Mode I interlaminar fracture toughness as a function of crack extension.....	65
<b>Figure 7.11 a</b>	SEM fracture surface micrographs of DCB specimen with 0 % wt. of binder.....	66
<b>Figure 7.11 b</b>	SEM fracture surface micrographs of DCB specimen with 3%wt. of binder.....	67
<b>Figure 7.12</b>	Ply lay up direction compressive stress vs. strain response of composites without binder.....	68
<b>Figure 7.13</b>	Ply-lay up direction compressive stress vs. strain response of composites with 3 wt.% of binder.....	68
<b>Figure 7.14</b>	Ply-lay up direction compressive stress vs. strain response of composites with 6 wt.% of binder.....	69
<b>Figure 7.15</b>	In-plane direction compressive stress vs. strain response of composites without binder.....	70
<b>Figure 7.16</b>	In-plane direction compressive stress vs. strain response of Composites with 3 wt.% of binder.....	70
<b>Figure 7.17</b>	In plane direction compressive stress vs. strain response of the composites with 6 wt.% of binder.....	71
<b>Figure 7.18</b>	The strain at maximum stress values as a function of binder weight percentage for the ply-lay up and in-plane loading directions.....	71
<b>Figure 7.19</b>	Ply lay up direction maximum compressive stress and compressive modulus as a function of binder weight percentage.....	72
<b>Figure 7.20</b>	In-plane direction maximum compressive stress and compressive modulus as a function of binder weight percentage.....	72
<b>Figure 7.21</b>	Fracture surface of compression composite specimen without binder loaded in ply-lay up direction.....	73

<b>Figure 7.22</b>	Fracture surface of compression composite specimen with 6 wt.% of binder loaded in ply-lay up direction.....	73
<b>Figure 7.23</b>	Fracture surface of compression composite specimen without binder loaded in in-plane direction.....	74
<b>Figure 7.24</b>	Fracture surface of compression composite specimen with 3wt.% binder loaded in in-plane direction.....	74
<b>Figure 7.25</b>	Fractured surface SEM micrograph of polyester matrix polymer without binder.....	74
<b>Figure 7.26</b>	Fractured surface SEM micrograph of polyester matrix polymer with 12.85 wt.% binder.....	75
<b>Figure 7.27</b>	Fractured surface SEM micrograph of polyester matrix polymer with 12.85 wt.% binder. The undissolved binder particles are visible in micrograph.....	76
<b>Figure 7.28</b>	The typical compressive stress and strain response of the model specimens without binder.....	78
<b>Figure 7.29</b>	The typical compressive stress vs. strain response of the model specimens with 6.5 wt.% of binder.....	78
<b>Figure 7.30</b>	The typical compressive stress vs. strain response of the model specimens with 12.85 wt.% of binder.....	79
<b>Figure 7.31</b>	Strain at yield values of the model specimens as a function of weight percentage of the binder.....	79
<b>Figure 7.32</b>	Yield stress and compressive modulus of the model specimens as a function of binder weight percentage.....	80
<b>Figure 7.33</b>	The viscosity values of the resin/binder blends (6.5 wt.% binder) stirred at room and at elevated temperatures.....	81

## LIST OF TABLES

<b>Table 2.1</b>	Examples for the application of fiber reinforced composites.....	5
<b>Table 2.2 a</b>	The properties of the typically used thermoset matrix material in composites Processing.....	6
<b>Table 2.2 b</b>	The properties of the typically used thermoplastic matrix material in composites processing.....	7
<b>Table 2.3</b>	Properties of some fibers and conventional materials.....	8
<b>Table 2.4</b>	Composition of glass used for fiber manufacture.....	9
<b>Table 6.1</b>	Charecteristic of composite panels fabricated with VARTM process for ballistic testing.....	48
<b>Table 7.1</b>	Ballistic delamination data for the composite panels with various concentration of preforming binder.....	59

# Chapter 1

## INTRODUCTION

Fiber reinforced polymer composites have recently become more popular engineering materials to be used in many industrial areas such as marine bodies, aircraft structures and armor for ballistic protection in military applications. This interest is due to their outstanding mechanical properties, impact resistance, high durability and flexibility in design capabilities and lightweight. Composite materials are playing a key role in the development of polymer composite/ceramic integral armor systems that contain multiple layers of glass fiber-reinforced polymer composites. For these applications, sized glass fibers are being employed with especially epoxy, vinyl ester and polyester resin systems.

Liquid molding processes such as Resin Transfer Molding (RTM) and Vacuum Assisted Resin Transfer Molding (VARTM) techniques are preferably used to fabricate affordable polymeric composite structures. These techniques provide higher fiber volume fraction, better surface quality and microstructural control as compared with traditional techniques such as spray up and hand lay up. The main processing steps in RTM or VARTM are/ placement of the reinforcing fabric into a mold cavity or on a flat tool, resin infusion, curing and demolding. There are some advantages of using fabric preforms that can be prepared in the shape and dimensions of the desired part prior to infusion process [1-4]. These include ease of handling and mold replacement of reinforcing constituent. Composites with higher volume fractions can be obtained from compacted preforms. Use of preforms offers significant potential in cost savings in terms of composite manufacturing duration. Furthermore, preforms may improve the control of dimensional specifications and fiber alignment of the final cured composite part.

Preforming can be done by weaving, knitting, braiding or stitching. The most recent technique to consolidate fiber preform systems is to introduce a thermoplastic binder between reinforcement fabrics to supply brief compaction [1,5]. Thermoplastic binders offer potential to make net shape thermoformable preforms to keep integrity of fibers during mold assembly. Preforms can be fabricated by uniformly spreading and then melting the binder onto the surface of the glass mats. The desired number of

binder-coated plies can be stacked together under application of heat and pressure. It was shown that final composite properties and microstructure depend to a great extent on compaction of the fiber preform to the designed thickness [6]. In addition, it was also shown that the distribution of plastic binders over the glass fabric surface affects the degree of compressibility of fiber preforms. Binders are desired to bond fibers together so that it is possible to tailor the properties of the composites at the interlaminar regions between the layers. In addition to chemical compatibility and reactivity of the binder with matrix resin as well as fiber sizing, physical properties of binder such as melt viscosity, wettability of the glass fabric and solubility in the applied matrix resin may significantly affect the properties of the final composite part. Dissolution of the binder may directly cause an increase in the resin viscosity. This is an important parameter on the composite processing because permeability of the resin through the binder path depends upon the degree of dissolution of binder in the matrix resin [7,8]. Binder properties such as modulus or the area of the binder coverage on the fibers have been found to have some considerable effects on fabricating net-shaped preforms with reduced springback [4]. It has been revealed by several studies that the presence of preforming binder has some significant effect on the mechanical and physical properties of the polymeric composites [1-8]. Furthermore, it was shown that the chemical compatibility of the binder with the matrix resin and fiber sizing is an essential for those composite properties.

The objective of this study is to investigate the effect of a thermoplastic preforming binder on the physical and mechanical properties as well as ballistic performance of the E-glass/polyester composite. Another objective is to develop techniques to fabricate fabric preforms with optimized characteristics.

In the present work, glass preforms were consolidated by application of heat and pressure over plies of the glass fabrics that were coated with various concentration of thermoplastic polyester binder. Composite laminates with and without binder were fabricated by utilizing VARTM technique. The peel strength of the preforms with various binder contents was measured to determine the optimum binder concentration. Preform compression test was also performed using universal test machine with preforms composed of eight plies of glass fabrics with binder (3,6 and 9 wt.%) and without binder. The flexural strength and modulus, compressive strength and modulus through ply-lay up and in-plane loading directions, apparent interlaminar shear strength,

mode I interlaminar fracture toughness of the composites with and without binder were measured to evaluate the effects of the binder on the mechanical properties of the composite plates. Ballistic test was performed on E-glass/polyester composite panels according to NATO standards 2920 using 1.1-gr. fragment-simulating projectiles (FSPs) to evaluate the effects of the binder on the ballistic performance of the E-glass/polyester composite laminates. To our knowledge, there is no work reported in the literature revealing the effects of a preforming binder on the ballistic performance of the polymeric composites. The ultrasonic C-scan test method was used to monitor the extent of the damage on the panels due to ballistic impact. A model matrix material was prepared adding various concentrations of the binder to the reacting resin system in order to follow the extend of binder dissolution within the matrix resin. Moreover, the viscosity measurements of the matrix resin with and without binder were performed in certain time intervals at room and elevated temperatures. Furthermore, to replicate the effects of thermoplastic binder on the compressive mechanical behaviour of the thermosetting matrix, compressive tests were conducted on the model matrix resin with and without binder.



## Chapter 2

### FIBER REINFORCED POLYMER COMPOSITES

Composite materials consist of two or more physically and chemically distinct materials in such that the properties of composite are superior and unique in some specific respects, as compared to the properties of its individual components. Composites are in general composed of matrix and reinforcing constituents as well as fillers [9]. Reinforcements for composites can be fibers, particles, or whiskers. Each of these materials has its own unique applications [10,11]. Fibers have usually high strength and modulus and serve as the principal load-carrying member. Fibers are most commonly used in high performance polymer composites. Some particulates including glass beads, calcium carbonate, mica, etc. are added into the matrix to produce particulate filled polymer composites. Matrix materials are generally polymers, ceramics and metals. The matrix holds the reinforcement together and acts as a load transfer medium between fibers and keep them away from any environmental damage that could initiate the fracture [12]. The matrix also keeps the fibers in a desired location and orientation, separating fibers from each other to avoid mutual abrasion during periodic straining of the composite. In fiber reinforced composites, both fiber and the matrix retain their identities in most of the cases. It results in unique properties that can not be achieved with either of them acting alone.

Reinforced composites may be classified based on the nature of the matrix material as polymer matrix composites (PMC) metal matrix composites (MMC) and ceramic matrix composites (CMC). PMCs have wider applications as compared with MMCs, and CMCs due to their unique properties such as low density and cost and easy handling. Moreover, they have high strength and stiffness, impact resistance, and durability and design flexibility depends upon the properties of the composite constituent. For those reasons, engineering metallic materials are currently being replaced with PMCs in structural designs. Selected examples with comments for the applications of PMCs in various industries are given in Table 2.1 [12].

**Table 2.1** Applications of fiber-reinforced polymer composites [12].

INDUSTRY	EXAMPLES	COMMENTS
Aircraft	Doors, elevators, rudders	- Usually result in 20 to 35% savings over metal parts
Aerospace	Space shuttle, space station	- Great weight savings - High dimensional and thermal stability using carbon / carbon composites
Automotive	Body frame, chassis components engine components, drive shaft, exterior body components, etc.	- High stiffness - Good surface finishing - Lower weight
Marine	Hulls and masts for boats, spars	- Weight reduction - Economy in fuel
Sporting goods	Tennis racquets, golf club shafts bicycle frames, skis, canoes, etc.	- Weight reduction - Vibration damping - Design flexibility
Chemical	Pipes, tanks, pressure vessels	- Weight savings - Corrosion resistance
Military	Helmets, portable bridges, armour plates.	- Weight savings - High stiffness and impact damage tolerance

## 2.1 Matrix Materials

The polymer matrix materials can be classified as thermoplastic and thermoset polymers. These two polymer types differ in their respective intermolecular structures that the thermoset materials are crosslinked in their final state, and the thermoplastics do not exhibit any crosslinking. The thermosets are generally liquid resins, which are cured with application of heat and chemical reaction to achieve the crosslinking of their molecular structures, while the thermoplastics are solids that can be melted, formed, and then cooled to achieve their final solid form. The matrix materials in fiber composites are extensive and vary in a wide range of properties. The chief polymers used in high

performance fiber reinforced composites are thermosetting resins with low molecular weight species and low viscosity. The property requirements for a matrix material are different from those for a reinforcement [10,11]. Matrix materials usually have relatively low modulus and strength and high ductility values as compared to fibers. Therefore, fracture toughness and crack propagation resistance in Mode I and II are commonly used to assess the potential of a matrix for use in damage-tolerant composites [9]. Moreover, the matrix determines the thermal stability of the composite. When the composite is under a compressive load, the matrix plays a key role in preventing micro buckling of fibers that is a major compressive failure mechanism in continuous fiber composites [13].

Composite performance is related to the following matrix properties; elastic modulus, yield and ultimate strengths under tension, compression or shear, failure strain or ductility, fracture toughness, durability or resistance to aggressive organic liquids and moisture, thermal and oxidative stability. When selecting a particular resin for a specific composite application, the processability of the matrix with appropriate viscosity must be also taken into consideration. Curing procedures can induce the defects in the form of delamination and flaws, voids, fiber debonding, wrinkles, inclusions, broken fibers, fiber misalignment and residual stresses. All of these factors determine the performance of the final composite part. Tables 2.2 (a) and 2.2 (b) show the properties of the typically used thermoset matrix and thermoplastic matrix materials, respectively [2,4]. In this study, the matrix material used to fabricate composite parts was chosen as a polyester resin. Brief information about polyester resin is given in the following part.

**Table 2.2 (a)** The properties of thermoset matrix materials typically used in composite processing [11].

Property	Units	Epoxy	Polyester
Density	Mg/m <sup>3</sup>	1.1-1.4	1.2-1.5
Young's modulus	GPa	3-6	2-4.5
Tensile strength	MPa	35-100	40-90
Compressive strength	MPa	100-200	90-250
Elongation to break	%	1-6	2
Shrinkage on curing	%	1-2	4-8

**Table 2.2 (b)** The properties of the thermoplastic matrix materials typically used in composite processing [11].

Property	Units	Polypropylene	Nylon 6.6	Polycarbonate
Density	Mg/m <sup>3</sup>	0.90	1.14	1.06-1.20
Young's modulus	GPa	1.0-1.4	1.4-2.8	2.2-2.4
Tensile strength	MPa	25-38	60-75	45-70
Elongation to break	%	> 300	40-80	50-100

### 2.1.1 Polyester Resin

The term polyester resin is used to describe a class of thermosetting resins consisting of an unsaturated backbone dissolved in a reactive monomer [13]. The most common backbone for the polymer is a saturated acid, an unsaturated acid, and one or more glycols. The most common reactive monomer is styrene. The polyester backbone polymer is synthesized by condensation polymerization. Polyester resins are commonly categorized as *ortho* and *iso* resins depending on the nature of the saturated acid portion of the backbone polymer. The difference between them is that, as the saturated acid portion of the backbone polymer, *ortho* and *iso* resins use orthophthalic acid and isophthalic acid, respectively. *Ortho* resins are used in contact molding such as marine applications, while *Iso* resins are used in matched die-molding, corrosion resistant applications and gel coats. Unsaturated polyesters are in general used where a good balance is required between the mechanical properties and chemical resistance at moderate or ambient temperatures [10]. The unsaturated polyesters are cured by adding free radical catalyst or initiators such as methyl ethyl ketone peroxide, plus an accelerator such as cobalt naphthenate and diethyl aniline. Anhydrides can be used to avoid the problem of by-product formation.

### 2.2 Fiber Materials

A wide variety of fiber materials are available for the polymer composites. The most commonly used fibers in polymer matrices are carbon, glass and aramid type fibers [11]. Although they are relatively more expensive, boron fibers also find some applications in military and aerospace applications. Alumina, silicon carbide, silicon nitride and other ceramic fibers and metal wires have still limited use as well [15]. High

strength and high modulus carbon fibers are manufactured by treating organic fibers with heat and tension, leading to a highly ordered carbon structure. The most commonly used precursors include rayon-base fibers, polyacrylonitrile, and pitch. Organic fibers like aramid and polyethylene is a class of the fibers based on the high strength and stiffness resulted from fully aligned polymers [10]. Aramid fibers are a generic term for aromatic polyamide fibers. As an example, Kevlar<sup>®</sup> developed by Du Pont Corp., is composed of poly(1,4-phenyleneterephthalamide). Two forms, Kevlar 29 and Kevlar 49, are available. The aramid fibers have an elastic modulus over twenty times greater than that of conventional polyamide (nylon) fibers [5]. Aramid fibers with high specific strength absorb much more energy than brittle fibers and widely used in lightweight armor and other impact-resistant structures [11]. Another example to organic fibers is polyethylene fibers produced from high-density polyethylene by solid state drawing. Like other polymer-based high performance fibers, the transverse and longitudinal compressive strengths of PE fibers are far from being satisfactory. Many of these fibers can be fabricated with a wide range of properties. The unique combinations of properties available in these fibers provide the outstanding structural characteristics of fiber-reinforced composites. Table 2.3 shows the properties of some fibers and conventional bulk materials [12].

**Table 2.3** Properties of some fibers and conventional materials [12].

Material	Tensile Modulus (GPa)	Tensile Strength (GPa)	Density (gr/cm <sup>3</sup> )
E-glass	72.4	3.5	2.54
S-glass	85.5	4.6	2.48
High modulus carbon	390	2.1	1.90
High tensile strength carbon	240	2.9	1.77
Carbon	190	2.6	1.76
Boron	385	2.8	2.63
Kevlar <sup>®</sup> -49	130	2.8	1.45
Kevlar <sup>®</sup> -29	60	2.8	1.44
Steel	210	0.34 to 2.1	7.8
Aluminium alloys	70	0.14 to 0.62	2.7
Tungsten	350	1.1 to 4.1	17.30

### 2.2.1 Glass Fibers

Glass is an amorphous material that consists of silica ( $\text{SiO}_2$ ) backbone with various oxide components like calcium, boron, sodium, iron and aluminum to give specific compositions and properties [12]. The most common reinforcement for polymer matrix composites is glass fiber. Glass fibers can be produced in either continuous filament or staple form. In the production of these fibers, the glass is melted and the melted glass flows through small orifices to form the fiber filaments. The advantages of glass fibers include low cost, high tensile and impact strengths, and high chemical resistance. Moreover, the three-dimensional network structure of glass filament exhibit isotropic properties in contrast to those of carbon and aramid fibers that have anisotropic structures [1,9]. The disadvantages include relatively low modulus, self-abrasiveness, low fatigue resistance.

Glass fibers are typically classified based on their compositions. This includes electrically resisted E-glass, chemically resisted C-glass and high tensile strength S-glass. Table 2.4 shows the composition of these types of filaments [11]. E-glass is the most commonly used glass because it draws well and has good strength, stiffness, electrical and weathering properties. C-glass has a borosilicate composition. It has a higher resistance to chemical corrosion than E-glass but it is more expensive and has lower strength properties. S-glass is more expensive than E-glass but has higher young's modulus and is more temperature resistant. For that reason, it is often used in advanced composites where strength is a premium.

**Table 2.4** Composition of glass used for fiber manufacture [11].

Composition	E-glass	C-glass	S-glass
$\text{SiO}_2$	52.4	64.4	64.4
$\text{Al}_2\text{O}_3, \text{Fe}_2\text{O}_3$	14.4	4.1	25
$\text{CaO}$	17.2	13.4	-
$\text{MgO}$	4.6	3.3	10.3
$\text{Na}_2\text{O}, \text{K}_2\text{O}$	0.8	7.6	0.3
$\text{Ba}_2\text{O}_3$	10.6	4.7	-
$\text{BaO}$	-	0.9	-

### **2.2.2 Fiber Reinforcement Architecture**

In the utilization of textile composites, an integrated approach from microstructural design and textile preform processing to performance characterization is indispensable [14]. This integrated approach exploits the intrinsic relation between the textile preform manufacturing technique and its resultant fiber architecture. For that reason, fiber reinforcement architecture associated with a suitable manufacturing technique is quite important in the design of the final composite properties. Reinforcing geometries of the composites can be roughly grouped by the shape of the reinforcing elements, including particles, continuous fibers or short fibers. By considering the degree of continuous fiber reinforcement in the thickness direction, textile preforms can be categorized as 2-D and 3-D [12]. 3-D can be further classed according to manufacturing techniques: woven, non-woven, braided, stitched and knitted [15]. In other words, sets of parallel continuous fibers are often embedded in thin composite layers, which are assembled into a laminate. Alternatively, each ply in a laminate can be reinforced with continuous fibers woven or knitted into a textile preform produced in the width and length of the finished composite structure [6]. Due to a variety of textile fiber architecture existing, composites may differ in fiber volume fraction, fiber type, fiber aspect ratio, fiber orientation and possibly fiber hybridization. So, it is really important to identify the structural element and the loading via the fiber reinforcement orientation and volume fraction. All these parameters enable one to determine which fiber preform manufacturing technique should be employed in the corresponding design of the final composite part.

## Chapter 3

### LIGHTWEIGHT COMPOSITE ARMOR

Composite materials are playing a key role in the development of integral armor systems that meet multifunctional requirements such as ballistic protection structural integrity, damage tolerance and multi-hit performance for military vehicles, structures and personnel protection. Integral armor is based on hybrid composite technology that employs various types of special and complex material constituents [17-19]. These systems include combinations of polymeric, metallic and ceramic materials and their reinforced composites with different configurations. The characteristic that all such systems have in common is that they employ two or more components in the corresponding configuration designed to give optimum ballistic performance [18]. What is meant by optimum ballistic performance is the best protection possible at minimum weight with best possible mechanical integrity. So, any integral armor configuration must include the mechanical integrity following ballistic impact. Density of the armor as well as armor bulk is a critical issue on the mobility of the armored systems. Ceramic backed by composite (glass or kevlar reinforced plastics) or metal (aluminum, titanium, hardened steel or their foams etc.) plate armors are becoming the subject of many investigations because their performance together against small or medium caliber projectiles is good enough when the areal density is a design condition.

Figure 3.1 illustrates an example for a multi-layered lightweight integral armor design [20]. As seen in the figure, the design of the integral armor consists of a combination of thick-section structural composite, ceramic tiles, resilient rubber, fire retardant laminate liner and a composite durability cover. Also, each constituent has unique tasks affecting the ultimate mechanical properties and ballistic resistance of integral armor. Table 3.1 shows the task of each integral armor component [21]. In such composite armor systems, the main role of the ceramic tile is the erosion and rupture of the projectile. When a ceramic is impacted by a projectile a compressive wave travels from the front to the rear face at the speed of sound, then it reflects back and becomes a tensile wave which breaks the ceramic in tension while traveling towards to back face [19]. Therefore, the involved back up plate is desired to delay the initiation of ceramic tensile failure initiating at the ceramic/backing plate interface and allows more projectile erosion [24]. The front plate to back plate thickness ratio and impact velocity



is important to investigate the mechanism of penetration process. However, the design of armour is really complex and need many sophisticated tools. The complexity of the system analysis lies in the fact that different deformation and failure mechanisms contributing to target perforation occur at different stages of the penetration process. Therefore, the design of the composite armor systems is based on the brief understanding of impact events. For that purpose, empirical methods are the most widely used ones because they offer reliability, but they are extremely expensive and the results do not give enough information: the history of the projectile, the trends when changing the configurations or the phenomenological process cannot be obtained in detail with the experimental approach. So, recently simulation techniques are widely employed to optimize the parameters to develop advanced armor. Such models have been checked both with ballistic tests and numerical methods to predict if good agreement is existing between them. J.G Hethorssonn *et al.* [17] studied the optimum thickness of two component composite armors (ceramic/reinforced plastic) using Florence model. He found that Florence model gives an valuable estimate of optimization of two components for a given areal density. Lee [18] investigated the ballistic efficiency of ceramic/metal composite armor systems against 40.7 gr. steel projectiles. In this study, the optimum thickness ratio of the constituents is found to be 2.5 and there is no significant difference between the ballistic performance of the two component armor systems when the thickness ratio is varied from 1.5 to 3.

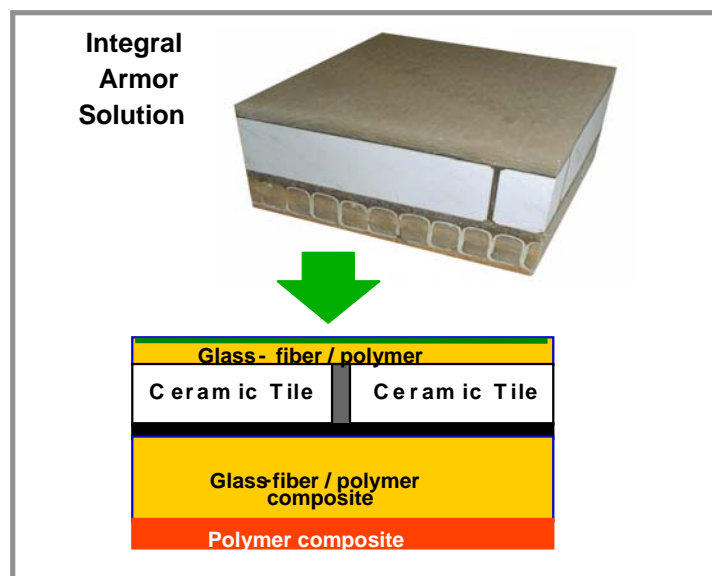


**Figure 3.1** Composite integral armor design [20].

**Table 3.1** Task of each integral armor components [19].

<b>Armor Constituents</b>	<b>Task</b>
Durability Cover	For outer shell comprising glass reinforcement
Ceramic tiles	For absorption of the initial kinetic energy of the projectile
Ethylene propylene diene monomer	For multi-hit damage tolerance
Thick section composite structural laminate	The primary structural load bearing component, glass fiber with appropriable resin matrix.
Electromagnetic mesh interference	For electromagnetic shielding
Phenolic laminate liner	Flammability protection for fiber reinforced composite structural laminate

### **3.1 Ballistic Impact Resistance of the Fiber Reinforced Polymer Composites**

Fiber reinforced polymer composites have demonstrated in a number of military applications that they can replace metals, ceramic and other ballistic materials. They can also take important place in integral composite armor systems with different design configurations, as stated in the previous section. These composites offer superior strength, ballistic resistance and significant weight savings [21-27]. Due to ease of fabrication, complicated components can have ballistic resistance without paying a weight penalty associated with coupling fixtures. The ballistic performance coupled with reduced weight is the primary factor for a number of composite applications. The combination of toughest resins such as epoxy or polyesters with lightweight reinforcing ballistic fibers such as glass, kevlar or aramid has shown good ballistic potential against fragmentation.

Fiber reinforced polymer composites respond differently to ballistic impact as compared to ideal materials such as metals in which the fundamentals of the mechanics of high strain deformation are based [22]. Ballistic failure modes for metal structures result in localized damage extension. Consequently, residual integrity of metal-based

armored structures is not a major issue. On the other hand, glass-reinforced plastic laminates demonstrate the large ballistic damage zones so that the extent of the damage and residual strength of glass reinforced plastic structures must be concerned in armor design.

The composite absorbs the kinetic energy of the fragments by stopping them through micro damages such as debonding and macro damages such as delamination. In brief, as the projectile proceeds through the target, the early phase being dominated by acceleration of target material, compression and crushing ahead of the projectile, and the latter stages being characterized by macro and micro fractures such as delamination. The delamination failure mode is the major life-limiting failure process for composite laminate in terms of damage tolerance [23-25]. This is because delamination can induce the strength and stiffness loss, local stress concentrations, and a local instability that can cause buckling failure under ballistic compressive loading. Delamination also may result in a redistribution of structural load paths. In summary, the process of the penetration and perforation of composite materials is extremely complex, involving not only the in-homogeneity and anisotropy of the material, but also complicated dynamic and thermal effects, finite displacement and rotation with inelastic strain, fracture and tearing, etc. [26]. Studies of ballistic penetration of fabrics and composites have examined fiber response, mechanisms of deformation and failure as well as energy absorption and dynamic loading [24]. Despite elucidating many characteristic features of fabric and composite behaviors, no single model has emerged which allows a quantitative description of the ballistic perforation process [27]. On the other hand, the ballistic limit  $V_{50}$  is critical parameter used in modeling of energy absorption of such targeted systems. Probabilistic in nature, all definitions of the  $V_{50}$  refer to the threshold velocity dividing penetration and non penetration events [28]. In most recent studies, considering  $V_{50}$  many authors have developed theoretical and numerical methods to analyze the dynamic plastic behavior of composites with various approximations, some of the results agreeing well with experimental observations. However, most of the methods are far complicated and are not suitable for use at the ballistic design state.

E.P. Gellert and co workers [29] examined thickness dependence of perforation of GRP composites for three projectile nose shapes by measuring ballistic resistance and examining sectioned and perforated specimens. An interesting attempt was made to analytically understand deformation process by comparison with observations on metallic laminates. For this purpose, GRP targets were constructed from woven roving

E-glass of 11 plies (4,5 mm 27% resin), 22 plies (9 mm, 28-29wt% resin), 33 plies (14 mm, 27wt% resin) and 44 plies (20 mm, 29-30wt% resin) of a nominal 608 g/m<sup>2</sup> cloth and vinyl ester resin. Hardened steel penetrators were fired from a commercial stud gun, and impact velocity was measured by the interruption of electromagnetic fields. The ballistic limit  $V_{50}$  for each target combination was calculated as the average velocity of impacting penetrators that just perforated and were just stopped by the target. Targets were impacted no more than four times, with the impacts spaced so that any delamination produced did not overlap with delamination damage from previous impacts. Because the penetrators of different geometry were of slightly different masses, the projectile kinetic energy to just defeat the target was calculated from the ballistic limit data, and this was plotted as a function of target thickness. So, the results from different penetrators can be compared to each other on the same scales. They concluded that energy absorption is largely independent of projectile nose geometry for thin GRP targets and thicker targets are more efficient ballistically against blunt projectiles.

N. Tarım and co-workers [30] have made an study on a new light-weight armored car-body manufactured from polymer based composite materials bonded to an Al-substrate as an alternative to the conventional steel product. Al-substrate thickness was 0.7 mm. Glass fiber prepregs were impregnated by epoxy resin using the hand-lay up method. In an experimental group; 6, 12, 18, 22, 28 and 36 layers of glass fiber prepregs were produced and (Al) was bonded on to both sides of these glass fiber groups. Ballistic impact tests then carried out on specimens with Al-substrates. During the ballistic testing at least 5 firing were performed to the plates and among the touching points of the bullets at least 4 diameters distance of a bullet was maintained in the investigation. They found that the thinner composite plates have higher elasticity than the thicker ones in the ballistic testing. The bending and tensile strength were increased with the increments of composite layers. The velocity of the bullet is decreased with the increment of the layer numbers. In contrast, output is obtained as the opposite behavior of speed. Another result is that the depth of trace of the bullets are decreased with the increment of the layer numbers. Also, there is a direct proportionality between speed and the trace depth for all layer numbers. In addition, the penetration depth is increased with the increment of bullet speed.

E.DeLuca and co-workers [31] described and quantified ballistic impact damage of S-2 glass fabric reinforced plastic laminate panels by measuring laminate strength

after ballistic impact. They tested the S-2 glass fabric reinforced plastics with two different size of fragment simulating projectiles at various velocities below the limiting velocity of perforation. The impacted specimen were examined by computed tomography to determine the extent of damage in the specimens. Prior to testing ballistically damaged plates, compression tests were conducted on ten undamaged S-2 glass fabric reinforced panels. They explored correlation of the residual strength with ballistic impact and damage parameters. They found that if the specimen size were different, the trend of strength degradation might be the same but the absolute value of strength degradation in percentage would be different.

A.P. Mouritz [32] studied whether the effectiveness of stitching in increasing the damage resistance of polymer composites against ballistic projectiles was better than unstitched one. For this purpose, E-glass reinforced vinyl ester composites stitched in the through-thickness direction with thin Kevlar-49 yarn were impacted with a bullet. He observed that the amount of the delamination damage to the composite caused by a ballistic projectile was reduced slightly with stitching. Stitching was highly effective in increasing the damage resistance against ballistic loading. The increased damage resistance was due to the stitching raising 60 % of Mode I interlaminar fracture toughness of the composite. He also found that the flexural properties of the stitched composites are similar to the properties of the unstitched laminate when damaged by a ballistic projectile because the amount of delamination damage was similar.

### **3.2 Energy Absorption Within Fiber Reinforced Polymer Composites Upon Ballistic Impact**

Upon ballistic impact, fiber reinforced polymer composites retard the projectile by reducing its kinetic energy, creating large conical damaged areas through some micro and macro failure modes. All of these failure modes are together responsible for the absorption of energy to different extends. The relative energy absorbing capability of each failure mode depends upon the basic properties of the target as well as the loading mode. In general, failure modes such as fracture of the matrix result in low absorbed energy whereas failures involving fiber/matrix frictional sliding and debonding result in significantly greater energy dissipation. The energy absorption of a ballistic projectile in a composite material is a complex combination of striking velocity, energy dissipation during the penetration, projectile characteristic and the

material properties of the target. For that reason, it is really necessary to quantify the energy absorbed by each of the mentioned mechanisms to efficiently design composite materials for ballistic protection. Several attempts are therefore made to develop a model for energy absorption of polymer composites at certain ballistic speeds. However, it is really difficult to get a theoretical energy absorption model of composites upon ballistic impact, results of which are reasonable with experimental ones.

S.S. Morye and co-workers [33] developed an energy absorption model of the composites under ballistic impact. In developing the model they made the following assumptions. The projectile is rigid and remains undeformed during the impact (this was confirmed by experiments which showed that the projectiles retained their shape and mass after impact). The energy lost in overcoming the frictional force between projectile and composite is negligible and also the heat generated during the projectile/composite interaction is negligible. The failure mechanism of the composite is uniform across its thickness. The energy absorbed in delamination is neglected. Three major components were identified as contributing to the energy lost by the projectile during ballistic impact, namely the energy ( $E_{TF}$ ) absorbed in tensile failure of the composite, the energy converted into elastic deformation ( $E_{ED}$ ) of the composite and the energy ( $E_{KE}$ ) converted into the kinetic energy of the moving portion of the composite. These three contributions are combined in the model to determine a value for the ballistic limit of the composite  $V_{50}$ .

$$E_{total} = E_{TF} + E_{ED} + E_{KE} \quad (3.1)$$

The energy lost by the projectile during impact is calculated using following equation

$$E_{KE} = \frac{1}{2} (V_s^2 - V_r^2) \quad (3.2)$$

where  $V_s$  is the strike velocity of the projectile and the  $V_r$  is the residual velocity. If the energy absorbed at the point of tensile failure of the composite per unit volume is  $E_C$ , then the total energy absorbed by tensile failure  $E_{TF}$  is given by the equation.

$$E_{TF} = E_C V \quad (3.3)$$

where  $V$  is the volume of the composite strained to its tensile failure and calculated from the equation,

$$V = 4R_C DT \quad (3.4)$$

where  $D$  is the projectile diameter,  $T$  is the composite thickness and  $R_C$  is the radius of the cone formed on the back face of the composite. So the final equation becomes,

$$E_{TF} = E_C 4R_C DT \quad (3.5)$$

The energy absorbed in elastic deformation of the composite at a strain of  $\varepsilon$  can be obtained from the area under the stress/strain curve of the composite. Kinetic energy of the cone formed on the back face of the composite upon ballistic impact is;

$$E_{KE} = \frac{1}{2} m_c V_c^2 \quad (3.6)$$

According to the model, the energy lost by the projectile is equal to the total energy absorbed by the composite.

$$E_L = E_{total} \quad (3.7)$$

$$\frac{1}{2} m V_0^2 = E_{total} \longrightarrow V_0 = \sqrt{\frac{2}{m} E_{total}} \quad (3.8)$$

The model gives a good agreement with the experimental data and the measured values of  $V_{50}$ . More information is available in the paper. However, this model is very simple and assumptions are not valid in every cases.

G.J Czarnecki [34] made a study on developing a set of simple energy-based algorithms capable of economically and accurately estimating the  $V_{50}$  of composite laminates. With the assumption that a fixed amount of energy, equal to the  $E_{50}$  must be absorbed by the laminate in order to achieve projectile penetration, any change of impact energy ( $E_1$ ) above the  $E_{50}$  must therefore equal the change of the projectiles

residual energy ( $E_R$ ) plus the spall energy ( $E_S$ ). From this point of view, they get the formula,

$$E_1 - E_{50} = E_R + E_S \quad (3.9)$$

During evaluation of this equation, three different procedures were followed. In procedure 1, the spall's energy is assessed by assuming the average spall velocity is the same with projectile residual velocity. In procedure 2, spall energy is ignored. In procedure 3, the kinetic energy required for penetration is assumed constant regardless of projectile mass. They found that the theoretical  $V_{50}$  prediction for the case 2 were better matched to the experimental  $V_{50}$  values, as compared to the other supposed models.

B. Wang and co-workers [28] evaluated the penetration resistance of fiber glass reinforced plastic plates under ballistic impact carried out using 7.62 mm armor piercing rounds with 759.54 m/s. Composites were made of E-glass fibers and chopped mats using epoxy and vinyl ester matrix. In parallel, a slow penetration test using a fabricated bullet profile was carried out to enable a comparison of the damage mechanism and the energy absorbing characteristics of the composites under the two different loading conditions. They observed that even though there are some differences in the failure mechanisms, the amount of the energy absorbed by the materials is quite close for the two different loading conditions. Thus, from the energy absorption point of view it is feasible to use the slow penetration test to predict the ballistic limit of the target. They declared a semi-empirical model to describe the resistant force at each penetration stage, from which the energy absorption can be calculated and the residual velocity of the projectile predicted approximately. They also found that the greatest kinetic energy absorbed per unit of plate areal density was recorded for the specimen consisting of layers of chopped strand mat in vinyl ester resin.



## Chapter 4

# FIBER REINFORCED POLYMER COMPOSITE MANUFACTURING METHODS

There is a number of manufacturing methods that are commercially available and optimized for the composite materials to be processed. The manufacturing technology for thermoset composites is quite different from that for thermoplastics. Thermoset composite manufacturing methods principally involve placing the uncured material into or onto a mold so that the material can be shaped into the final part [9].

### 4.1 Wet-Lay Up/Spray-Up

Wet lay up is one of the oldest but still one of the most commonly used methods to manufacture composites [35]. In wet-lay up, fabric or mat is laid into or onto a mold which is treated with mold-release agent. Then, catalyzed resin is applied either by hand or spray. In hand lay up technique, the resin is worked into reinforcement with a hand-held roller, which compacts laminate and removes voids and air bubbles. The reinforcement layers are satisfactorily impregnated and stacked together one by one. This sequence is repeated until the desired thickness is obtained. The layered structure is then allowed to cure to get the cross-linking of the resin. To get better uniformity, the reinforcement is prewetted with the resin before being layed into the mold. The dry fabric and liquid resin can be weighed to obtain specific fiber/resin ratio. This method helps preventing the formation of resin-rich and resin poor areas caused by vertical drainage [36]. To prevent the composite from sticking the mold, a mold release is applied to the mold.

For many commercial applications, a layer of catalyzed resin is applied to release coated mold and is allowed to cure to the gel state before the dry or saturated reinforcement is applied. This resin layer, called the gel-coat, forms a protective surface layer through which fibrous reinforcements do not penetrate. Specially formulated gel-coat resins are generally used to improve the flexibility, weatherability and toughness. The spray up method is similar to hand lay up process except the method of applying the resin and reinforcement. Instead of using cloth or mat, the spray up method uses

roving that is chopped and then blown into the mold. The resin and initiator are sprayed into the mold simultaneously with the chopped fiber. Although much of the manual work of wet lay-up is reduced by employing spray up, manual rolling still may be required and may be important in the final compaction of the laminate to remove voids and to improve impregnation. Since spray up gives faster production cycles, it is useful for fabricating very large structures and parts with rather than complex geometries. The physical properties of the final composite parts by spray up method are not as good as those by hand lay up. Characteristics of the wet lay up methods can be considered as follows [9];

- Require small capital investments
- Typically use resins that crosslink at room temperature with little or no applied pressure and that are tolerant to variations in processing temperature.
- Use simple tooling due to modest crosslinking requirements
- Labor-intensive process
- Very cost effective for short production series and prototype production
- Suitable for any size structures, notably very large.
- Evoke worker health concerns due to the active chemistry of the resin.

Due to low capital and high labor costs, wet hand lay up is used for products manufactured where the requirements on structural and environmental properties are not excessive, typically meaning low to moderate loads and ambient temperatures. Applications include; motor and sailing yachts, high – speed passenger ships, storage tanks.

## **4.2 Prepreg Lay Up**

Prepreg is a reinforcement that has been pre-impregnated with resin, which is cured slightly to increase viscosity to facilitate easy handling and lay up with prepreg lay up technology [35]. Superior composite part with higher performance can be produced with less resin and fiber handling difficulty. The prepreg is normally produced at a facility dedicated to the manufacturing of prepreg by using a method that permits better control of the resin /fiber ratio. The fibers are usually arranged in a unidirectional

tape or a woven fabric, impregnated with catalyzed resin, partially cured and then rolled up for the process. Prepregs are used in applications where part performance is critical, since the prepreg lay up method is more precise than the wet lay up method. At a composite manufacturing, prepreg tapes already provided with the matrix resin are profiled and cut to specific dimensions and shapes, laid up ply-by-ply into a mold and then cured. This technique usually requires vacuum bagging and often autoclaving. The prepregs typically are leathery and have a slight tackiness so that the layers will not slide over one another during lay up. They should also be conformable to the mold so that parts with complex shape may be produced. Characteristics of the prepreg lay up method can be considered as follows [9].

- Requires medium capital investments.
- Uses resins that require increased temperature, vacuum and often externally applied pressure to crosslink an intended and that are fairly intolerant to variations in processing conditions.
- Labor intensive
- Suitable for short production series and structures of any size.

Prepreg lay up is the most suitable for manufacturing products in short series where the need for good exceptionally properties can motivate the high costs. Lay up of prepregs directly onto the core is common in the aerospace industry , where applications include; vertical and horizontal stabilizers, control surfaces, landing-gear doors, rotor blades.

### **4.3 Compression Molding**

Three types of matched die molding are existing; preform molding, sheet molding compounds (SMC) and bulk molding compounds (BMC) [35,36]. These three methods utilize the same type of high pressure molding equipment, but differ in the form of the material that is placed in the molds to form the part. The materials most commonly molded by these techniques are fiberglass. The fiber lengths generally preclude the use of this technique for high performance parts. The equipment is a hydraulic press that is fitted with both male and female dies. The dies are generally made of hard metal and

can be highly polished and chrome-plated in order to get a fine finish. The pressures developed by press can range up to several hundred thousand kilos, which is useful for obtaining good part uniformity and compression of the voids that may develop.

In preform molding, a dry mat of the reinforcing material is preformed to the approximate shape of the part and placed into the open mold. Resin is added to the preform, and the mold halves are then pressed together and heated to cure the part. Sheet molding compounds (SMC) process consists of chopping glass fibers onto a sheet of plastic film on which a mixture of resin-catalyst-fillers have been applied. Another film, which also has the resin mixture applied onto it, is placed on top, and the sandwich of resin mixture and chopped glass is passed between compaction rolls to wet the fibers and thoroughly mix the constituents. The material is then cured slightly and rolled up. A typical SMC incorporates 30-50% fibers, 25% resin (generally polyester) and 25-45% filler (generally clay, alumina, or calcium carbonate) [11]. Some care must be taken with SMC because it has already had initiator added and therefore, kept refrigerated until use. After aging, the SMC material has a leather like texture. When it is to be molded, it can be cut off the roll, the plastic film backing removed, and loaded into the compression molding process. This technique, for instance, widely used in production of car bodies.

Bulk molding compounds (BMC) has a similar composition to SMC, but the fiberglass content is slightly lower and lengths are shorter. BMC is usually mixed in bulk rather than as a sheet and is employed in a log or rope form. BMC is molded by placing a weighed amount of the material into the lower mold. The molds are then closed, and pressures, temperatures, and cycles are much like those for SMC. Advantages of match die molding can be considered as follow.

- Both interior and exterior surfaces are finished
- Complex shapes( including ribs and thin details) are possible.
- Production rate can be high
- Labor costs are low.
- Minimum trimming of parts is needed.
- Products have good mechanical properties and close part tolerances.
- Good consolidation of parts.

Disadvantages of match die molding process;

- More equipment is needed than for lay up.
- Molds and tooling are costly compared with lay up molds.
- Transparent products are not possible with SMC and BMC.
- Molding problems (trapped water, etc.) may cause surface imperfections, such as pitting or waviness.
- SMC and BMC have limited shelf lives.

#### **4.4 Filament Winding**

A continuous band or tape of resin-impregnated fibers is wrapped over a mandrel to produce a hollow part. A large number of fiber roving is pulled from a series of payoff devices, collimated into a band through the use of a textile thread board or a stainless steel comb, passed into a liquid resin bath and a wiping device, and then wrapped over a mandrel. Either the mandrel or the application head can rotate to give the fiber coverage over the mandrel. Although the rotating mandrel is far more common, simultaneous rotation/translation of both mandrel and application head permits filament winding of complex non-uniform shapes [11,13].

The process which incorporates the resin impregnation as part of the winding process is called wet filament winding. The process which uses prepreg tow as the winding medium is called dry filament winding. In wet winding, fiber tension is controlled by the fiber guides or scissor bars located between each payoff device and the resin bath. A wiping device is normally a set of squeeze rollers where the clearance gap between rollers can be adjusted to control the resin content. The traversing speed of the carriage and the winding speed of the mandrel are controlled to provide the desired winding angle patterns. A helical winding pattern is created with a rotating mandrel and a translating a carriage. By adjusting the carriage speed and the mandrel rotation rate, any wind angle between near 0 and 90 can be achieved. For a circular mandrel rotating with a constant rotational speed,  $N$  (revolutions per minute) and a constant carriage feed of  $V$ , the wind angle is given by;

$$\theta = 2\pi Nr/V$$

where ( $r$ ) is the radius of the mandrel. A constant ( $\theta$ ) can be maintained in a thick part if the ratio  $N/V$  is adjusted from layer to layer.

Most standard matrix resins can be used for filament winding, provided that they are low in volatile content and have proper viscosity characteristics. Viscosity of the resin should be high enough so that resin dripping in the mandrel can be avoided and yet low enough so that good fiber wet out can be achieved. Resins such as epoxy, polyester, etc. can be used for filament winding. The parts can be left on the mandrel and a mold is placed over the part for autoclave curing. In some cases, parts can be simply oven cured. The effects of gravity may be minimized if the part is rotated while being cured. Characteristic of Filament winding [13];

- Parts of widely varying size may be produced.
- Non-cylindrical shapes can be made.
- Panels and fittings for reinforcement or attachment can be easily included in the winding process.
- Low void content and good fiber/resin ratio can be achieved.
- Parts with high pressure ratings can be fabricated.

Some applications of filament winding include pressure vessels, fuel and water tanks, rocket motor cases, pipelines, automotive drive shafts, and helicopter blades. In sporting goods, the filament winding process is used also to manufacture tennis rackets from prepreg sheets. The sheets are formed by slitting the wound shape parallel to the mandrel axis or at an inclined angle to provide adequate normal and shear strengths to the tennis rackets.

#### **4.5 Pultrusion Method**

Pultrusion is a continuous fabrication technique used to produce constant cross section composite structures. The process involves pulling resin-impregnated fiber reinforcements through a preformer and a heated die to cure the resin. Pultrusion differs from filament winding in that filament winding places the primary reinforcement in the hoop direction, while pultrusion has the primary reinforcement in the longitudinal direction [36]. The heart of the pultrusion process is the impregnation of the fibers with

the resin and the shaping of the material into the desired shape. In most pultrusion processes, the dry fibers are pulled through a resin bath which has several mechanical rollers or other devices to assist in assuring that the fibers are well wetted. The wetted fibers are then pulled through a die or forming bushing. Alternately, the dry fibers can be formed by passing them through a die and then into a cylindrical chamber made of perforated metal through which the resin can be forced to wet the fibers. Three curing methods are traditionally associated with pultrusion. The most common of these methods is called the tunnel oven method in which the part is usually gelled in the die and fully cured as the part travels through the oven after exiting the forming die. The second curing method is called the split die. In this method, two female molds are brought up against the part as it exits the die. The third one is called die curing. It involves the rapid curing of the part while it is still in the die. The mechanical properties of the pultruded parts are generally good compared with similar parts made by other methods. However, parts made from all unidirectional material have very poor transverse strength. Advantages of pultrusion [13];

- Pultrusion has a much higher material usage (95%) than lay up (75%) therefore, it is more productive in time and material.
- High throughput rate
- High resin contents available

#### Disadvantages of pultrusion

- Part cross sections must generally be uniform
- Problems can arise when resin or fibers accumulate and build up at the die opening. This can increase the friction to the point that the equipment will be jammed or the fibers will break.
- Voids can result if the dies are run with too much opening for the fiber volume.

## 4.6 Resin Transfer Molding

Figure 4.1 shows the schematic of the RTM process [37]. In RTM, a mold is loaded with dry reinforcement materials. Reinforcement material can be originally in the form of roving, mat, fabric, or a combination. Individual fabrics or fiber preforms may be used in a RTM mold [1-8,38]. However, preforms prepared in the shape and

dimensions of the final composite part prior to infusion process would be employed rather than individual fabrics in a RTM mold. The preform is being normally pre-rigidized by using a small amount of fast-curing resin or employing other techniques such as stitching, knitting or use of binder between fabric layers before being placed in a RTM mold. The preform must not extend beyond the desired seal or pinch off area in the mold to permit the mold to close and seal properly. Resin is injected into the mold cavity where it flows through the reinforcement preform, expelling the air in the cavity and impregnating the reinforcement. When excess resin starts to flow from the vent areas of the mold, the resin flow is stopped and curing begins. Completion of curing can take from several minutes to several hours. When the cure process ends, the part is removed from the mold, which is prepared to accept another preform. The cured part may require a postcure to complete the resin reactions. RTM offers the promise of producing low cost composite parts with complex structures and large near net shapes. Relatively fast cycle times with good surface finishing and appearance are easily achievable.

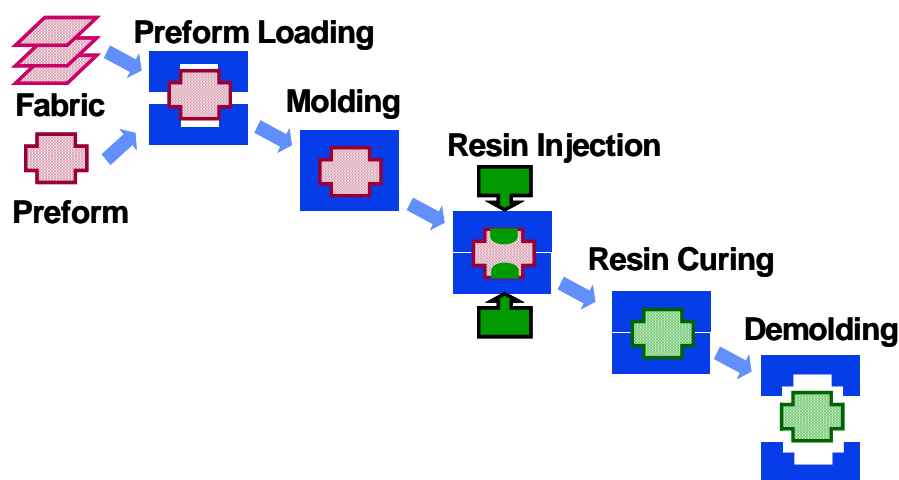


**Figure 4.1** Schematic of RTM method [37].

Structural Resin Transfer Molding (SRIM) is a derivative of RTM process. Once the mold has been closed, the resin and the crosslinking agent is injected separately into the mold and reacts quickly within the mold to cure fully within a few seconds. This chemical reaction proceeds as the resin penetrates through the preform and, therefore, SRIM requires fast fiber wet-out and air displacement. Through impregnation of reinforcement is quickly followed by complete cure of resin. The resin rapidly becomes



too thick to permit resin flash through vents. SRIM parts normally do not require postcuring. Advantages of RTM and SRIM Method [9-13];

- Very large and complex shapes can be made efficiently and inexpensively through the use of preforms.
- Surface definition is superior to lay up. In addition, using matched tools for the mold one can improve the finish of all the surfaces.
- Production cycles are much faster than with lay-up.
- One or both mold surfaces can be gel-coated to improve surface performance.
- Mechanical properties of molded parts are comparable to other composite fabrication processes
- Volatile emissions is low because RTM is closed mold process.

Disadvantages of RTM and SRIM;

- The mold design is critical and requires great skill. Improper gating or venting may result in defects.
- Properties are equivalent to those with matched die molding and not as good as with vacuum bagging, filament winding or pultrusion
- Control of resin uniformity is difficult. Radii and edges tend to be resin rich.
- Reinforcement movement during resin injection is sometimes a problem.

RTM and SRIM have become popular in the automobile, aerospace, military and sport industries; RTM for short to medium sized production series and SRIM for long series. The major reasons for this interest are that complex parts may be economically produced in one step using low cost moulds and that the parts may have high-class surfaces. In the manufacturing of sandwich composite parts for the vehicle bodies, they both find widespread use.

#### **4.7 Vacuum Assisted Resin Transfer Molding**

The most commonly used derivatives of the RTM is Vacuum Assisted Resin Transfer Molding (VARTM) process. It has been widely used for application in both commercial and military, ground-based and marine composite structures. The process has some advantages over conventional RTM. For example, the matched metal tool commonly found in RTM is replaced in the VARTM process by a formable vacuum bag material and the vacuum provides the dual advantage of the pressing the layers together by simultaneously withdrawing the excess volatiles [9.35,36]. Vacuum pressure is selected in the range 0.01-10 KPa.

VARTM technique similarly consists of four steps; loading the dry fabrics into mold cavity, resin injection, curing and demolding. Figure 4.2 shows the schematic of VARTM process. A preform or individual fabrics are placed in a flat tool. Then, a peel ply material that permits resin flow through and separation of the parts from the processing constituents is placed over the fabrics. Peel materials are generally Teflon-treated nylons. A distribution (resin transfer) media is next applied on top of the peel ply to aid the flow of the resin over the surface of the fabrics. There are several types of distribution media in various pore geometries such as sphere or triangular to achieve designed resin permeability. The bleeder material (Vacuum transfer media) is a mat that absorbs the excess resin. Common bleeder materials are surface treated polyester mat or felt. It is important that the bleeder material has good absorption qualities and does not compact under vacuum pressure. The barrier is layer that limits the upward movement of the resin and prevents resin from reaching or clogging the breather and vacuum lines. Finally, vacuum bag that can be made of any plastic film material that is strong enough to hold a vacuum is applied through the sealing tape or sealant around the mold. The resin is injected via vacuum through single or multiple inlet ports depending upon part size and shape.

The most common problems associated with VARTM are material quality and bag leaks. Bridging is also a common problem in VARTM. Bridging occurs when the shape of the part does not allow the VARTM materials to press against all of the part surface. So, these areas can not be compressed properly. To overcome such problems, as well as the pressure gradient caused by the vacuum pressure, gravity and capillary flow effects must also be considered [5]. The preform infiltration time is a function of the resin viscosity, the preform permeability and the applied pressure gradient [6].

The infiltration time can be greatly reduced by utilizing a distribution medium with a higher permeability than the preform. Consequently, the resin flows in the distribution medium first and then the infiltration process continues through the preform thickness.

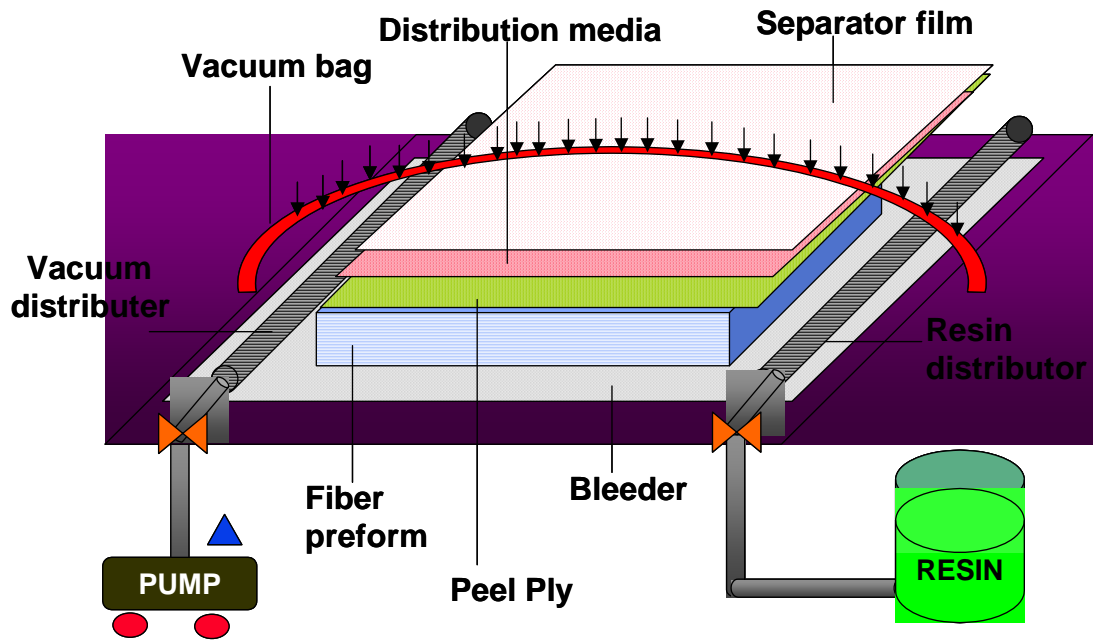


Figure 4.2 Illustration of VARTM processing.

## Chapter 5

### FIBER PREFORMING

In RTM and VARTM processes, holding fabric reinforcements together and undeformed to the final shape is a key issue. Cutting and shaping the individual layers of the reinforcement fabrics via various curvatures of the tool surfaces is very time consuming [39]. Employment of fiber preforms is the obvious advantage of RTM and VARTM methods. The recent trend in order to handle the fiber reinforcement in a rigid form as a single unit in the mold is the use of fabric preforms. A preform is a pre-shaped fiber form in which fibers arranged in one, two or three dimensions in the approximate shape and dimensions of the final composite part. A variety of preforms can be produced by automated manufacturing methods using braiding or weaving techniques [40]. Interweaving of the roving or yarns serves as the means to hold the preform together. An alternative new approach is the application of a binder material onto dry fiber plies at various concentrations and bonding of fabrics together by melting and resolidification [1-8].

#### 5.1 Advantages of Fiber Preforms

The use of preforms offers some superior advantages [41]. Preforming fixes the fibers in a desired orientation and it may improve the control of dimensional specifications and fiber alignment of the final part. Another advantage is that fibers can be easily obtained with shape and dimensions of the part prior to composite processing [39-44]. Preforming also presents the opportunity to combine a variety of fiber architectures and materials within the same part. As a result, preforming makes possible to locally tailor the microstructure of the final part to meet the structural intricacies of the global and local loading conditions. Thus, preforms allow composites with higher fiber volume fraction ( $V_f$ ) and can enhance the part performance properties. Many studies showed that use of preforms has significant effect on the physical and mechanical properties of the composites. In addition, use of preforms has significant potential in cost savings in terms of composite manufacturing time. The cost and the

process time of RTM and VARTM processes can be reduced by employing preforms, which result in throughput increase for higher manufacturing.

## **5.2 Fiber Preforming Techniques**

Preform refers to all of the reinforcement materials placed into the tool prior to resin injection. Preforming is associated with converting the dry, unimpregnated yarns, roving and fabrics into the complex three dimensional precursor of the part prior to composite processing. So, the preforming methods provide a mechanism to develop the configuration of the part in itself microstructure. The most common preforming techniques includes [39-45];

- a) Cut and place
- b) Directed fiber preforming
- c) Textile preforming
- d) Use of preforming binder

### **5.2.1 Cut and Place Preforming**

With this method, random fiber mat, either chopped or continuous, and directional reinforcement, primarily woven or knitted fabrics, are cut prior to the shape of the final part. By trial and error hand shaping, the reinforcement is arranged into the female side of the mold cavity [41]. This method is extremely labor intensive and preform cycles time of several hours are existing. The large quantities of the material that are wasted make hand preforming an extremely expensive method for liquid molding processes. However, there are some distinct advantages of using the cut and place preforming method. High performance components may be formed as a result of the precision by which the fibers are laid down and through the inclusion of directional reinforcement. Furthermore, geometrically complicated preforms may be developed with that process.

### **5.2.2 Directed Fiber Preforming**

In this technique, the preform is usually made by spraying chopped reinforcements onto a perforated screen. A vacuum applied to the rear of the screen holds the reinforcement in place until some resin, which is sprayed along with reinforcement, has time to cure [45]. After a post cure, the preform becomes an easily handled. Directed fiber preforming appears to be the method of choice for producing preforms for RTM and VARTM. However, there are some drawbacks to this process. Only glass fibers can be used with the direct preforming process. A primary concern with this system is volume fraction of fibers within the preforms; above 28 %, which is very low, is not achievable. This shows that directed fiber preforms tend to have a great deal of entrapped air. Thus, they must be pre-compacted to arrive at the desired thickness for higher performance. Other issues that are crucial is preform to preform weight variation and glass weight consistency.

### **5.2.3 Textile Preforming**

Textile preforming including braiding, knitting, stitching and weaving have become gradually popular for the development of preforms for RTM and VARTM methods. Using the advanced CAD/CAM simulation programs, complex shapes of 3-D processed textile preforms are sometimes directly formed to be used in liquid molding processes [40-43].

#### **5.2.3.1 Braided Preforms**

In its original form, braiding is a textile process in which yarn bundles are intertwined to form a continuous flat or tubular fabric. Tubular fabrics are much more common in the composites industry. These fabrics are formed by laying down yarns onto a mandrel that moves through the center of the machine's cross section at a predetermined rate [42-45]. With the feed and braiding rate varied, the yarn can be deposited at angles ranging from 10 to 85 relative to the mandrel direction. Circular braiding is ideal to develop a preform for high aspect-ratio parts like snow skis, tennis racquets and helicopter blades. Some recent studies showed that complex cross-sectional preforms can be produced in 3-D with multi-layer interlock braider.

### **5.2.3.2 Knitted Preforms**

Knitting is a process through which looped yarns known as stitches are interconnected to form a fabric. The two simplest techniques for developing a knitted fabric are warp and weft knitting. Warp knitting involves the conversion of the yarn into a looped structure in the warp or machine direction, while weft knitting forms loops across the width of the fabric or the weft direction. Although not a mechanically efficient use of fiber reinforcement, knitting offers a versatile way of manufacturing complex 3-D shapes. The primary types of directionally reinforced knitted fabrics include multi-axial warp knits (MWK) and weft-inserted warp knits (WIWK) [45].

### **5.2.3.3 Stitched Preforms**

Stitching is the simplest way of fabricating 3-D textile preforms. Stitching is primarily used as a means of adding through-the-thickness reinforcement to a 2-D reinforced preform. Because of their layered nature, 2-D reinforced preforms have low damage tolerance, especially in-plane fiber damage that results in a degradation of the in-plane mechanical properties of the composite. Thus, stitching can be locally used to decrease the extent of delamination and increase the through-the-thickness properties of the composites. The types of the stitch geometry are the chain, lock and tricot stitches. Stitching has benefits that it can be added locally, as required in areas of high interlaminar stresses, and it is possible to vary the pattern, type, or material that is stitched to arrive at the desired performance level. The application of stitching dry fiber preforms is for structural components of aircraft.

### **5.2.3.4 Woven Preforms**

The process of weaving is suited for the production of flat panels and woven fabrics have been used for a number of years in two-dimensional laminated composites. However, these composites exhibited poor impact resistance, delamination strength. Furthermore, typical 2-D weaves only possess fibers in the zero (warp) and ninety (weft) degree directions, reducing in-plane shear properties. To improve the impact and interlaminar properties, some extensions have been made to the basic form of weaving

so that it is possible to produce 3-D reinforced woven composites. The two main techniques to develop these preforms are angle interlock and orthogonal weaving.

#### **5.2.4.5 Use of Preforming Binder**

To consolidate well fiber preform systems, the key is to supply brief compaction. The use of binders helps in obtaining net-shaped thermoformable preforms with desired fiber volume fraction, which are critical for the fabrication of high performance parts. The binder also needs to provide adhesion between the fiber layers so that preform keeps its integrity.

The two most common types of binder are low melting thermoplastics and uncatalyzed thermosets. Binder is either applied by spraying over the fabrics with solvent in which it dissolved or applied by spreading in powder form onto fiber mats with sifter apparatus. Spraying the reinforcement fabrics with a dissolved binder is better than use of powder in that the binder is present in small pockets on the fiber bundles rather than being evenly spread across the fibers [1-5]. Powders are uniformly applied per specified concentrations and melted to one surface of a continuous roll of fabrics. This binder-coated roll of fabrics can be thought of as a very low resin content prepreg that can be made into ply kits using conventional cutting equipment. Preforms can be easily made by stacking plies as desired and forming to near net part geometry using inexpensive tooling with moderate heat and pressure [39-44]. The ideal binder should be able to eliminate any springback of the fiber layers after preforming in order to control the preform dimension. The presence of the fiber however affect the permeability and fiber wetting of the preform in the mold filling process, as well as mechanical properties of the final part. To optimize the preform consolidation process and therefore to tailor the final properties, amount of the preforming binder used is vital.





### 5.3 Fiber Preform Compressibility

Preform compressibility is a critical issue that ties processing and performance together. Figure 5.2 shows the influence of preform compression on the microstructure with examples [45]. The compaction of the preform flattens the yarn bundles reduces the pores and gaps among the fibers and yarns. This results in fiber re-orientation, nesting and interlayer packing [40-46]. It was revealed that final composite properties and microstructure depend to a great extent on compaction of the fiber preform to the designed thickness [42-44]. Furthermore, the degree of the compaction of the fiber preform has some significant effect on the permeability of the reinforcement during resin infusion and mutually fiber volume fraction and porosity. As the compressive force increases, the thickness of the fabric preform decreases, while the fiber volume fraction increases [43]. However, when the force reaches the limiting value, the fabric can not be further compressed [6,44-46].

In liquid molding processes, resin infiltration time is also critical parameter. It was shown that both the degree of the compaction and the type of the preform affect the resin infiltration time. The experimental results also demonstrated that for a given preform, the infiltration time increases with the fiber volume fraction, due to decrease in preform permeability. Thus, an understanding of the relations between compression force, fiber volume fraction and preform thickness reduction per layer is essential to optimize and to control the properties of the final part during processing [39-45].

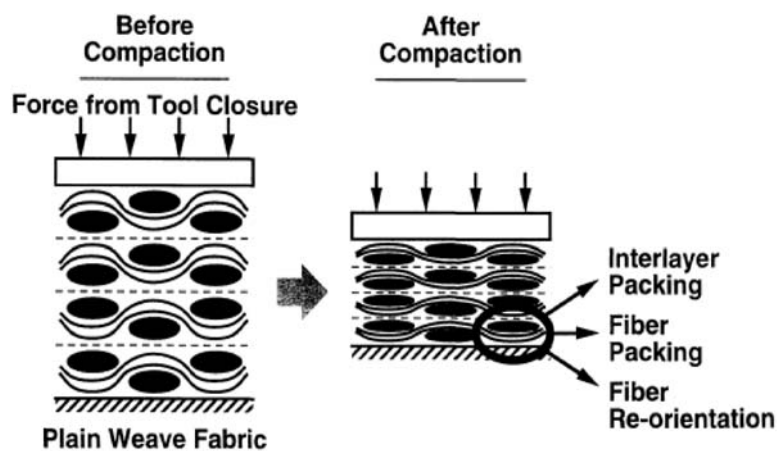


**Figure 5.1** An example to preformed woven glass fabric structure

A number of theoretical models have been developed to briefly define the compressibility of preform and its effects on the final properties of the composite part. Chen *et al.* [6] reported results of compaction experiments for three types of preforms, continuous strand mats, plain woven fabrics and unidirectional knitted materials. They observed that for a given compaction pressure and preform material, the thickness per layer for a stack of 10 or 25 layers of preform is less than the thickness of a single layer. They concluded that the reason for that is the nesting of the hills and valleys of adjacent layers. They also found that nesting was existing at the beginning of compression for plain woven and unidirectional materials, but not for continuous strand mat.

Chou and co-workers investigated [40] the single layer deformation. They examined the behaviour of woven-fabric preforms under compaction predicting the compressive behaviour of the yarns, and the relationship among composite fiber volume fraction, applied compressive force and preform thickness reduction. Since only a single layer woven fabric preform was modeled, nesting was not considered. They attributed the linear relation between the preform thickness and the applied pressure to the bending deformation of the preform. From this point of view, they proposed a 3D model of the unit cell of plain weave fibrous preform with certain assumptions to predict the compressive behaviour of the yarns. They found that maximum thickness reduction for a single layer is about 36 % of the original thickness. In their next study [46], they modeled the nesting and the elastic deformation for multi-layer plain weave fibrous preforms. Analytical expressions for non-nesting case and the maximum nesting case were developed. They finally concluded that thickness reduction and fiber volume fraction from nesting is caused only by geometric shifts between adjacent yarns.

Rohatgi and Lee [7] investigated the physical phenomena and mechanisms of fiber consolidation and springback in the preforming process. For this purpose, certain layers of woven graphite fiber mats with binders were placed between two plates which were then bent into a U shape and then held in that position with a clamp. Binders are applied over the fiber mats with two different methods; solvent and powder. After allowing the samples to cool down to room temperature, the preform was taken out of the bending device and springback angles were measured. Springback was then obtained by taking the difference in the laminate thickness with and without applied pressure. At any particular concentration level, increasing the degree of cure resulted in decreasing the springback level. Another interesting result was that application of 3 wt. % of the binder by powdering did not show the same decrease in the springback

compared to when it was applied by spraying. This is because solvent coating makes the filament become stiffer, causing an increase in the elastic modulus of fibers. As binder concentration increases, springback decreases. However, spring back is kept constant, while the binder concentration is about 9 wt.%. This results show that preform compression is dominated by binder amount up to a limited peak.

R.A Saunders *et all* [42] studied the mechanical compression behaviour of fiber plain woven fabric preforms by performing a series of mechanical tests on dry and resin impregnated cloths and from microstructural studies of the specimens cured under compression. The experiments included investigations of the effects of applied pressure, speed of compression and cloth orientation on the fiber volume fraction of the compressed assembly. They found that compression of dry cloths followed a power law relationship between pressure and volume fraction with a power law index ( $P=cV_f^n$ ) of 10 for assemblies of 5,10 and 20 dry cloths. They also conclude that the compression of resin impregnated woven cloths could be considered as a combination of modes of deformation composed of nesting of cloths, deformation of the yarn waveform and deformation of the yarn cross-section.

In their next study [44], they examined the compression of fiber reinforcements during the processing of polymer composites. They used plain weave, twill, satin and non-crimped, stitch bonded fabric. The assemblies were dry or impregnated with three alternative resins; high viscosity polyester, low viscosity polyester and equal low viscosity of epoxy. They found that for wet fabrics, the viscous resin pressure component was dominant at high compression rates (1 mm/min). Especially for the assemblies of the wet plain weave compression curves moved to higher pressures and lower fiber fraction as the compressive force was increased. At low compression speeds (0.05 mm/min), the curve was more like that for dry cloth. The type of fabric has an influence on compression. Assemblies of twill weave were the most difficult to compress in both dry and wet state.

There are really a few studies on the compression properties of the preforms consolidated with thermoplastic binders. The structure of the fiber preform is an important factor in determining the load required for a given change in fiber volume fraction. Batch and Macoska [47] presented the viscosity characteristics of a typical thermoplastic binder in conjunction with the consolidation behavior of continuous strand random glass mats. They performed a study on the same kind of mat at two different temperatures below the binder melting point were seen to be nearly identical;

above the melting point, higher temperatures led to progressively greater compaction. This indicates that the effect of temperature on preform consolidation is tied to binder flow characteristics.

The extent of binder redistribution is also governed by the binder viscosity characteristics. The binder viscosity is a strong function of strain rate and temperature. Knight and co-workers [2] made a study on consolidation and relaxation behavior of continuous strand random glass mats with thermoplastic binders. Attention has been given to the effect of preforming conditions on binder flow around the fibers, and on the rearrangement of fiber tows making up the preform. They have revealed with SEM that degree of fiber tow flattening which is closely related with binder distribution around the fiber tows is the greatest at high temperatures and at low closing speeds. They also indicated that flattening of the fiber tows introduces small gaps along which binder flows mainly due to squeezing force and capillary forces which play a minor role here. The redistribution of binder then facilitates further compaction. The shear thinning viscosity of the binder leads to a reduction in pressure at the highest closing speed, even though the pressure increased with increasing closing speed. Another interesting point is that the lower binder viscosity at higher temperatures allows more rearrangement of the tows, resulting in no loss of binder from the stacks.

#### **5.4 Effect Of Preforming Binder On The Mechanical Properties Of Composite Parts**

Employment of thermoplastic binders may enable to achieve simultaneously high strength and high toughness for composites when an appropriate matrix resin is chosen. From this point of view, the interactions between the binder, matrix resin and the fiber sizing are important to design high performance composites. In other words, chemical compatibility and reactivity of the binder with matrix resin, binder viscosity, wettability of the reinforced fabric, and binder solubility in the matrix resin may all together significantly effect the mechanical properties of the final composite part. The effect of fiber/matrix interfacial adhesion is also important. If the interface bond is too weak, the material will not bear the loads in shear and compression. However, much stronger interface bond would not allow effective crack diverting , and this would make a brittle composite. A weaker interfacial bond results in intraply splitting and interply delamination and allow the composite to absorb a greater amount of impact energy,

provided that the splitting and delamination are the dominant failure modes. However, when fiber tensile or compressive failure modes become significant, then a weaker interfacial bond may cause a weak flexural strength of the laminate. So, the binder may have ability to tailor the properties of interlaminar region by altering the adhesion mechanism via design. Therefore, toughening composites with thermoplastic binders has received considerable attention by researches in recent years and much effort has been undertaken to understand the effect of interlayer with binder on the final composite properties [48].

Theoretical and experimental studies revealed that there are several advantages of using thermoplastic binders, such that larger increases in impact resistance is obtained. As the concentration of binder typically ranges from 4 to 7 percent by weight of the fibers, preforms with binders can be thought of as very low resin content prepregs [8]. Also, since the density of the fibers is nearly twice that of the resin, the binder constitutes about 8 to 14 percent of the total resin in the molded part. Therefore, in order to obtain a homogeneous matrix and to avoid any deterioration in the mechanical properties, chemical compatibility of the binder with the matrix resin is taken carefully into consideration. It was also found that incomplete dissolution of the binder in the reactive matrix resin can adversely effect the mechanical properties due to residual micro stresses at the binder/resin interface. During the preforming stage, the binder powder melts, coagulates and flows along the capillaries blocking the pore spaces within the preform. Since mold filling is governed primarily by macro flow, blocking of the larger gaps by binder powder results in lower permeability or increased flow resistance. Blocking of the interstitial pore spaces can however effect the fiber wetting by lowering the capillary pressure.

Broutman and Agarwall [49] reported a theoretical study which showed that a lower modulus interphase can maximize the composite strain energy release rate without significantly reducing the composite modulus. By increasing the interface modulus, the composite strength is predicted to increase until the interphase modulus reaches a value of about 69 MPa. At this point, the strain energy absorbed; a measure of impact strength reaches a maximum and the composite strength remains constant. It was found that a good combination of tensile strength and toughness may be expected with an interlayer modulus about one-tenth that of the matrix. Using binders, it may be possible to increase the interlaminar toughness and tensile strength, consequently bigger interlayer modulus. This can be certainly a reason of employment of binder.

James C. Seferis [3] and co-workers compared the mechanical properties of the composite laminates fabricated by VARTM through epoxy resin. Composite laminates with (4, 7 and 11 %wt.) epoxy binder and without binder (control) with the addition of elastomeric particles in 50% wt. were prepared. They found the same trend of increasing laminate thickness with increasing binder concentration. In the case of fabric with the highest binder loading, a thick resin and particle rich interlayer between the fabric plies was present. Mode I and mode II interlaminar fracture toughness tests were employed to investigate the effect of binder content on the fracture properties of the cured laminates. The  $G_{IC}$  values were found to increase greatly as the binder percentage in weight increases. The  $G_{IIC}$  values followed a similar trend as  $G_{IC}$  except less incremental gain in toughness with increasing binder content. The three point bend test characterized overall flexural properties of the laminates. These values are criterion to consider as the toughness increase might have caused a decline in the elastic properties to be observed for toughening modifications.

They also observed that the glass transition temperatures were decreased slightly by the addition of the binder. In the next research of James C. Seferis and co-workers [50], the effects of tackifier application and composition were investigated by modifying spray and powder epoxy tackifier with polyamide 6 elastomeric particles in the ratio (67 % wt. epoxy and 33 %wt. elastomeric particles). They found that spray tackifier provided 30% improvements in mode II interlaminar fracture toughness, and slight increases in the interlaminar shear strength without reducing the thermal properties. The powder tackifier showed a slightly lower performance increase due to less homogeneous laminate structure. They also showed that mode I interlaminar fracture toughness was not improved using modified tackifier. In addition, for both techniques, compressive strength of the composites was found to be unaffected by the introduction of modified tackifier.

M. Tanoglu et al. [51] investigated the effects of thermoplastic preforming binder on the properties of S2-glass fabric reinforced epoxy composites. They showed that the highest peel resistance of the preforms was obtained from the preforms that have full coverage of the binder on the glass fabric. Further addition of the binder does not affect the peel strength. They found that about 2.6 wt.% of the polyester binder reduces the mode I interlaminar fracture toughness and interlaminar shear strength of the composites about 60 and 25 %, respectively, by reducing the glass temperature of the matrix polymer about 6°C.

S. Ziaee and co-workers [5] studied the effects of a polyester and an epoxy – amine binder on properties of E-glass fabric reinforced vinyl ester composites. They showed that the use of 3 wt. % of the polyester binder in S2-glass/epoxy-amine system that is made of epoxy-amine compatible sizing lowers the mode I interlaminar fracture toughness values by 61 %. On the other hand, it was found that for the S2-glass/vinyl-ester systems that is made of vinyl ester in-compatible sizing, the reduction of mode I interlaminar fracture toughness values were only limited to about 10 % due to the presence of the 3 wt. % of polyester binder. These results clearly demonstrates the interactions between the fiber sizing and matrix resin, and also the effect of the non-reactive binder on the adhesion within the composites.

## Chapter 6

### EXPERIMENTAL

#### 6.1 Materials

E-glass fabrics and polyester resin (Neoxil 266) were purchased from Cam-Elyaf Corp., Turkey. The accelerator and initiator for this resin are Cobalt Naphthenate (CoNAP) and Methyl Ethyl Ketone Peroxide (MEKP), respectively. Figure 6.1 gives the gelation time as a function of CoNAP weight percentage with 1.5 and 2 MEKP weight percentages. For the fabrication of the composites, the concentration of MEKP and CoNAP was selected as 1.5 and 0.28 wt.% of the resin to complete the infusion of the composite part prior to gelation of the resin.

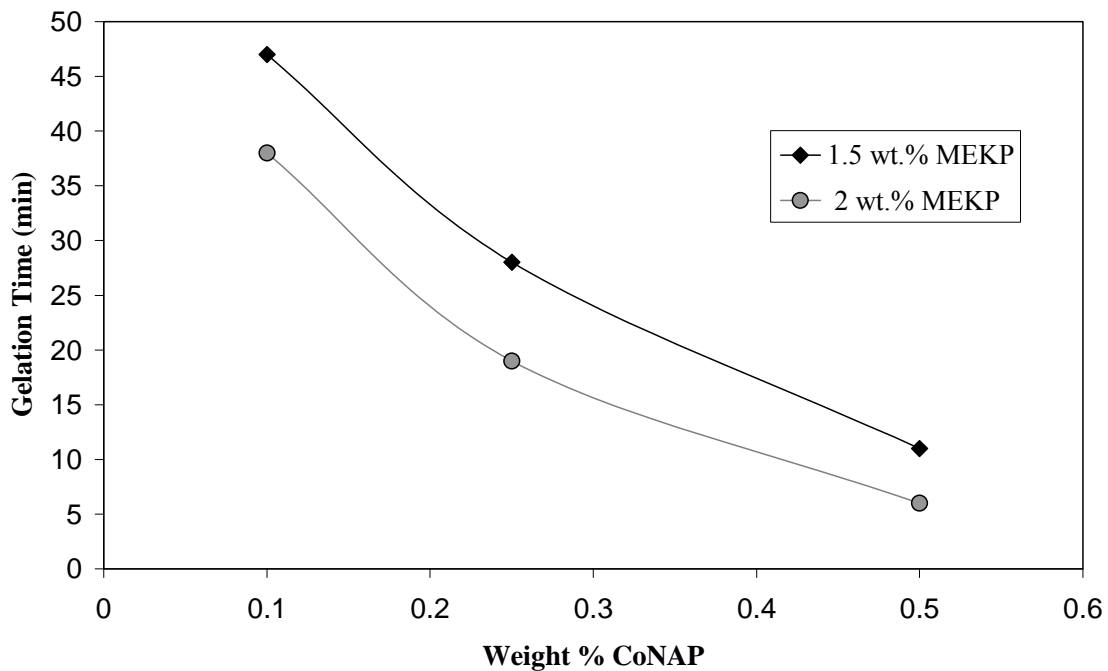


**Figure 6.1** Gelation time as function of CoNAP and MEKP weight percentage



The preforming binder used for this work was ATLAC 363E, a bisphenol -(A) based polyester with fumarate groups in the backbone. Figure 6.2 illustrates the chemical structure of the binder.

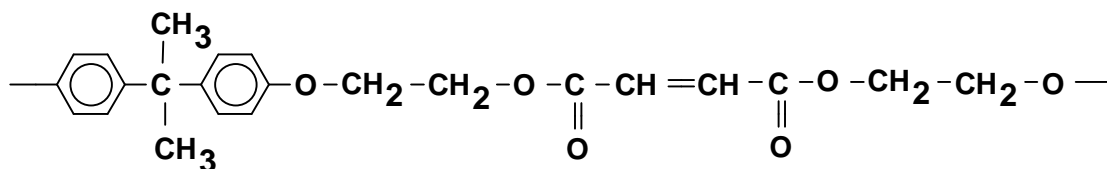


**Figure 6.2** Chemical structure of the binder

### 6.1.1 Binder Characterization

The DSC profile of the binder is shown in Figure 6.3. The melting point ( $T_m$ ) of the binder was measured as 60 °C.

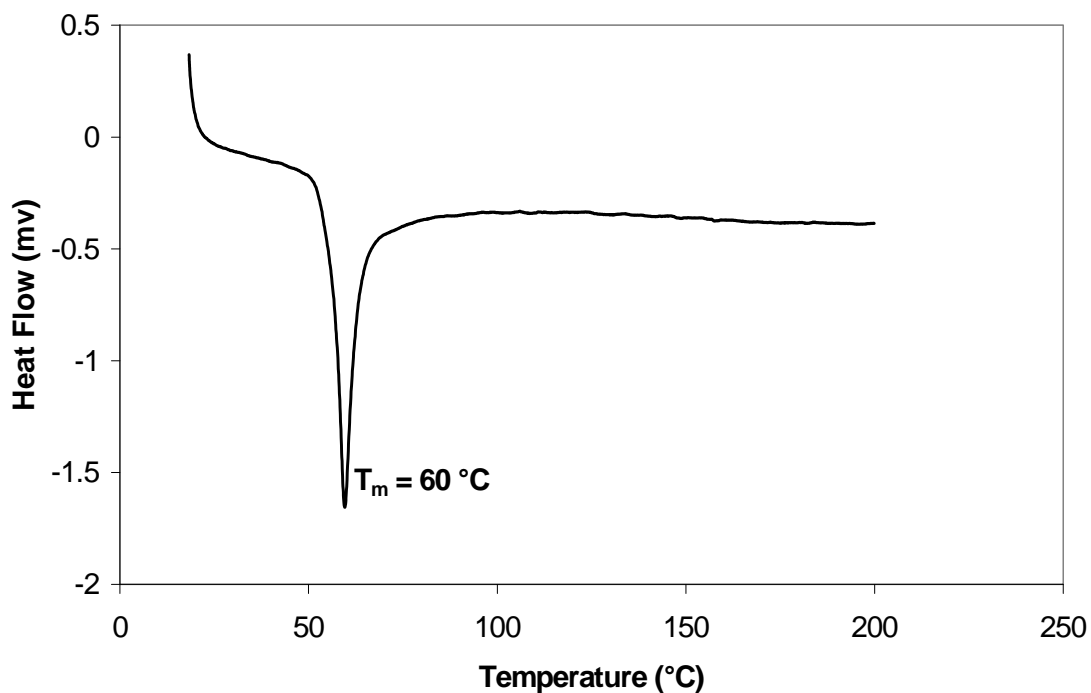


**Figure 6.3** DSC profile of the ATLAC 363E polyester preforming binder.

## 6.2 Preform consolidation and characterization of peel strength and compaction behaviour

### 6.2.1 Preform Consolidation

Glass preforms were consolidated from the glass fabrics by uniformly spreading of 3 and 6 wt. % of the thermoplastic polyester binder onto the glass mats. Figure 6.4 illustrates the schematic of preform consolidation process. The desired number of binder-coated plies were stacked together under compression pressure of 2.7 KPa for about 45 minutes at a temperature of 80°C, which is above the  $T_m$  of the binder. After completion of the preform consolidation, the preforms were allowed to cool down to room temperature under the pressure. Upon re-solidification of the binder, well-consolidated preform was obtained.

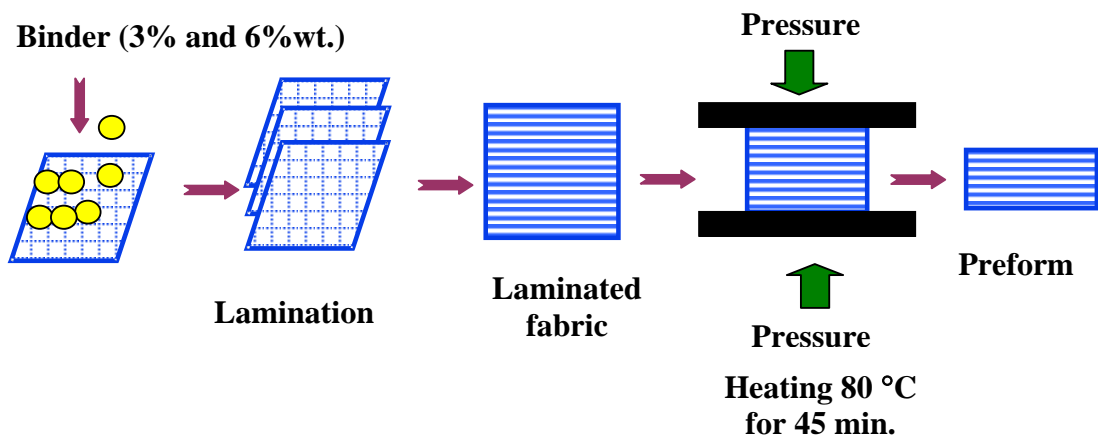


**Figure 6.4** Schematic of preform consolidation

### 6.2.2 Preform T- Peel Test

The peel strength (bonding strength) of the preforms was determined with T-peel test method, ASTM D-1876-95 [52]. The peel test was also used to optimize the concentration of the binder on the glass fabric. For the peel test, two layers of the glass fabrics 200 mm in length and 25 mm in width were bonded with 3, 6, 9 and 12 wt.% of the binder. Kapton<sup>®</sup> film was inserted in the midplane of one end of the specimen such that an initial unbond peel length of 500 mm was obtained. Specimens were tested using

Shimadzu universal test machine with a cross head speed of 5 mm/min. Figure 6.5 shows the peel test configuration. Average peel strength ( $\delta_{peel}$ ) of the samples was calculated based on the average peeling load ( $F_{peel}$ ) per unit width of the bond line ( $w$ ) as;

$$\delta_{peel} = \frac{F_{peel}}{w} \quad (6.1)$$



**Figure 6.5** T-Peel test configuration.

### **6.2.3 Preform Compaction Test**

To determine the compaction of the preforms composed of eight fabric layers with various binder contents (0, 3, 6 and 9 wt.%) were consolidated based on the procedure described in the previous section. Preform compaction experiments were performed using the universal testing machine at a cross head speed of 1 mm/min by applying a compressive load normal to the plane of the fabric preforms placed between compression plates and measuring the distance between the steel circular plates. The average thickness per layer as function of compaction pressure was calculated for each preform based on the initial thickness, stroke value, applied force and the area of the preforms.

### 6.3 Composite Fabrication

Composite laminates were manufactured using VARTM technique. Figure 6.6 shows the schematic of the VARTM process. In this technique, preforms were placed on a flat tool, which is coated with a releasing agent in order to ease the peeling of the tool. Preforms were infused with the reacting resin under vacuum. The applied pressure to the VARTM system by the vacuum pump was about 10 Pa. After completion of the resin infusion and curing of the part, the panels were demolded and subjected to post-curing at 110°C for 2 hours. Ballistic test panels (dimensions and areal densities (mass per unit area) as shown in Table 6.1) were fabricated with various binder concentrations. In addition to ballistic panels, composites laminates were fabricated for Short Beam Shear (SBS) (10 mm thick), Double Cantilever Beam (DCB) (2.5 mm thick), flexural test (4 mm thick) and compression test (10 mm thick). For DCB specimens, a 65 mm long Kapton® film was inserted in the midplane of the composites as a crack initiator for interlaminar fracture toughness test specimens.

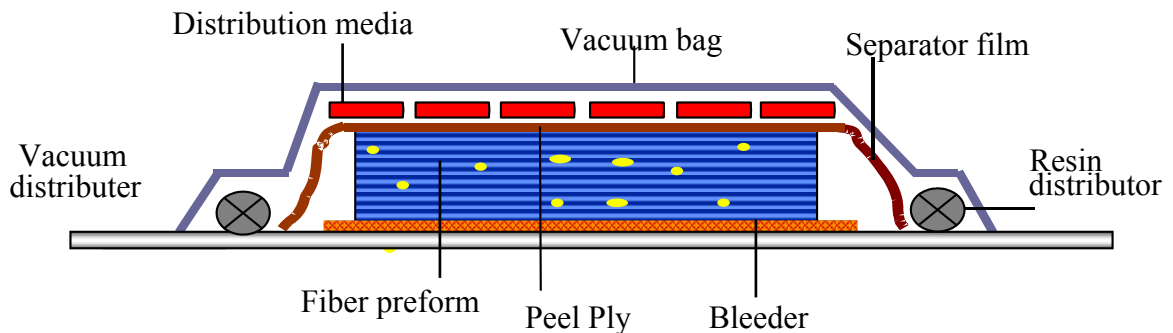


**Figure 6.6** Schematic of VARTM process

**Table 6.1** Composite panels fabricated with VARTM process for ballistic testing.

Ballistic panel	Binder Concentration (wt. %)	Thickness (mm)	Area (cm <sup>2</sup> )	Mass (gr)	Areal Density (gr/cm <sup>2</sup> )
1	6	13.788	750.7	1859	2.47
2	6	13.697	731.7	1851	2.52
3	3	12.642	731.7	1720	2.35
4	3	12.637	753.5	1766	2.34
5	0	11.852	737.1	1671	2.26
6	0	11.854	734.4	1667	2.26

#### 6.4 Matrix Burn-Out Test

The burn-out test method was used to determine the fiber volume fraction of the E glass/polyester panels. In this method, a small sample of composite is burned off in a high temperature oven. The ash is rinsed from the remaining fiber (using acetone or alcohol) and the fiber is dried and weighed. The volume of the fiber is calculated by dividing the mass of the fiber by the density of the fiber material. The average fiber volume fraction obtained from the samples of the composite panels were calculated to be 45.3 ( $\pm 1.05$ ), 50.1 ( $\pm 1.2$ ) and 46.6 ( $\pm 0.55$ ) % for the composites with 0, 3 and 6 % wt. binder, respectively.

#### 6.5 Ballistic Testing

Ballistic testing on composite panels has been conducted using 1.1-gr. fragment-simulating projectiles (FSPs) in accordance to NATO Standart 2920 [53]. Figure 6.7 shows the schematic of the ballistic test set up. The specimen was mounted on a hollow frame and the striking and residual velocity of the projectiles were measured using a chronograph. The specimens were examined after the test and the size of the impact damage zone was measured at the front and the back surfaces of the panels by visual inspections and non-destructive C-scan testing. The failure modes occurred in the composites during the ballistic loading and the effect of binder on the damage modes were evaluated using microscopic techniques.

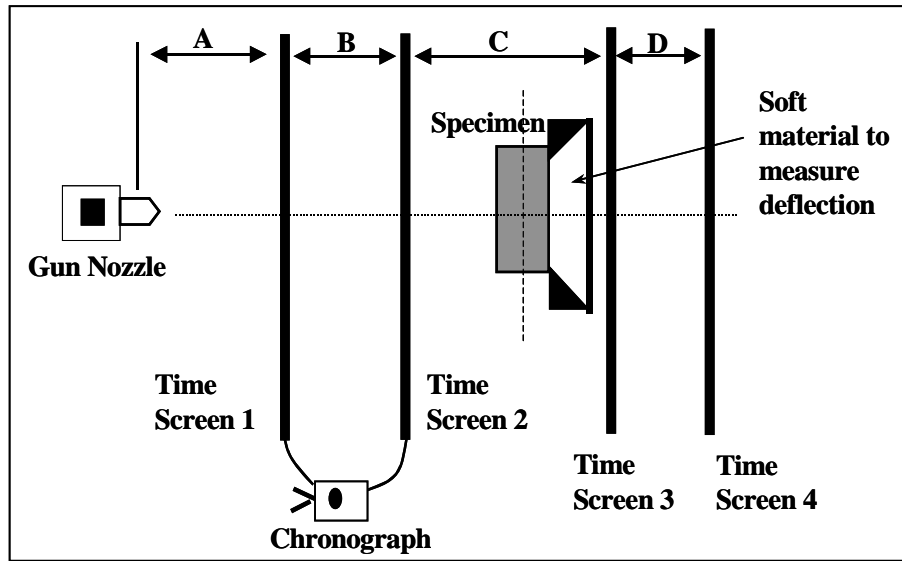


**Figure 6.7** Schematic of the ballistic set up.

### 6.5.1 Ultrasonic C-scan Test

The ballistically damaged composite panels were non-destructively tested to determine the extent of delamination resulting from the projectile impact. All of the targets were C-scanned using 1 MHz scan frequency. Transducer with a nozzle diameter of 6.3 mm was used in order to record delamination through the thickness of the panel. After the panels were C-scanned, the images were imported into an image processing software package to determine the fraction of damage in the panel. Percent delamination was determined through edge enhancements of the images.

## 6.6 Mechanical Property Characterization

### 6.6.1 Flexural Tests

The flexural test technique, ASTM D 790-92 [54] was used to determine the effects of binder on the flexural strength and modulus of the composites. For this purpose, test specimens with 25 mm in width and 80 mm in length were sectioned from the VARTM processed panels using a diamond saw. Figure 6.8 is the photo showing the flexural test specimen under load. Specimens were tested in 3-point bending configuration with a span to thickness ratio of 32. At least five specimens from

composites with 3 and 6 wt. % of binder and without binder were tested using the universal test machine at a cross-head speed of 5 mm/min. Force vs. deflection at the center of the beam was recorded. The flexural strength, ( $S$ ), values were calculated using the following equation [54].

$$S = \frac{3PL}{2bd^2} \left[ 1 + 6 \left( \frac{D}{L} \right)^2 - 4 \left( \frac{d}{L} \right) \left( \frac{D}{L} \right) \right] \quad (6.2)$$

where  $P$  is the applied load at the deflection point,  $L$  is the span length,  $d$  and  $b$  are the thickness and the width of the specimen, respectively and  $D$  is the deflection. The flexural modulus values,  $E_b$ , were calculated using the following equation [54].

$$E_b = \frac{L^3 m}{4bd^3} \quad (6.3)$$

where  $m$  is the slope of the tangent to the initial straight line portion of the load-deflection curve.



**Figure 6.8** Photo of flexural test specimen under load.

### 6.6.2 Short Beam Shear Test (SBS)

The apparent interlaminar shear strength of the composite specimens with (3 and 6 wt. %) and without binder were determined by a short beam shear test according to ASTM method D2344-84 [55]. The SBS specimens 80 mm in length and 10 mm in width were sectioned from the composite laminates. The length to thickness ratio and span to thickness ratio were kept constant at 7 and 5, respectively. Figure 6.9 shows the SBS test specimen and test configuration. The cross-head speed was remained constant at 5 mm/min. Ten specimens from each set were tested using universal test machine and load at break was recorded. The apparent shear strength ( $\tau_{max}$ ) was calculated using the following equation [55].

$$\tau_{max} = \frac{0.75P_B}{bd} \quad (6.4)$$

where  $P$  is the breaking load,  $b$  and  $d$  are the width of the specimens and thickness of the specimen, respectively.



**Figure 6.9** Photo showing the SBS specimen under load and SBS configuration.

### 6.6.3 Double Cantilever Beam Test (DCB)

To investigate the effect of the binder on the fracture toughness of the interlaminar region, mode I interlaminar fracture toughness of the composites with various binder contents (0, 3 and 6 wt. %) was measured using double cantilever beam (DCB) method, ASTM D-5528 94a [56]. The DCB specimens were sectioned from



composite laminates with the length of 280 mm and width of 25 mm. The loading hinges were bonded at the insert side of the specimens such that the initial delamination length,  $a_o$  was about 65 mm. Figure 6.10 shows the DCB test specimen under load and DCB test configuration. The specimen were tested at cross-head speed of 1.5 mm/min. The crack length and cross-head displacement were measured using the universal test machine. Mode I fracture toughness,  $G_{Ic}$ , values were calculated based on modified beam theory equation [56].

$$G_{Ic} = \frac{3P_c\delta_c}{2b(a + |\Delta|)} \quad (6.5)$$

where  $P_c$  is the applied load and  $\delta_c$  is load displacement at the crack initiation. The terms  $a$ ,  $b$  and  $\Delta$  are the delamination length, specimen width, and a correction factor determined experimentally from beam compliance and delamination length, respectively. Fracture surface of DCB specimens were observed using scanning electron microscopy to investigate the failure modes of Mode I fracture specimens.

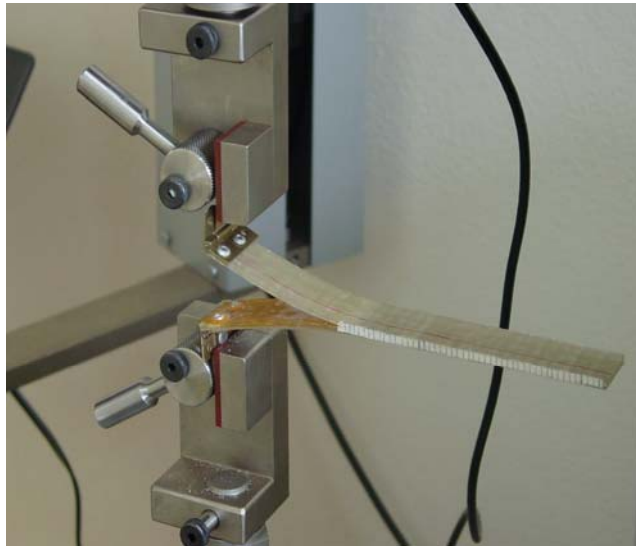


**Figure 6.10** DCB test specimen under load and configuration of DCB test set up.

#### **6.6.4 Compression Tests**

Compression test method according to ASTM D 695-M [57] was utilized to measure the ply-lay up and in-plane compressive strength, modulus and strain to failure values of the composite panels with various binder content (3 and 6 wt.%) and without binder. For this purpose, compression test specimens in the length of 10 mm and the width of 13 mm were sectioned from larger VARTM processed composite panels. Compression tests along the ply-lay up and in-plane loading directions were performed using the universal test machine at a cross-speed of 1.3 mm/min. At least 10 specimens for each set were tested and force vs. stroke data were recorded. The compressive stress values were obtained by dividing load values with cross-sectional area of the specimens. The strain was estimated by dividing machine compliance corrected (for machine compliance) stroke values with the initial specimen thickness. The yield stress values were estimated considering the transition value from linear to non-linear behavior. The modulus values were estimated from the slope of the stress-strain graphs.

#### **6.7 Microstructure Characterization**

Scanning electron and optical microscopy on the fracture surfaces of tested specimens were performed in order to investigate the failure modes and degree of adhesion. For this purpose, Phillips™ SEM and Nikon™ optical microscope were used. Moreover, ballistic damage modes in the panels were observed for composites with various binder contents. For that reason, ballistic test panels were cross-sectioned through the impacted zones using diamond saw. The cross sections of the panels were prepared metallographically. In addition, the microstructural characterization techniques were also used to follow the extent of the binder dissolution within the reacting resin system.

#### **6.8 Determining the interaction between thermoplastic binder and the matrix resin**

Interactions between the thermoplastic binder and the thermosetting polyester matrix were followed to determine the effects of the addition of the preforming binder on the compressive strength and modulus of the polyester matrix and also the extent of the binder dissolution in the reacting resin. For this purpose, 6.5 and 12.85 wt.% of

binders (corresponding to 3 and 6 wt.% of the binder in the matrix for 50 % fiber volume fraction) were added into the reacting system to replicate the blend of the binder and matrix materials. The blend samples were then subjected to post-curing at 110°C for 2 h upon room temperature curing. The compressive mechanical properties of the cured model matrix materials were evaluated using the same procedure described in compression testing of the composites. The model specimens were also loaded under flexure and the fractured surfaces of these materials were examined under SEM to assess the level of binder dissolution within the resin. Moreover, the viscosity measurements using a Brookfield LV+ rheometer with spindles no. 2 and 3 were performed for neat resin and resin/binder blends. The blends (6.5 and 12.85 wt.% of binder added neat resin) were stirred at room temperature and the viscosity values were recorded in the certain time intervals. In addition, blends with similar compositions were stirred at about 65°C (above  $T_m$  of the binder) for 3 h to simulate the extensive dissolution of the binder by melting.

## Chapter 7

### RESULTS AND DISCUSSION

In this chapter, the results of investigation of the effect of the thermoplastic binder on the mechanical properties and ballistic performance of E-glass fiber reinforced polyester composites are presented. As mentioned in Chapter 6, composites with fiber preforms containing various amount of the binder (0, 3 and 6 wt.%) were prepared. The peel strength of the preform and the effect of the binder content on peel resistance were evaluated. Moreover, woven fabric reinforced polymer composite were fabricated using VARTM technique. The flexural, compressive and interlaminar shear strength, and mode I interlaminar fracture toughness of the composites made with consolidated preforms were also evaluated. Ballistic performance of the composite panels was also determined and the effects of various binder content on the damage extend were evaluated. Moreover, the interaction between the thermoplastic binder and the matrix resin was also followed.

#### 7.1 Peel Strength of Glass Preforms

Peel strength between glass plies was measured to determine the adhesion between the glass fabric and the binder. For this purpose, 3, 6, 9 and 12 wt.% of binder content were used to bond two E-glass plies together. Figure 7.1 shows the average peel strength of the specimens as function of binder concentration. As seen in the figure, there is a linear increase of the peel strength with the binder content and the highest peel resistance was obtained from preforms with about 9 wt. % of the binder. The linear increase of the peel strength is due to the improved adhesion by increased surface coverage of the fabric by the binder. At about 9 wt.%, the binder covers almost full surface and the further increase in the amount of the binder does not affect the preform peel strength.

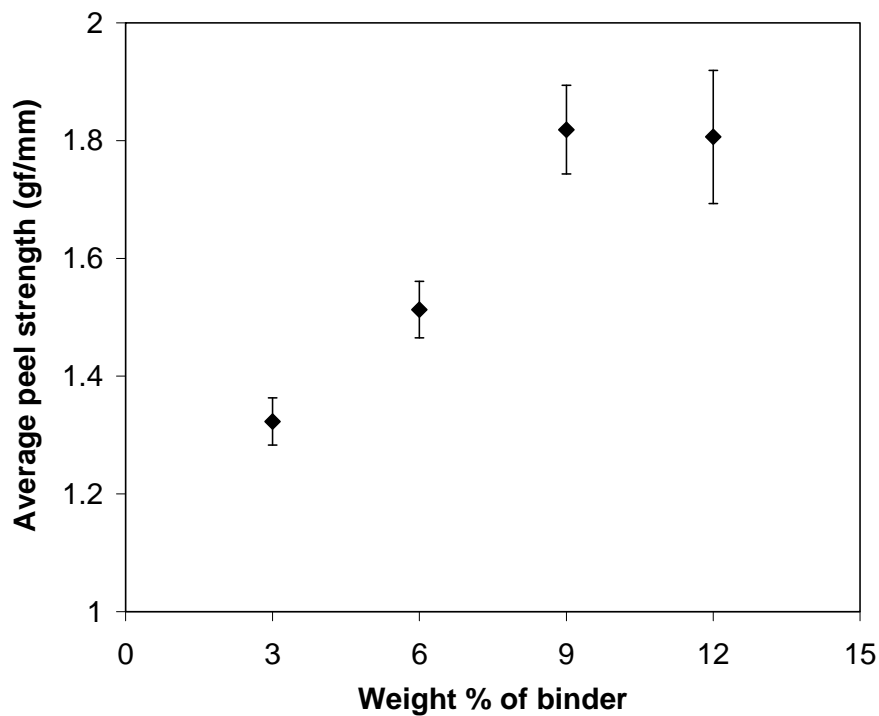


**Figure 7.1** Average peel strength as a function of binder weight percentage

## 7.2 Effects of Binder on Preform Compaction

Preform compression tests were performed to evaluate the effect of binder on the preform compaction under compressive loads. This is a particular interest to be considered especially in VARTM processes. Note that the preforms with binder were prepared by stacking the fabric layers together by the application of heat and pressure as described in Section 6.2.1. The fabric layers were compacted together upon the solidification of the binder particles between the fabrics. Therefore, the thickness of preforms obtained after the thermal consolidation process is much lower as compared to the layered fabrics without any addition of the binder. Fig.7.2 shows the average thickness per layer for the preforms composed of eight fabric layers with 0, 3, 6 and 9 wt.% of the binder as function of pressure applied by the mechanical test device. The thickness reduction with applied pressure was minimum for the preform with 9 wt.% of binder, while the reduction was maximum for the preforms without binder. In addition, the minimum thickness per layer with applied pressure was achieved with 3 wt.% of

binder. Therefore, the highest fiber volume fraction may be expected from this materials under pressure applied during VARTM and RTM processing.

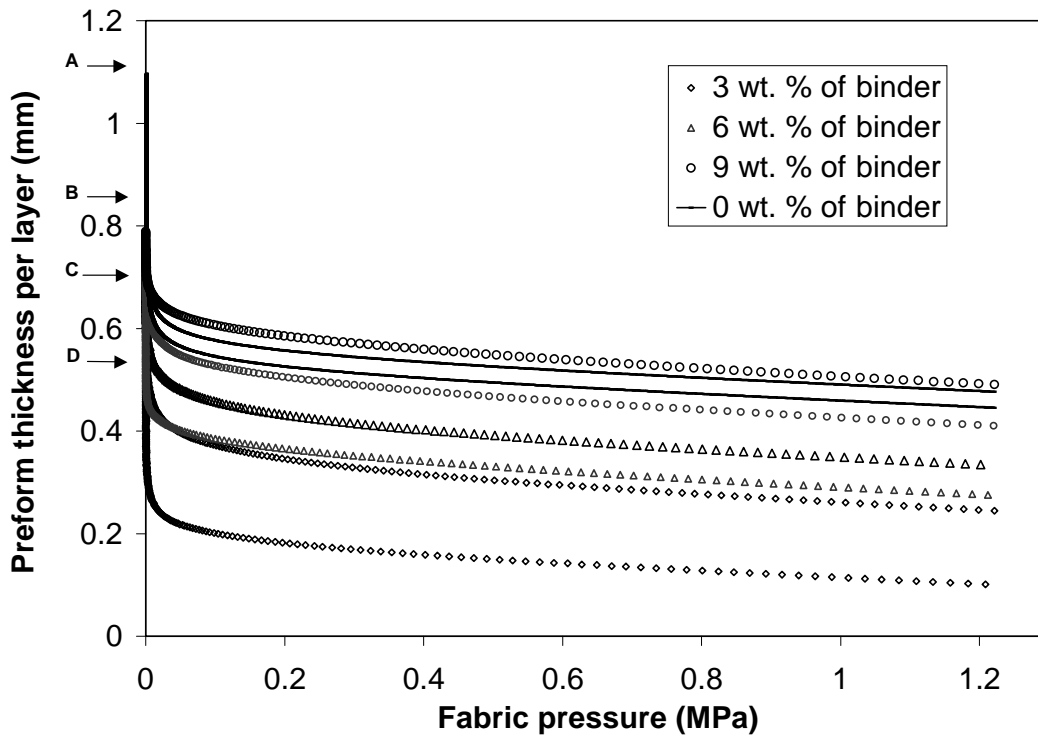


**Figure 7.2** Preform thickness per layer as a function of fabric pressure for various binder content (A, B,C,D refer to initial thickness of the preforms with 0, 9, 6 and 3 wt.% of binder, respectively)

As mentioned previously, the volume fraction values of the composites with 3 wt.% of binder were measured to be only about 5% greater than those with 0 and 6 wt.% of the binder. However, the extend of binder dissolution within the reacting resin is a critical issue on the compaction behavior of the preforms. If the binder dissolves partially during the infusion of the reacting resin prior to the gelation, the binder may be detached from the fiber surface and its compaction effect may be lost and the thickness of the preforms may increase during VARTM. In other words, depending on the type of interaction between the binder and resin, the initial low thickness of the preforms with binder may arise during infusion and reaches to the value of the fabric stacks without the binder [58]. For the material systems studied in this work, partial dissolution of the binder within the resin was observed as mentioned in detail in Section 7.5. So, the detachment of the binder from the fabric surface due to binder dissolution and increase

of the preform thickness may be expected. In this case, the thickness of the composite panels with and without binder approaches to each other. The thickness of the composite panels fabricated with and without binder were close to each other (about 13.65, 12.60 and 11.90 for 6, 3 and 0 wt.% binder for the stacks of 25 fabric layers) indicating the thickness increase of the preforms with binder due to dissolution.

Moreover, the peel strength of the E-glass preforms made with polyester powders are in the range of 1.5-1.9 gf/mm as reported in section 7.1. It was also reported [59] that the peel strength may decrease by up to 80% due to the exposure of the binder to the resin components. Also, note that the vacuum pressures applied during VARTM technique, in general, are relatively low (typically in the range of 0.01-10 KPa) to keep the initial preform thickness. However, the thickness may be kept constant and higher volume fractions may be obtained with binder in the case of application of RTM technique that applies much greater pressures on the fabric layers. These results reveal that application of the binder has some considerable effect on the degree of preform compaction especially prior to resin infusion.

### **7.3 Effect of the Binder on the Ballistic Performance of the Composites**

Figure 7.3 is the photographs showing front and back surface of the ballistic panels with 3 wt. % and without binder. The type of the impact damage seen in the figure are typical for all panels and the projectile was stopped by the targets with only partial penetration without perforation in all cases. The energy level impacted to the targets caused sufficient damage to the laminate without completely penetrating the target. This allowed for comparison of the ballistically impacted panels based on extent of damage given at relatively equivalent input energies. In this way, the effects of material variations such as binder concentration introduced along the interlaminar region were assessed. The size of the damage and the percentage of delamination areas on the front and back surface of the panels, measured by visual inspection are given in Table 7.1.

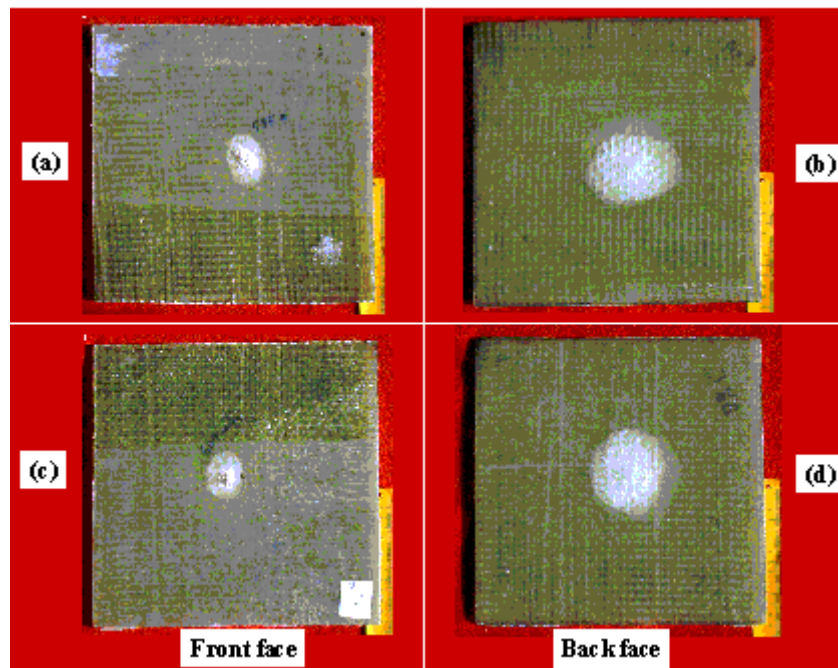


**Figure 7.3** Ballistic impact damage on front and back face of VARTM processed composite panels. (a and b – panels without binder), (c and d – panels with 3 wt. % binder)

**Table 7.1** Ballistic delamination data for the composite panels with various concentration of preforming binder

No:	Binder Conc. (wt.%)	Velocity (m/s)	Front Damage Diameter (cm)	Back Damage Diameter (cm)	Delamination % (Front Face)	Delamination % (Back Face)
1	6	614	4.25	7.5	1.88	5.88
2	6	578	3.5	5.5	1.31	3.24
3	3	609	4.25	8	1.93	6.86
4	3	579	4	6.75	1.66	4.74
5	0	585	4.5	9	2.15	8.62
6	0	575	4	8	1.71	6.84



A relatively less damage is observed at the front where projectile entered, as compared to the back surface. Delamination type damage is visible and the delaminated area through the thickness increases, forming a conical damage zone. The results showed that as the concentration of the binder increases in the composites, a relatively less damage, i.e.; less delamination, was occurred within the composites.

In order to approve the same findings analytically, the ballistically impacted panels were also subjected to non-destructive ultrasonic C-scan testing. Figure 7.4 shows the C-scan images of the ballistic panels. Area of the delaminated damage zone on the ballistic panels is calculated through an image analysis program and the fraction of the damage was found to be 1010, 875, 790 mm<sup>2</sup> for 0, 3, 6 wt.% of binder, respectively. This revealed that the damage area was reduced by 21.7 % by the use of 6 wt.% of the binder. All these results may indicate a relatively higher energy absorbing capability of the composites with preforming binder material due to tailored properties. The damage modes occurred during ballistic impact within the panels were observed by optical microscopy on the cross sections of impact-damaged zones.

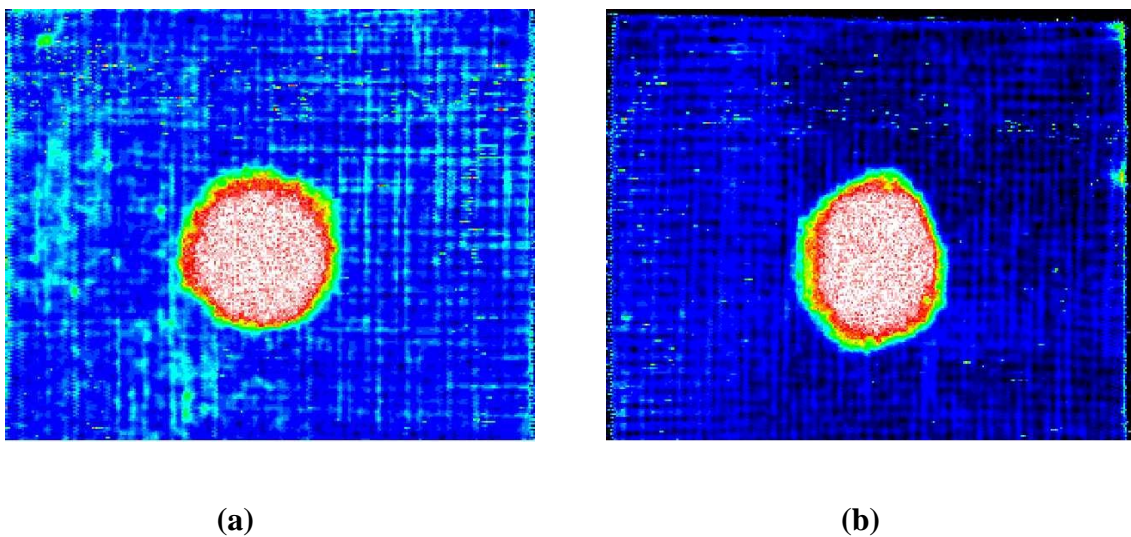


**Figure 7.4** C-scan imaging of the ballistically impacted panels ( a and b refer to 0 and 6 wt.% of the binder, respectively)

Figure 7.5 shows the cross sections of the impacted panels with various binder concentrations. Observations revealed that microscopic (fiber fracture, etc.) and macroscopic (delamination, matrix cracking, etc.) type damage mechanisms occurred in composites due to ballistic impact. Delamination type damage is visible and the delaminated area through the thickness increases, forming a conical damage zone. Figure 7.6 illustrates the delamination and intra-bundle cracking type failure modes occurred within the impact-damaged zone. Interfacial debonding of the fibers and the matrix caused by intra-bundle cracking within the tows is also apparent. A cavity at the projectile contact region was formed due to the penetration. Around cavity region, significant amount of fiber and matrix failure besides folding and buckling of fibers is apparent as illustrated in Figure 7.7.

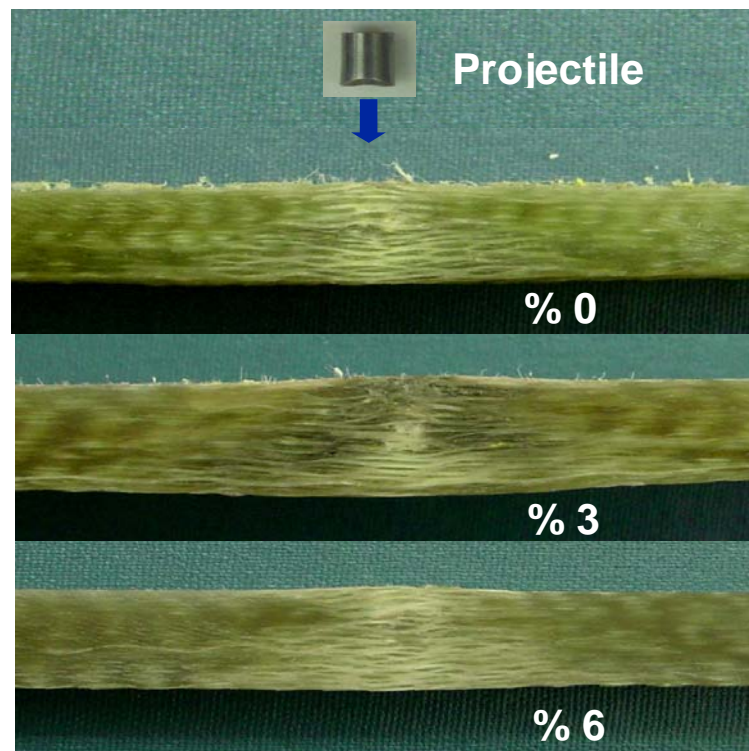


**Figure 7.5** Cross sections of the impacted panels with various binder concentrations.



**Figure 7.6** Optical micrographs from the cross-section of E-glass/polyester composite panel (with 3 wt. % of the binder) after ballistic impact showing delamination and intra-bundle cracking.



**Figure 7.7** Optical micrographs from the cross-section of E-glass/polyester composite panel (with 3 wt. % of the binder) after ballistic impact showing fiber fracture and buckling around cavity region.

## 7.4 Effect of the binder on the mechanical properties of the composites

### 7.4.1 Flexural properties

Figure 7.8 shows the plot of flexural strength and modulus values as a function of binder weight percentage. The results show that the presence of the polyester binder along the interlaminar region affects the flexural properties of the composites. The strength is reduced about 20 % due to the presence of 6 wt. % of the binder. On the other hand, the modulus values are increased about 40 % due to the same amount of the binder material. The flexural strength values decrease and the modulus values increase as the binder content increases. So, the decrease of the strength values with binder may be related to the reduced bonding between the binder and matrix. The increase of the modulus values with binder content may be associated with the mechanical interlocking of the fabrics and increased fiber volume fraction as a result of using preformed fabrics.

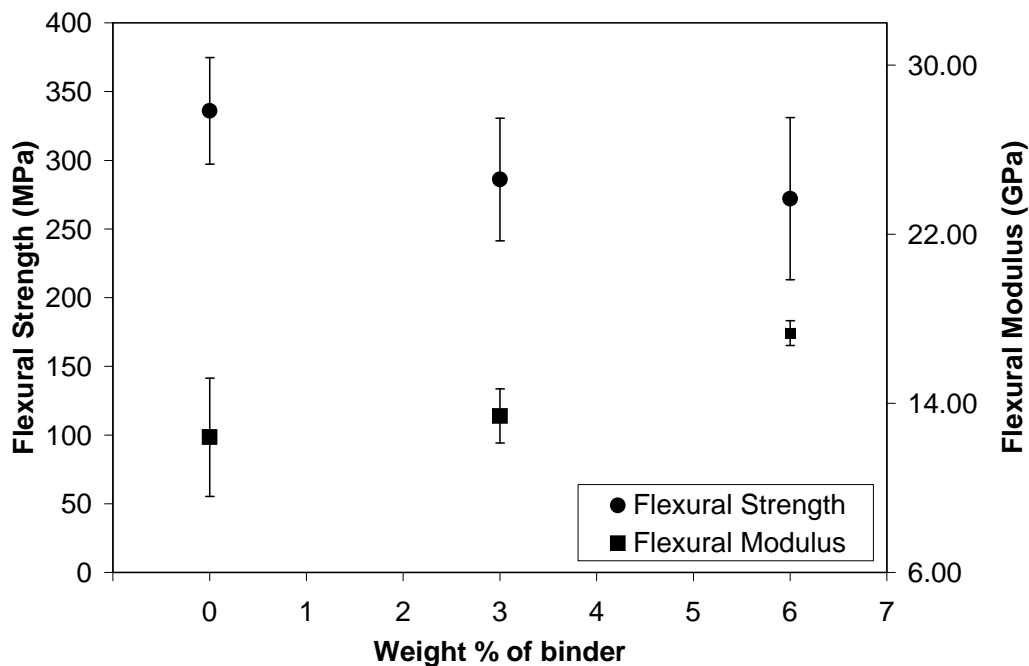


**Figure 7.8** Flexural strength and modulus of the E-glass/polyester composites as a function of binder weight percentage.

### 7.4.2 Interlaminar Shear Strength

Figure 7.9 shows the apparent average interlaminar shear strength versus binder weight percentage values. The results indicate that presence of the binder has no

significant effect on the interlaminar shear strength of E-glass / polyester system. The reason for this may be the fact that the matrix properties is dominant for shear properties. In other words, the shear strength is primarily dependent on matrix properties.

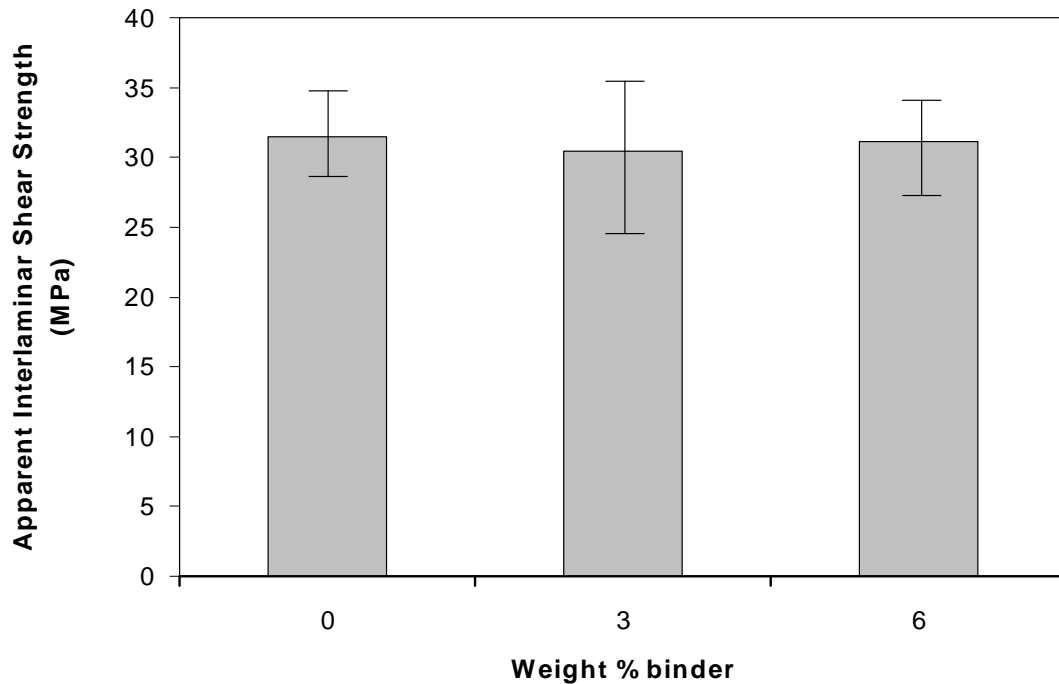


**Figure 7.9** Apparent interlaminar shear strength of the composites as a function of binder weight percentage.

### 7.4.3 Interlaminar Fracture Toughness

Mode I interlaminar fracture toughness of the composite specimens with (3, 6 wt. %) and without binder was measured using DCB specimens. Figure 7.10 shows the  $G_{Ic}$  values as a function of delamination crack extension ( $\Delta a$ ). It was found that composites with binder and without binder exhibit rising delamination curve behaviour. The average  $G_{Ic}$  values increase with crack extension and reach a constant propagation value. The average crack propagation values are 720, 432 and 235  $J/m^2$  for 0, 3 and 6 wt. % of the binder, respectively. The results reveal that the fracture toughness of the composites is reduced about 67 % due to the presence of the 6 wt. % polyester binder. The chemical compatibility of the sizing on the fibers with the polyester resin is a critical issue on the mechanical properties of the composites. In the present study, glass

fibers used are compatible with the matrix resin system and the polyester binder does not react with the polyester matrix resin and the sizing of the fiber. Therefore, the binder acts as a barrier between the fiber sizing and the matrix resin and the chemical bonding between the fiber and the matrix resin is inhibited as the binder content increases. So, the decrease of the flexural strength and  $G_{Ic}$  values with the presence of the binder may be associated with the reduced bonding between the fiber and matrix.

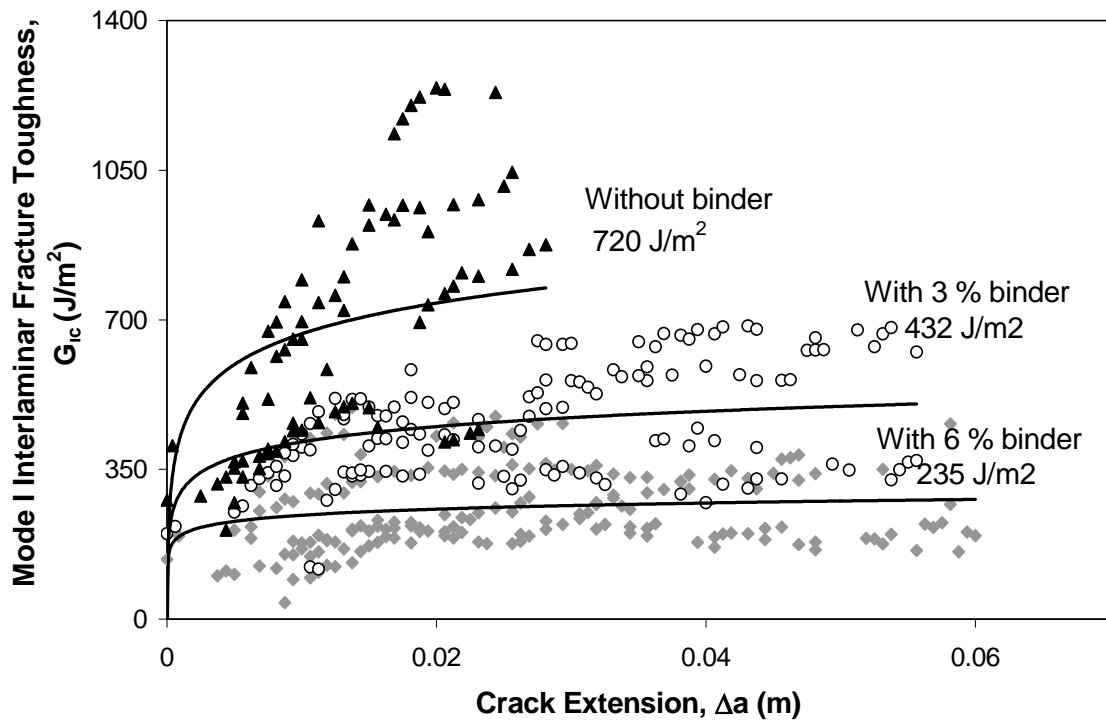


**Figure 7.10** Mode I interlaminar fracture toughness as a function of crack extension

The effect of the fiber sizing compatibility with the resin was studied previously [2,5]. It was reported that the use of 3 wt. % of the polyester binder in S2-glass/SC-15 epoxy-amine system that is made of epoxy-amine compatible sizing lowered the  $G_{Ic}$  values by 61%. On the other hand, it was found that for the S2-glass/vinyl-ester systems made of vinyl ester in-compatible sizing, the reduction of  $G_{Ic}$  values were only limited to about 10 % due to the presence of the 3 wt. % of polyester binder. In the present study, use of 3 wt. % of polyester binder reduces the  $G_{Ic}$  values of the E-glass/polyester composites made of polyester compatible sizing by 40 %. These results clearly demonstrates the interactions between the fiber sizing and matrix resin, and also the effect of the non-reactive binder on the adhesion within the composites.

Fracture surface morphologies of the DCB specimens were examined using SEM to evaluate the failure mechanisms at the interlaminar region. The results show some considerable differences in the morphology of the mode I fracture surfaces for composites with and without binder. As presented in Figure 7.11-a and 7.11-b, composite with binder exhibit great amount of interfacial failure in which the fibers are stripped of matrix material easily. This may also indicate hindered bonding between sized fiber and matrix resin due to coverage of the fiber surfaces by the binder. However, the composites without binder show some considerable amount of matrix failure besides interfacial failure and some fiber pull-out. Because of the better adhesion between the fiber and matrix, matrix deformation is also dominant rather than interfacial failure.

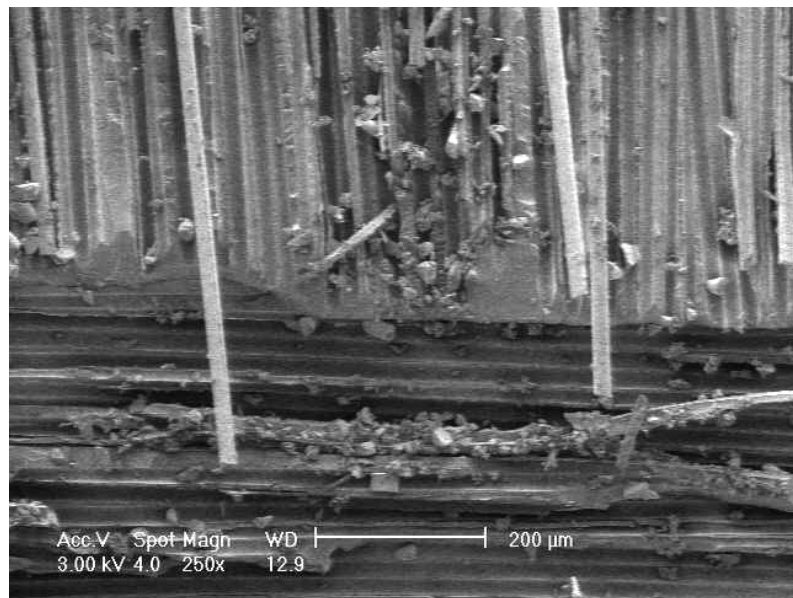


**Figure 7.11a** SEM fracture surface micrographs of DCB specimen with 0 % wt. of binder

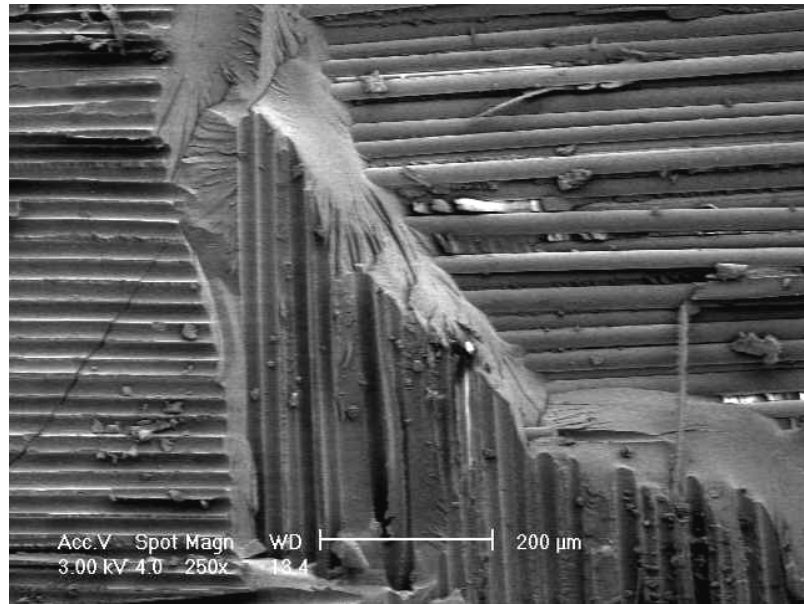


**Figure 7.11b** SEM fracture surface micrographs of DCB specimen with 3% wt. of binder.

#### **7.4.4 Compression Properties of the Composites**

Figures 7.12 to 14 show compressive stress vs. strain responses of E-glass/polyester composites loaded along the ply-lay up direction with 0, 3 and 6 wt. % of binder, respectively. Also, compressive stress vs. strain responses of the same type of composites loaded along the in-plane direction are given in Figures 7.15 to 17. For loading in ply-lay up direction, stress-strain response of the composites is almost linear up to the maximum stress level at which damage initiates. There is a sudden drop of the stress after the maximum stress at which failure occurs and the material loses its integrity. The stress-strain behaviour of the composites loaded along the in-plane direction is less linear as compared to those for ply-lay up direction. In some cases, stress increase up to a maximum level without the indication of any damage occurrence. On the other hand, some of the specimens show kinks at stresses prior to maximum level at which the initial cracking occur. The stresses drops suddenly after the maximum stress at which macroscopic damage may occur and material losses its integrity.



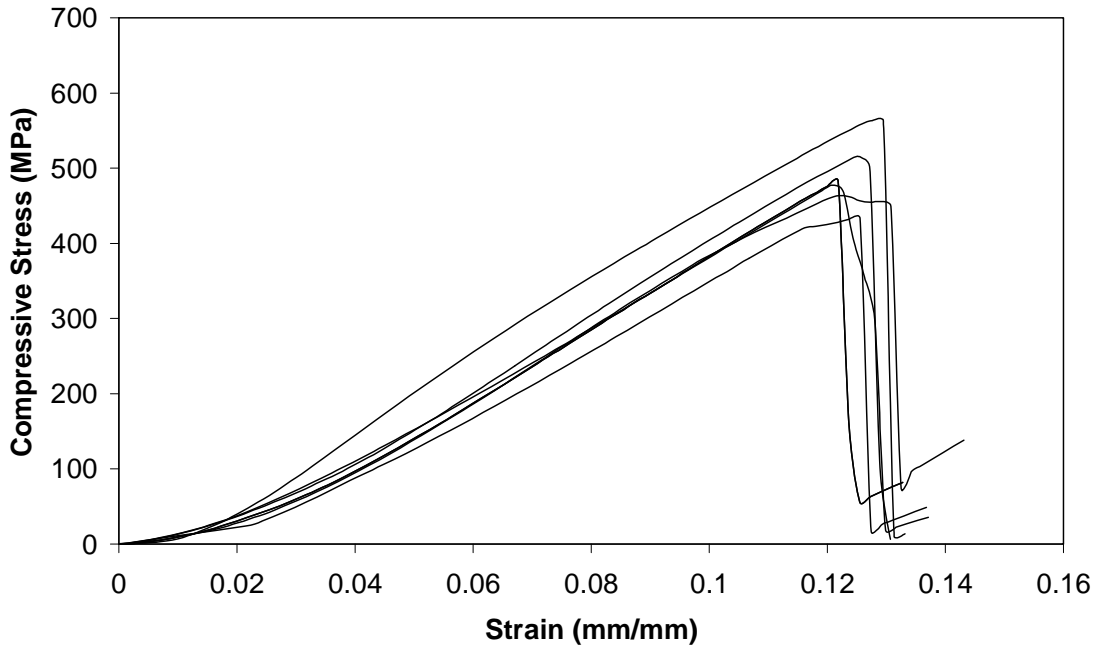


**Figure 7.12** Ply lay up direction compressive stress vs. strain response of composites without binder.

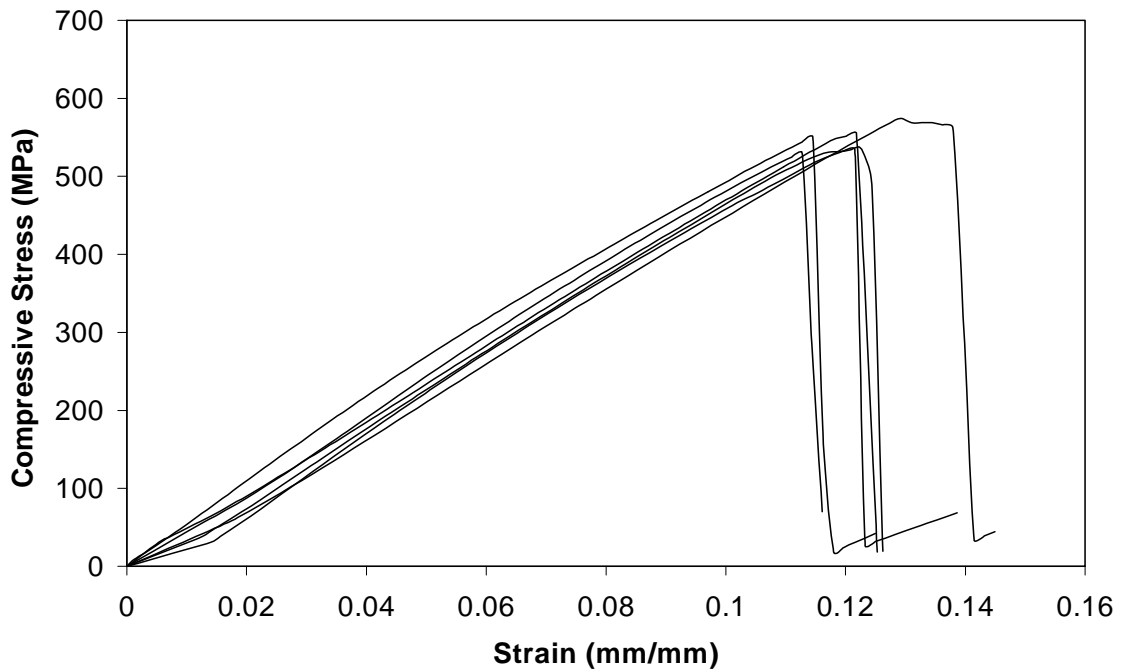


**Figure 7.13** Ply-lay up direction compressive stress vs. strain response of composites with 3 wt.% of binder.

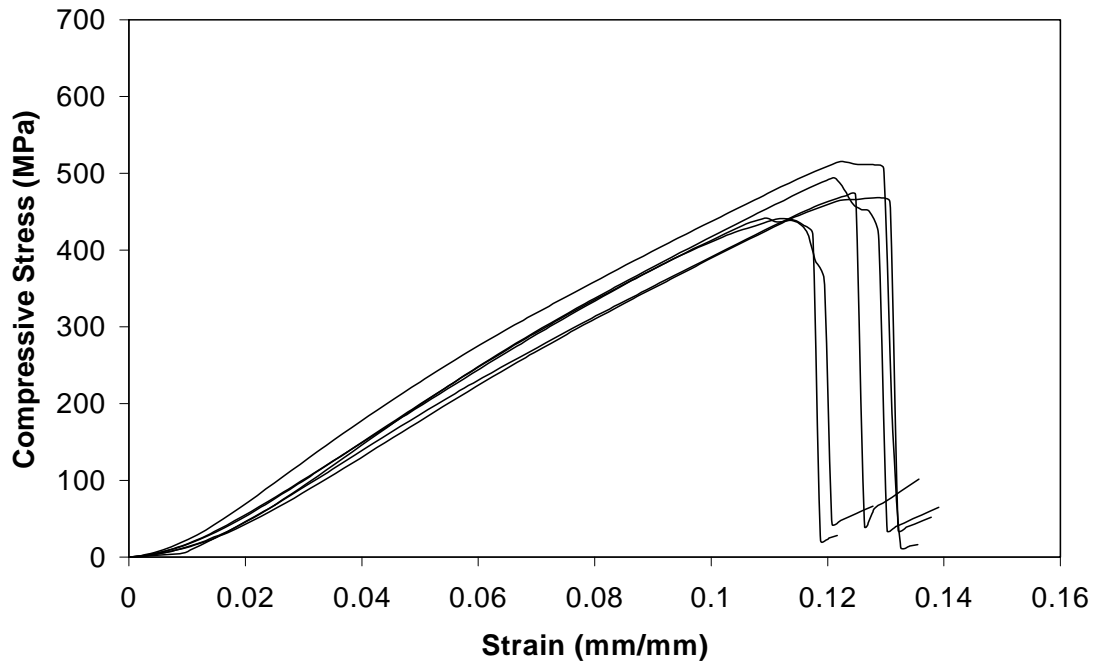


**Figure 7.14** Ply-lay up direction compressive stress vs. strain response of composites with 6 wt.% of binder.

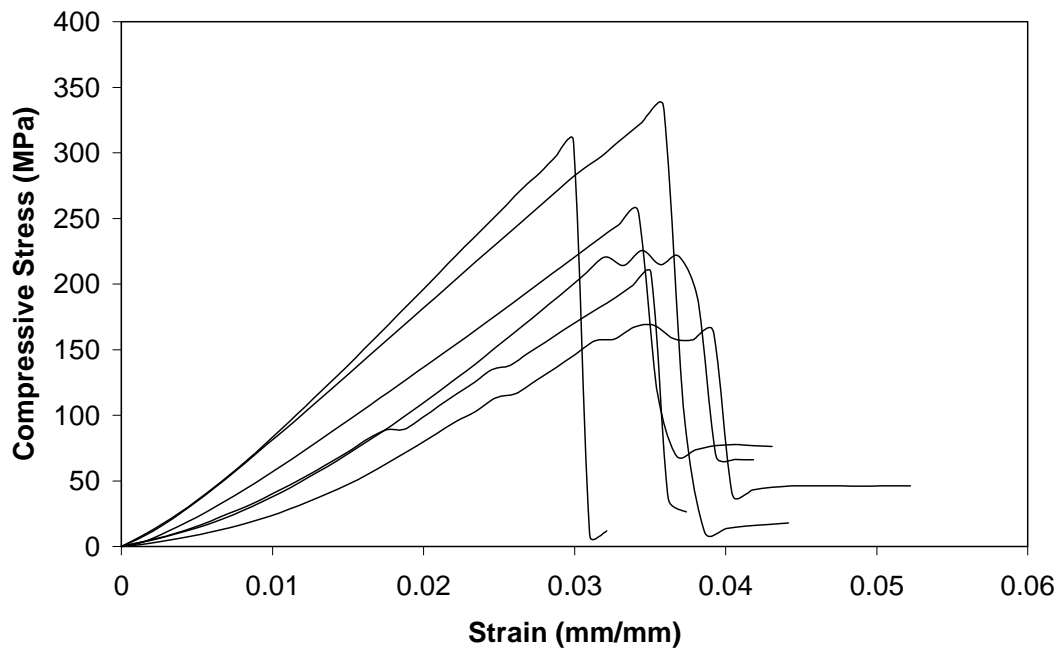


**Figure 7.15** Ply-lay up direction compressive stress vs. strain response of composites without binder.

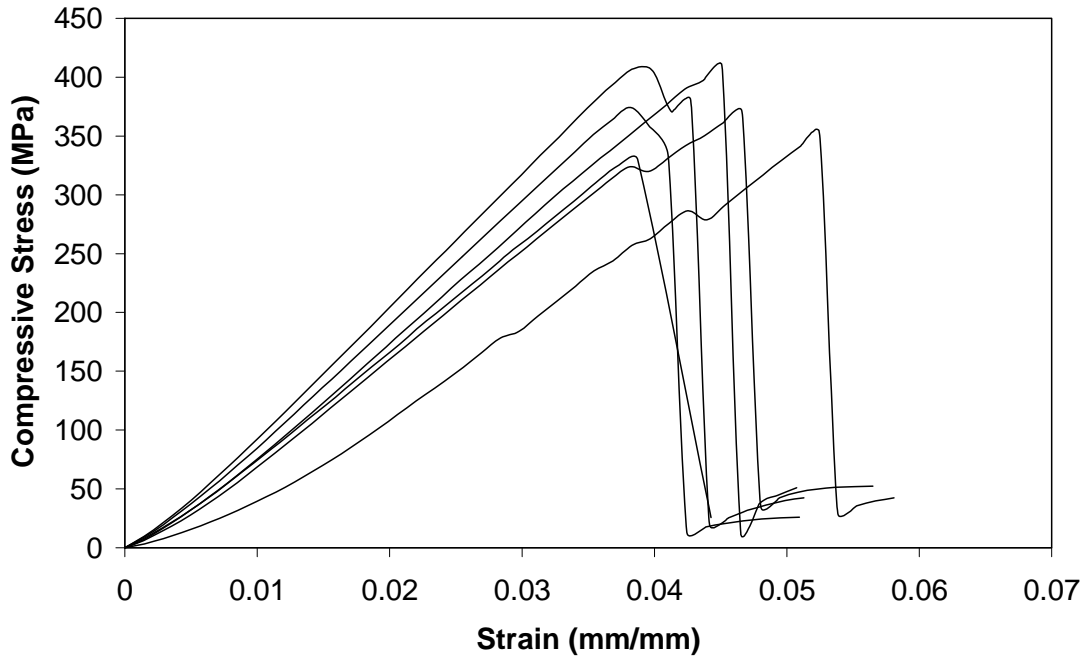


**Figure 7.16** In-plane direction compressive stress vs. strain response of composites with 3 wt.% of binder.

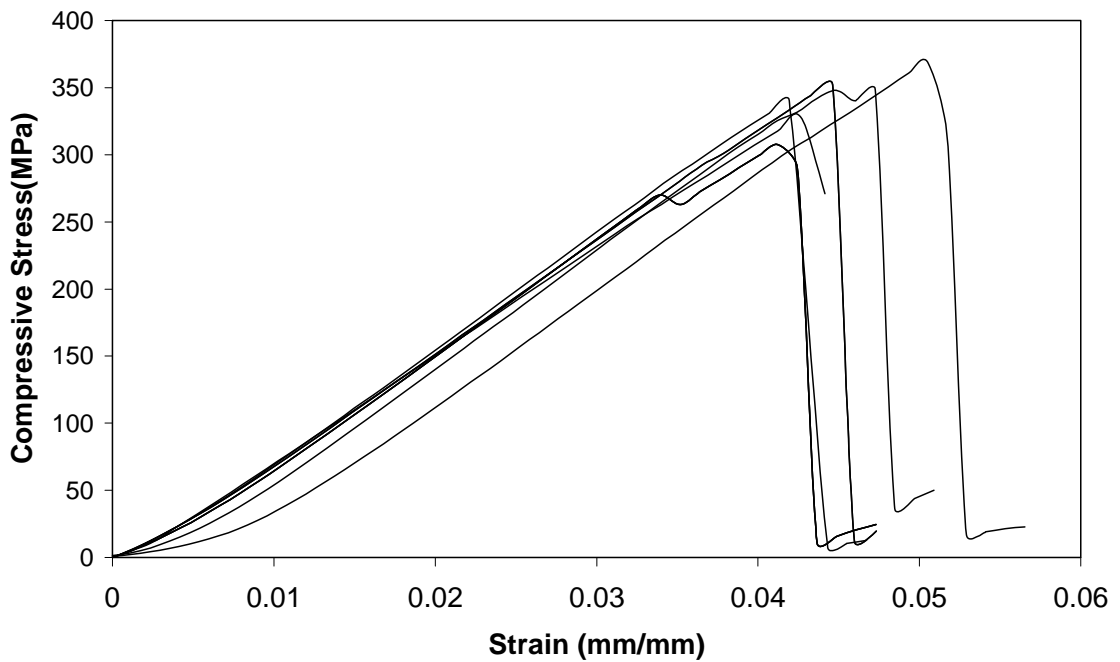


**Figure 7.17** In plane direction compressive stress vs. strain response of the composites with 6 wt.% of binder

Figure 7.18 shows the strain at maximum stress values as a function of binder weight percentage for both the ply-lay up and in-plane loading directions. It was found that the average strain values at maximum stress for the specimens loaded along in-plane and ply-lay up directions are about 0.035 and 0.110, respectively. The results also indicate that the strain values along ply-lay up direction are almost constant with the presence of the binder, while those along in-plane loading direction seem to be slightly increased by introduction of binder. This may be due to the fact that the fracture in in-plane loading is considerably related to the interlaminar properties that are modified by the plastic binder.

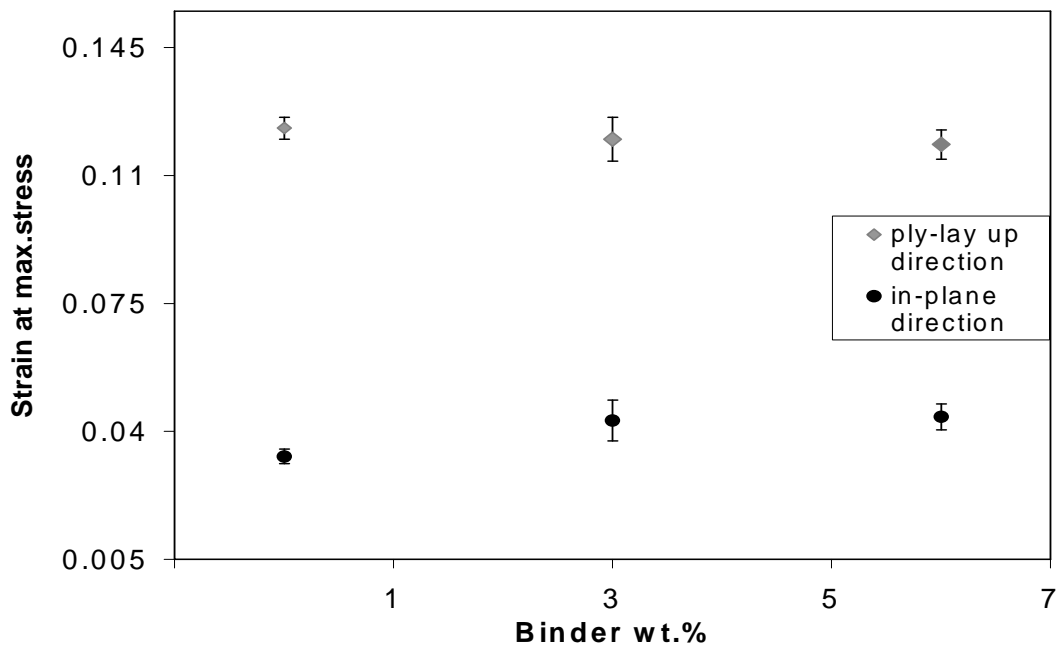


**Figure 7.18** The strain at maximum stress values as a function of binder weight percentage for the ply-lay up and in-plane loading directions

Figures 7.19 and 20 show compressive strength and modulus values of E-glass/polyester specimens as function of binder weight percentage for the ply-lay up and in-plane loading directions, respectively. The strength values are in the range of 400-600 MPa and 150-300 MPa for ply-lay up and in-plane directions, respectively. Also, the modulus values are in the range of 4500-6000 MPa and 5000-11000 MPa for ply-lay up and in-plane directions, respectively. The higher strength along ply-lay up direction may be due to the fact that the compressive strength is more matrix-property dominant in this

direction while along in-plane direction is more related to interlaminar and interfacial bonding. Furthermore, for the both loading directions, both average strength and modulus values increase slightly up to 3 wt.% of the binder while the further addition of the binder results in slight decrease. This may be associated with the optimum interlaminar strength and the highest fiber volume fraction. Surfaces of the fractured compression test specimens for both loading directions were examined using SEM to reveal the compressive failure modes at the interlaminar region. The results show that compressive failure modes of specimens for both loading directions were altered by the introduction of binder within the interlaminar region.

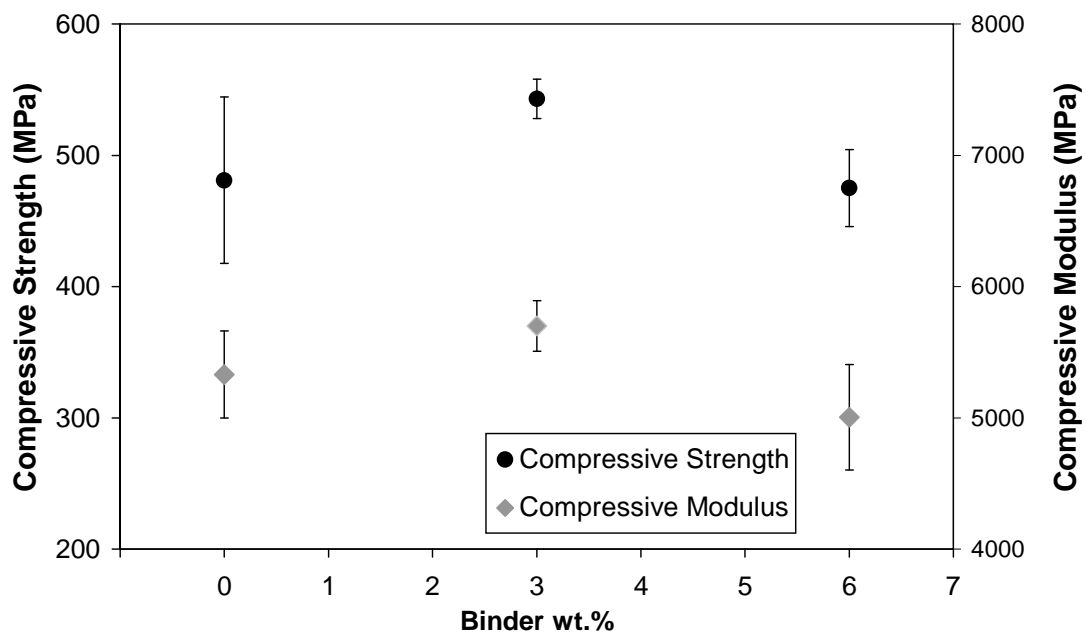


**Figure 7.19** Ply lay up direction maximum compressive stress and compressive modulus as a function of binder weight percentage.

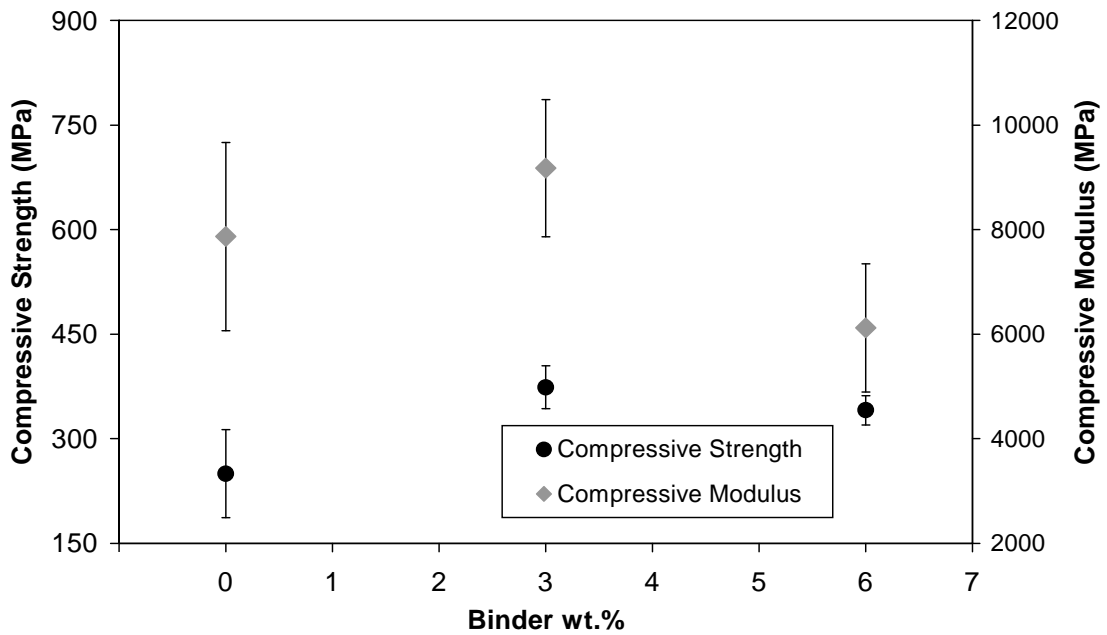


**Figure 7.20** In-plane direction maximum compressive strength and compressive modulus as function of binder weight percentage.

Figures 7.21 and 22 show the fracture surface SEM micrographs of compression test specimens without binder and with 6 wt.% of the binder for ply–lay up direction, respectively. As seen in these figures, fibers normal to the loading direction were observed to fail due to Poisson expansions. Also, matrix cracking and intrabundle cracks are visible for the specimens with and without binder. Figure 7.23 and 24 show the fracture surface of the composite specimens without binder and with 3 wt.% binder for in-plane loading direction. As seen in these figures, fibers along the loading directions were observed to buckle and formed kink band. In detail, the fact that composites without binder have more local kink band regions than those with binder. This may be due to higher interfacial strength of the composites without binder. Also, longitudinal splitting, along the interlaminar region is visible. Furthermore, a weaker interfacial bond resulted in intraply splitting and fiber/matrix interfacial debonding. It was also observed that the extend of longitudinal splitting is greater in composites with binder. This may be due to the lower interlaminar strength of the composites made with addition of preforming binder.

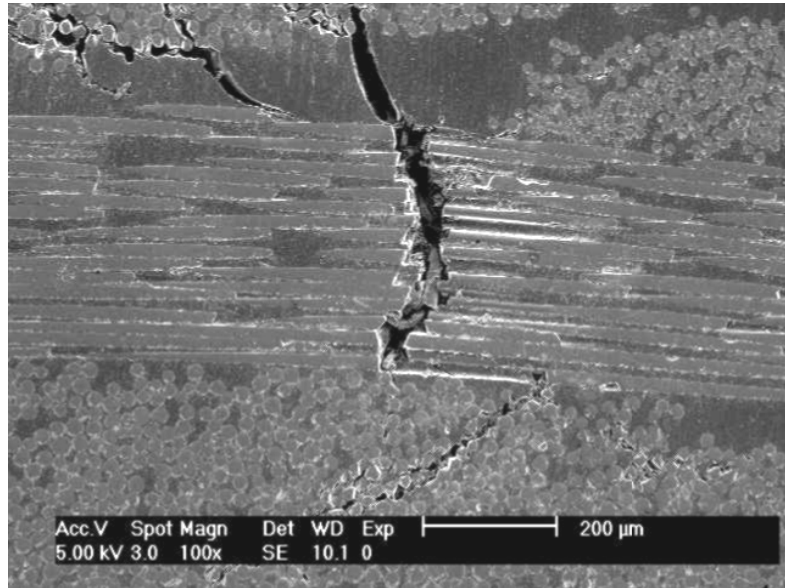


**Figure 7.21** Fracture surface of compression composite specimen without binder loaded in ply-lay up direction.

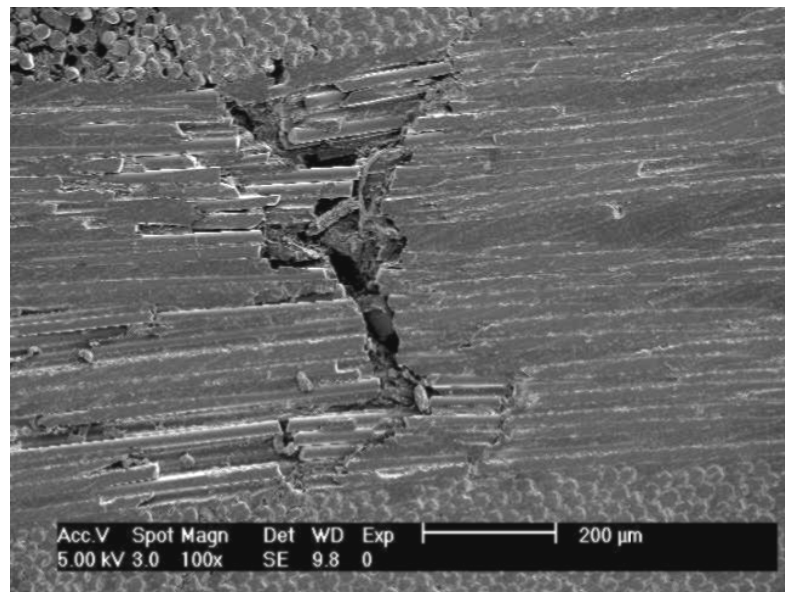


**Figure 7.22** Fracture surface of compression composite specimen with 6 wt.% of binder loaded in ply-lay up direction.

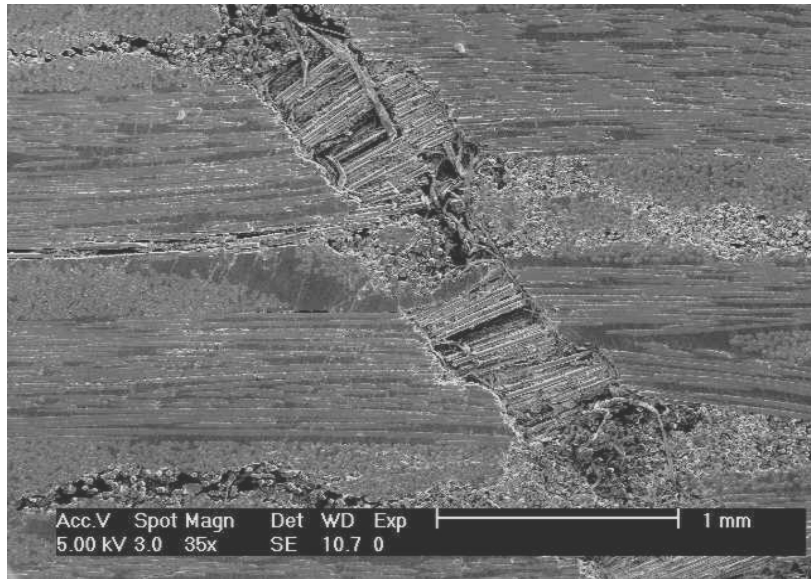


**Figure 7.23** Fracture surface of compression composite specimen without binder loaded in in-plane direction.

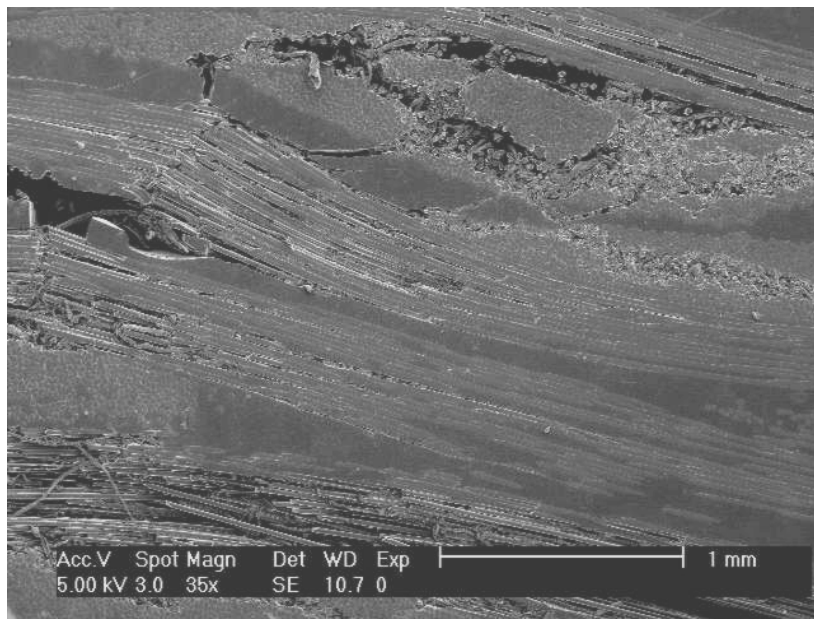


**Figure 7.24** Fracture surface of compression composite specimen with 3 wt.% binder loaded in in-plane direction.



## 7.5 Interactions between binder and matrix resin.

Interactions between the thermoplastic binder and the thermosetting polyester matrix were followed to investigate the effects of the binder on the mechanical behaviour of polyester matrix and extent of the binder dissolution within the reacting matrix resin. For this purpose, various amount of binder was added into the reacting system to replicate the matrix material. Figures 7.25 and 26 show the fracture surface SEM micrograph of the matrix polymer without binder and with 12.85 wt. % binder, respectively. The specimens were loaded under flexure using three point bending configuration. As seen in Figure 7.27, undissolved binder particles embedded in the matrix are visible. This indicates that there is no complete dissolution of the binder within the reacting resin system. Moreover, as the polyester matrix exhibits a brittle fracture mode (Figure 7.25) that is typical for thermosetting polymers, the presence of the binder within the matrix alters the mode of the fracture of the polymer.

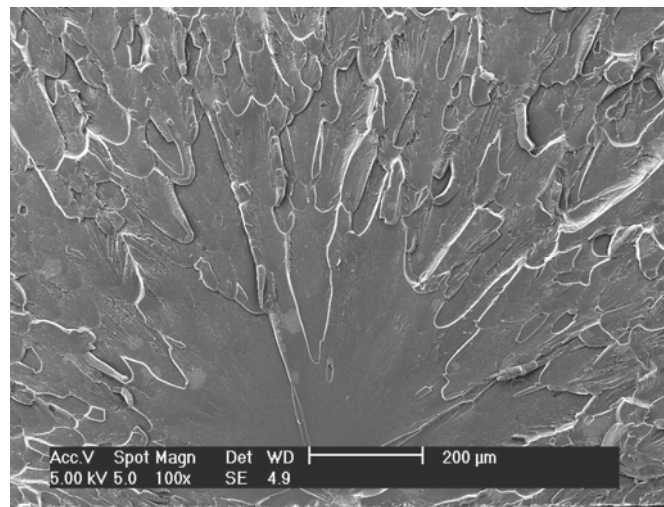


**Figure 7.25** Fractured surface SEM micrograph of polyester matrix polymer without binder.

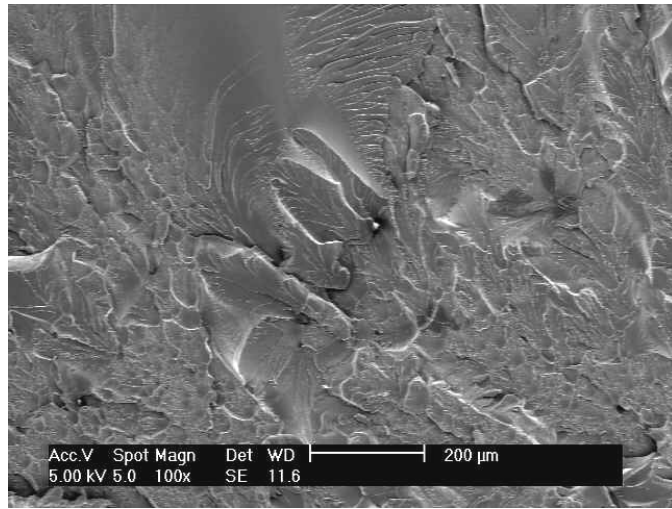


**Figure 7.26** Fractured surface SEM micrograph of polyester matrix polymer with 12.85 wt.% binder.

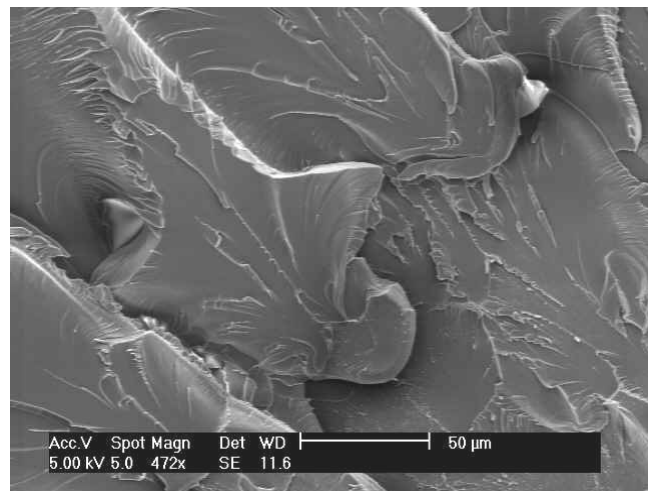


**Figure 7.27** Fractured surface SEM micrograph of polyester matrix polymer with 12.85 wt.% binder. The undissolved binder particles are visible in micrograph.

Mechanical behaviour of the cured model materials was also evaluated to reveal the effects of the addition of the binder on the compressive behaviour of the matrix polymer. Figures 7.28 to 30 exhibit the compressive stress and strain response of the model specimens with and without binder. The stress strain behaviour of all the specimens showed linear elasticity up to the yield point. The yield point is defined as the point at which deviation was observed in the linear part of the stress-strain curve. For all specimens, deformation involved significant plastic flow beyond the maximum stress and the flow stress remained constant up to relatively high strains.

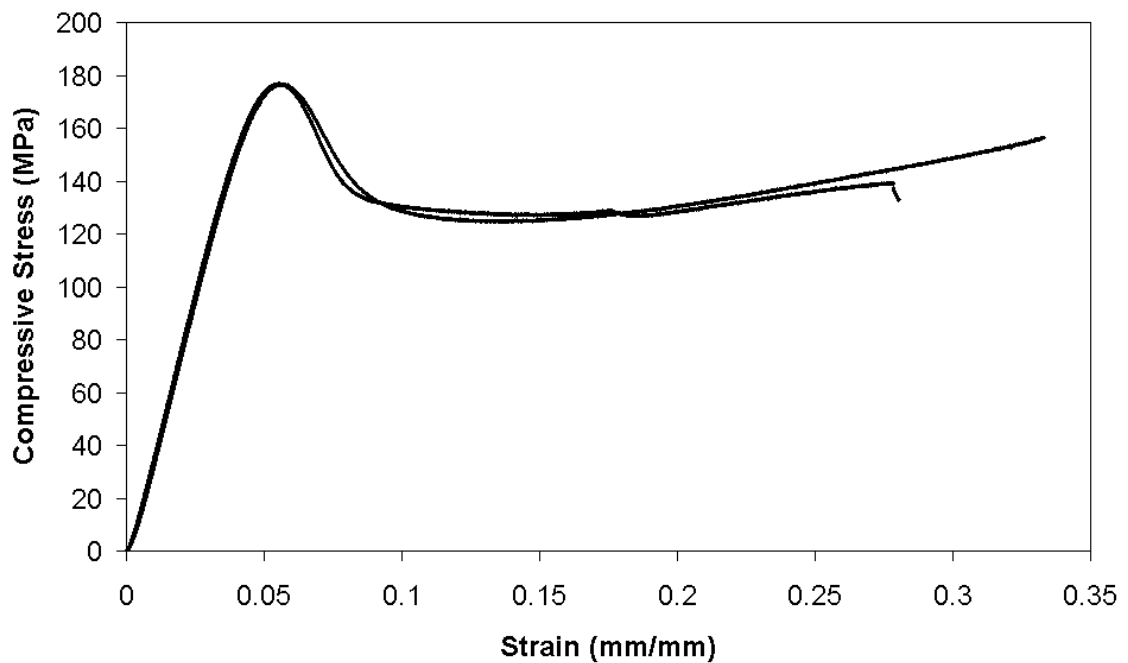


**Figure 7.28** The typical compressive stress and strain response of the model specimens without binder

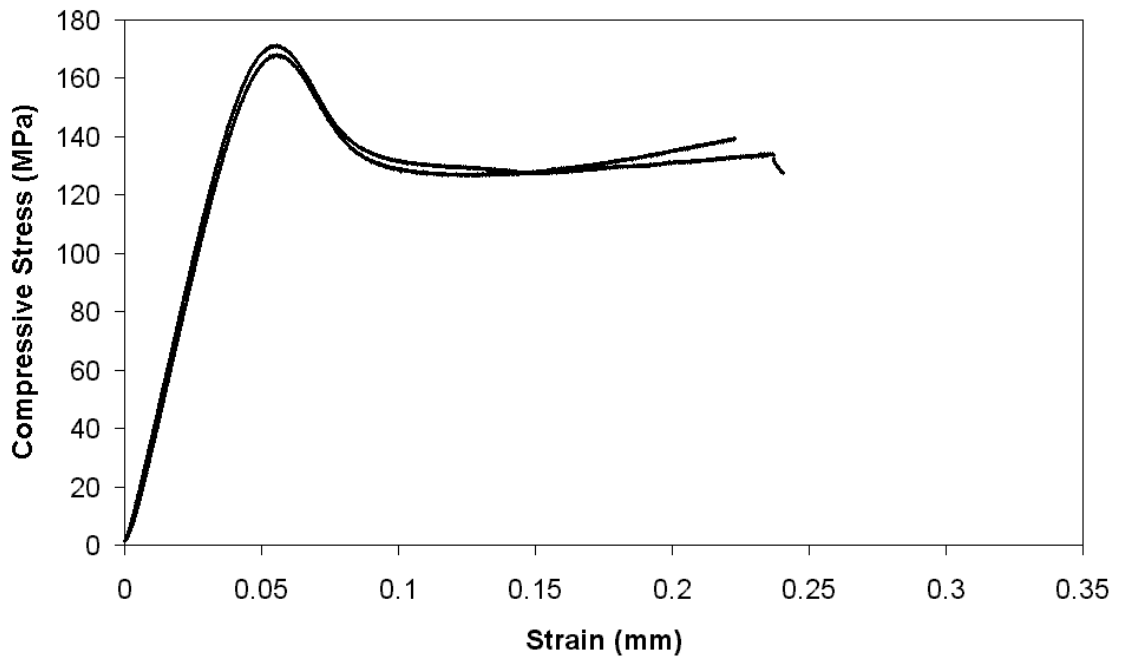


**Figure 7.29** The typical compressive stress vs. strain response of the model specimens with 6.5 wt.% of binder.

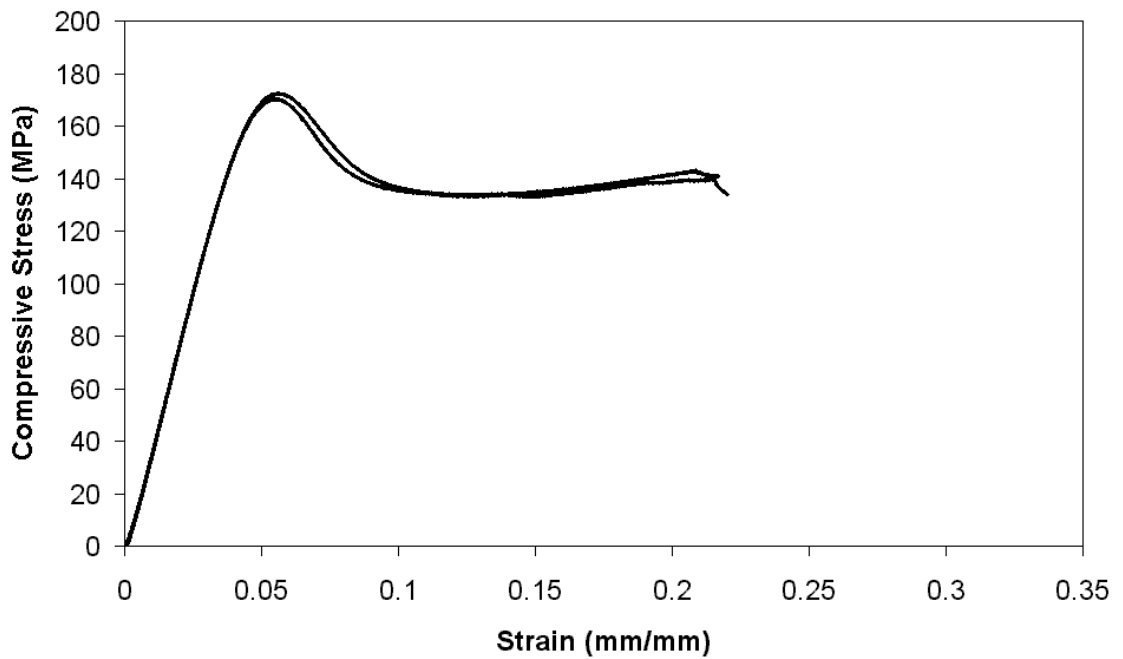


**Figure 7.30** The typical compressive stress vs. strain response of the model specimens with 12.85 wt.% of binder.

Figures 7.31 and 32 show the strain at yield values and the compressive yield stress and modulus of the polyester matrix resin as a function of binder weight percentage, respectively. The results reveal that compressive modulus and the strain at yield values of the model specimens are not significantly affected by the introduction of the binder. On the other hand, the compressive yield stress decreases insignificantly with increasing binder content.

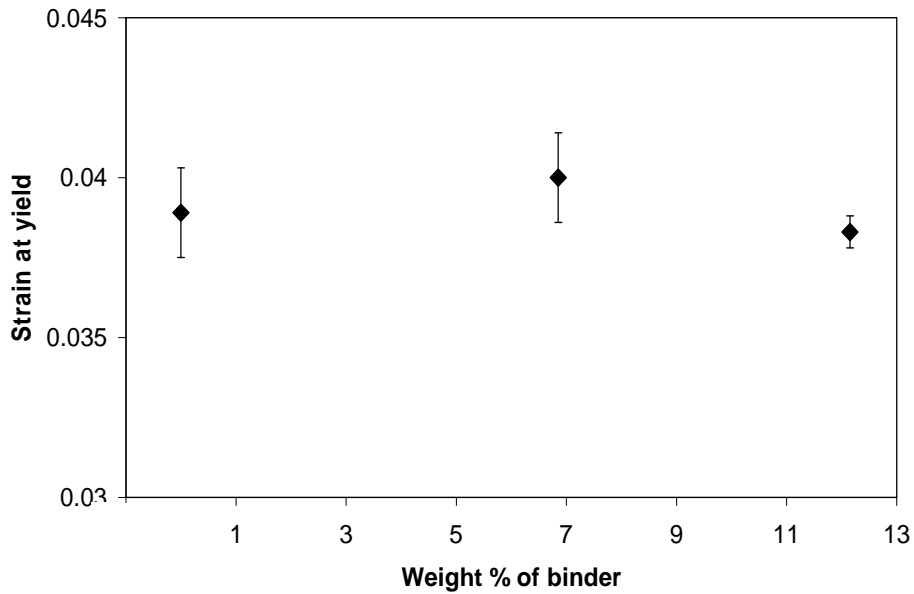


**Figure 7.31** Strain at yield values of the model specimens as a function of weight percentage of the binder.

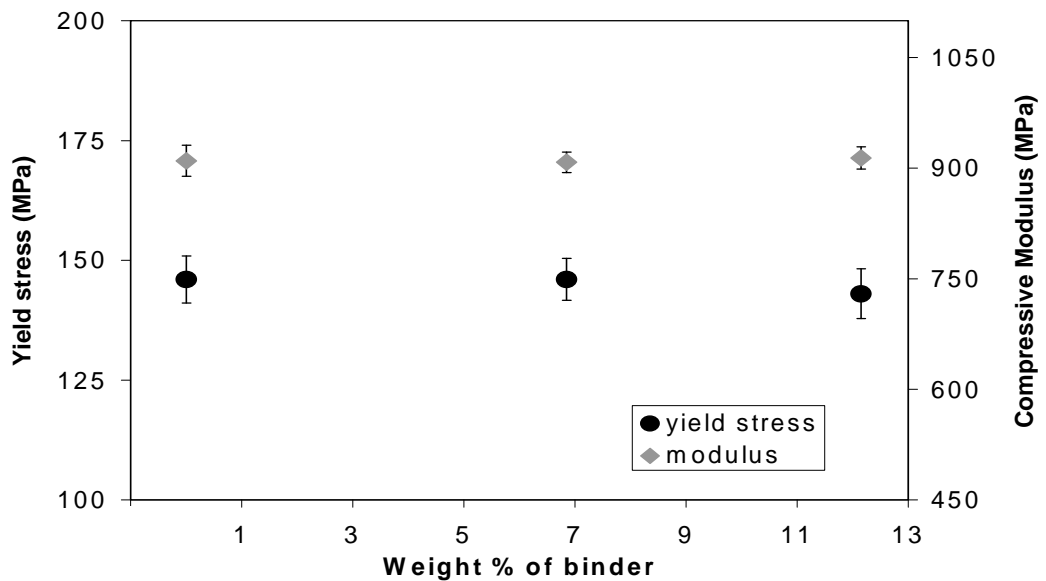


**Figure 7.32** Yield stress and compressive modulus of the model specimens as function of binder weight percentage

The viscosity values of the resin/binder blends stirred at room temperatures at constant shear rate of  $5 \text{ s}^{-1}$  are given in Figure 7.33. The viscosity of the neat resin at room temperature was measured as 1135 cp. As seen in the figures, the viscosity values of the resin lift up to higher values initially by the addition of the powdered binder. The further increase and the saturation of the viscosity values was observed due to stirring at room temperature and approaches to a constant value. This further increase may indicate the partial dissolution of the binder within the matrix. The viscosity increase was measured to be about 30 % and 35 % for 6.5 and 12.85 wt.% of the binder, respectively, up to the gelation time ( $\approx 50 \text{ min.}$ ) of the resin in real composites. Moreover, the viscosity value for the blend (6.5 wt.%) increased at elevated temperature ( $65 \text{ }^\circ\text{C}$ ) and reached to the highest value of 10360 cps. at complete dissolution by melting. The results indicate that in real composites partial dissolution of the binder within the resin and therefore an increase in the viscosity of the infusing resin possibly occurs.

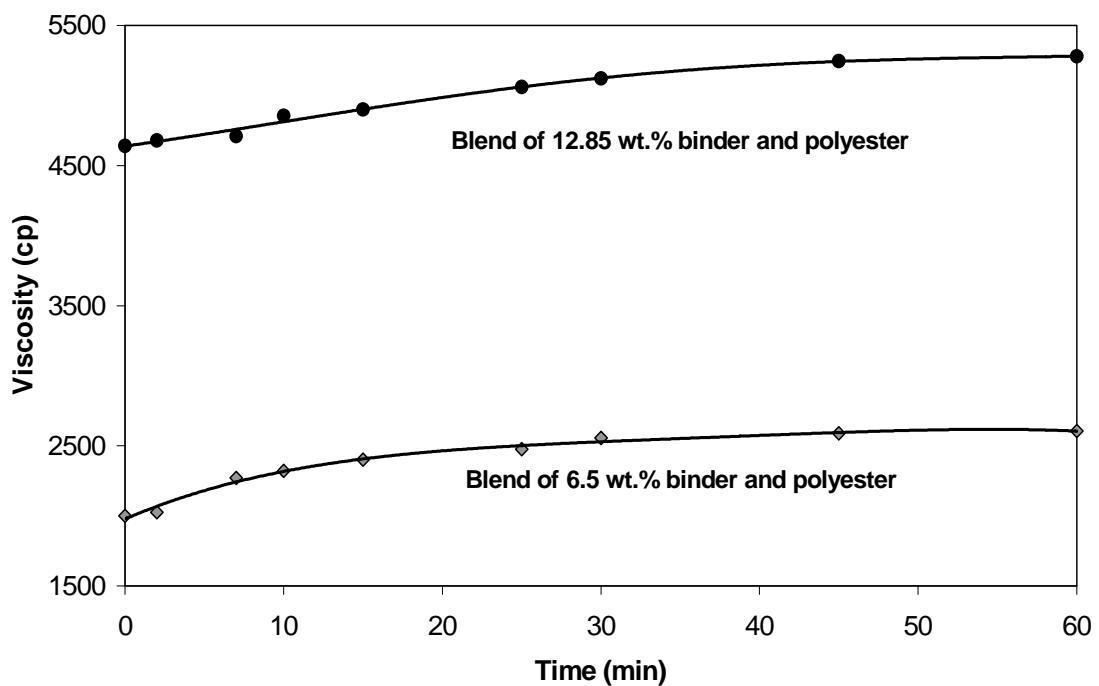


**Figure 7.33** The viscosity values of the resin/binder blends (6.5 wt.% binder) stirred at room temperatures.

## Chapter 8

### CONCLUSIONS AND RECOMMENDATIONS

In this study, the effects of the preforming binder on the mechanical properties and ballistic performance of the E-glass/polyester composite systems were investigated. The results showed that the powdered thermoplastics have high potential to produce thermoformable glass fabric preforms. It was found that approximately 9 wt.% of the binder provides full coverage of the glass fabric surface. The highest peel strength was measured from the preform that has almost full binder coverage on the fabric. The further increase on the binder concentration has no significant effect on the peel strength values. Preform compressibility was found to be affected by introduction of binder. Furthermore, the preform compaction experiments revealed that the initial fabric compaction can be achieved by application of preform consolidation technique using powdered binders and the highest compaction and therefore the highest fiber volume fraction can be obtained with 3 wt.% of the binder.

Polymer composites were successfully fabricated by VARTM technique and using consolidated preforms. Flexural strength and modulus, interlaminar fracture toughness and compressive strength and modulus of the composites have gone under considerable changes by the introduction of the preforming binder. Flexural strength is decreased while flexural modulus is increased with increasing binder content. Compressive stress and strain responses of the E-glass/polyester composites loaded along the ply-lay up and in-plane direction were also considerably affected by the preforming binder. It was found that compressive strength and modulus through ply-lay up direction is higher than that for the in-plane direction. The effect of presence of the binder on the strain values at maximum stress for both directions were insignificant. For both loading directions, compressive strength and modulus values of the composites increases up to 3 wt.% of the binder and the further increase of the binder concentration results in slight decrease of these values. Mode I interlaminar fracture toughness of the composite laminates is also significantly affected by the thermoplastic binder, i.e., 40 % reduction by the presence of 3 wt.% binder. It was found that interlaminar shear strength is not significantly affected by the presence of the binder.

The results of the ballistic tests showed that failure damage due to the ballistic impact is also considerably affected by the presence of the binder. Ultrasonic C-scanning test showed that the extend of the delamination type damage was reduced due to the presence of the preforming binder. Microstructure characterization of the composite specimens was performed using Scanning Electron Microscopy (SEM) and optical microscopy. The fracture surface examination of the composites revealed that the failure modes alter with the presence of the binder. This study also showed that there is no complete dissolution of the binder in the reacting polyester resin. Partial dissolution of the binder increases the viscosity of the resin that is critical for the infusion process within the VARTM and RTM techniques. Also, the presence of the binder has some effects on the mechanical behaviour of the matrix polyester. All these results indicate that the potential of the preforming binder to modify the properties at interlaminar region and to tailor the mechanical and ballistic performance of the polymeric composites

In the future studies, different binder concentration may be studied by following the same methods described in this study. In addition, the effects of preform consolidation parameters such as heat and pressure may be investigated at different heat and pressure applications on the final composite part properties. Also, the effect of vacuum applied during composite manufacturing may be determined on the final properties of the composites with and without binder.



## REFERENCES

1. R. Griffiths, A. Ball, An Assessment of the properties and Degradation behavior of Glass Fiber-Reinforced Polyester Polymer Concrete, *Composites Science and Technology* 60, 2000 , 2747-2753.
2. J.C Knight, D. Backes and K. Jayaraman, Consolidation and Relaxation Behaviour of Continuous Strand Random Glass Mats with Thermoplastic Binder, *Polymer Composites*, 17;3, 1996, 451-457.
3. R.W. Hillermeier, B.S. Haye, and J.C. Seferis, Tackifier/Binder Toughened Resin Transfer Molding Composites, *Journal of Advanced Materials*, 31;4, 1999, 52-59.
4. C.H. Shih, Q. Liu, L. J. Lee, 45 In: International SAMPE Symposium, 21;25, May 2000, 776-787
5. S. Ziaee, J. C. Brody, M. Tanoğlu, Jr. J. W. Gillespie, S.H McKnight, Effects of a Polyester Preforming Binder on Properties of E-glass Fabric Reinforced Vinyl-Ester Composites, Conference Proceedings of 16 th Annual Technical Conference of American Composite Society, Blacksburg, Virginia, Sept. 10-12, 2001.
6. B. Chen, T.W. Chou, Compaction of Woven Fabric preforms: nesting and multi-layer deformation, *Composite Science and Technology*, 60-2000 , 2223-2231.
7. V. Rohatgi, and L.J. Lee,. Moldability of Tackified Fiber Preforms in Liquid Composite Molding. *Journal of Composite Materials*,31;7, 1997, 720-744.
8. J. Chen, D. Backes, and K. Jayaraman, Dynamics of Binder Displacement in Liquid Molding, *Polymer Composites*, 17;1, 1996 , 23-33.
9. K. F. Karlsson and B. T. Astrom, Manufacturing and Applications of Structural Sandwich Components, *Composites Part A*, 28, 1997 , 97-111.
10. R. Marissen and J. Linsen, Variability of Flexural Strength of Sheet Moulding Compounds, *Composites Science and Technology* 59 1999 , 2093-2100.
11. D. Hull, An introduction to composite materials, Cambridge Solid State Science Series 1995, 31-47.
12. A. B. Strong, Fundamentals of composites manufacturing, Society of Manufacturing Engineers, 1989 , 99-116.
13. B. Z. Jang, Advanced polymer composites: principles and applications, ASM International, 1994 , 1-21.

14. S. K. Akhtar, U. Ö. Colak , P.Centala, Compressive Failure Strengths and Modes of Woven S2-glass reinforced Polyester due to Quasi static and Dynamic loading, *International Journal of Plasticity* 5 2002 , 574-595.
15. N.J.Pagano and R.B.Pipes, Interlaminar response of composite materials, Volume 5 Composite Materials Series, 1989 , 184-215.
16. H. Albertson, J. Ivens, P. Peters, M. Wevers, Interlaminar Fracture Toughness of CRFP Influenced by Fiber Surface Treatment Part1: Experimental results, *Composites Science and Technology* 54, 1995 , 133-145.
17. J.G. Hetherington, The Optimization of Two Component Composite Armours, *Int. J. of Impact Engineering* Vol.12 No:3 1992, 409-414.
18. M.Lee and Y.H.Yoo, Analysis of Ceramic/Metal Armour Systems, *Int J. Impact Engineering* 25, 2001, 819-829.
19. I.S. Chocron and V.Sanchez, A New Analytical Model to Simulate Impact Onto Ceramic /Composite Armors, *Int.J. Impact Engineering*. 21; 6 1998, 461-471.
20. M. Tanoğlu, S.H. McKnight,G.R. Palmese, Jr. J.W. Gillespie, Effects of Glass Fiber Sizings on the Strength and Energy Absorption of the Fiber/Matrix interphase under high Loading Rates, *Material Science and Engineering* 61,2001 , 205-220.
21. M. Skrifvars, T. Mackin , B. Skagerberg, An Application of Experimental Design to the Development of Glass Fiber Reinforced Polyester Laminates with Enhanced Mechanical Properties, *Polymer Testing* 17 1998 , 345-356.
22. U. K. Vaidya, A. Abraham, S. Bhide, Affordable Processing of Thick Section and Integral Multi-Functional Composites, *Composites: Part A*, 32, 2001, 1133-1142.
23. A. Bhatnagar, L.C. Lin, D.C. Lang, H.W. Chang, Comparison of Ballistic Performance of Composites. Proceedings of International SAMPE Symposium, 1989, pp.1529-1537.
24. F. A. Milton, Army after next proposal for ground combat vehicles, Army Science Conference, Norfolk, VA, June 1998.
25. S. Jr., W. N., “Light Weight Armor”, US Patent # 4,732,803, 1988.
26. K. R., Bernetich, B. K. Fink, Jr. J.W. Gillespie, Ballistic Testing of Affordable Composite Armor. Proceedings of American Society for Composites, September 1998, Baltimore, Maryland.
27. W.J. Cantwell, J. Morton, The impact resistance of composite materials-a review, *Composites*, 1991 , 347-362.

28. B.Wang and S.M.Chou, The behaviour of Laminated Composite Plates as Armour, *Journal of Materials Processing Technology* 68, 1997, 279-287.
29. E.P. Gellert, S.J. Cimpoeru, R.L. Woodward, A Study of the Effect of Target Thickness on the Ballistic Perforation of Glass Fiber Reinforced Plastic Composites, *Int. J. of Impact Engineering* 24, 2000 ,445-456.
30. N.Tarim, F.Findik and H.Uzun, Ballistic Performance of Composite Structures, *Composite Structures* 56, 2002, 13-20.
31. E.D.Luca, J.Prifti, W. Betheney, S.C. Chou. Ballistic impact damage of S-2 Glass Reinforced Plastic Structural Armor, *Composite Science and Technology* 58, 1998, 1453-1461.
32. A.P. Mouritz, Ballistic Impact and Explosive Blast Resistance of Stitched Composites, *Composites Part B* 32, 2001, 431-439
33. S.S. Morye, P.J Hine, R.A. Duckett, D.J Carr, I.M.Ward, Modeling of the Energy Absorption by Polymer Composites Upon Ballistic Impact, *Composites Science and Technology* 60, 2000, 2631-2642.
34. G.J. Czarnecki , Estimation of the  $V_{50}$  Using Semi-empirical procedures, *Composites Part B* 29, 1998, 321-327.
35. W.E Lawson, *Composites in Manufacturing*, SME, Los Angeles, 1, 1986
36. G.M Knoblach, Processing of Polymeric Composites- a review , *Composites Part A*, 21, 1991 , 87-101.
37. C. F. Johnson, *Resin Transfer Molding*, Ford Motor Company, 1995, Composites
38. G-W Lee N.J., H.Lee, J. Jang, K.J. Lee, J.D.Nam, Effects of Surface Modification on the Resin Transfer Moulding (RTM) of Glass fibre/unsaturated Polyester Composites, *Composites: Part A*, 40, 2002, 214-223.
39. High Performance Composites, "Preforms get lean and mean" March 2002 pp.42-47
40. B. Chen, T.W. Chou, Compaction of Woven Fabric Preforms in Liquid Composite Molding Processes: Single Layer Deformation, *Composite Science and Technology* 59 1999, 1519-1526.
41. R. Kamiya, A. Bryan, Cheeseman, P. Popper, T.W. Chou, Some Recent Advances in the Fabrication and Design of Three Dimensional Textile Preforms : a review, *Composite Science and Technology* 60, 2000, 33-47.

42. R.A. Saunders, C. Lekakou and M.G. Bader, Compression and Microstructure of Fibre Plain Woven Cloths in the Processing of polymer composites, *Composites Part A*,29, 1998 , 443-454.
43. Tsu-Wei Chou, Roy L. McCullough and R. Byron Pipes, *Composites*, 1997
44. R.A.Saunders, C. Lekakou, M.G. Bader, Compression In the Processing of Polymer Composites 1. A mechanical and microstructural study for different glass fabrics and resins, *Composites Science and Technology* 59, 1999 , 983-993.
45. D. A. Steenkamer, The Influence of Preform Design and Manufacturing Issues on the Processing and Performance of Resin Transfer-Molded Composites, University of Delaware, 1994 .
46. B. Chen, T.W. Chou, Compaction of Woven Fabric preforms: nesting and multi-layer deformation, *Material Science and Engineering: A* 317 (2001) 188-196
47. Batch and Mocasko, Consolidation behaviour of the preforms with binder, *Material Science and Engineering: A* 116 (1996) 24-32
48. K. Jang, W. J. Cho, C. S.Ha, Influence of Processing Method on the Fracture Toughness of Thermoplastic Modified Carbon Fiber Reinforced Epoxy Composites *Composite Science and Technology* 59, 1999 , 995-1001.
49. Broutmann and Awargall, A Theoretical Study on the Energy Absorption of the Composites, *Composites A*, 122 (1994) 12-19.
50. R. W Hillermeier,., J. C Seferis,., Interlayer Toughening of Resin Transfer Molding composites” *Composites: Part A*,32, 2001, 721-727.
51. M. Tanoglu, S. Robert., D. Heider, S.H McKnight, Jr. J. W Gillespie,., Effects of Thermoplastic Preforming Binder on Properties of S2-Glass Fabric Reinforced Epoxy Composites. *International Journal of Adhesion and Adhesives*, 2001, 187-185
52. Standard test method for peel strength of textile fabrics . Annual book of ASTM standards ,Vol. 08. 03, 1991
53. Ballistic testing method, NATO Standards Vol. 08. 03 1987
54. Standard test method for flexural properties of unreinforced and reinforced plastics and electrical insulating materials. Annual book of ASTM standards, Vol. 08.03, 1986, 290-298.
55. Standard test method for apparent interlaminar shear strength of parallel fiber composites by short-beam method. Annual book of ASTM standards, Vol. 08.02, 1989

56. Standard test method for mode I interlaminar fracture toughness of unidirectional fiber-reinforced polymer matrix composites. Annual book of ASTM standards, Vol. 15.03, 1995, 280-289.
57. Standard method for compressive properties of rigid plastics. Annual book of ASTM standards, Vol 14.02, 1996, 76-82.
58. A.T.Seyhan, M. Tanoglu , Compressive mechanical behaviour of E-glass /polyester composite laminates tailored with a preforming binder, Material Science and Engineering A, 2003
59. M. Tanoglu, A. T. Seyhan, Investigating the Effects of a Polyester Preforming Binder on the Mechanical and Ballistic Performance of E-glass Fiber Reinforced Polyester Composites, Int. J. of Adhesion and Adhesives 23, 2002, 1-8.